Meddelanden från Stockholms universitets
institution för geologiska vetenskaper No 341

Stockholm University

Oden Southern Ocean 0910
OSO 0910

Cruise Report

John Anderson, Martin Jakobsson
and OSO 0910 Scientific Party

Stockholm 2010

MEDDELANDEN
från
STOCKHOLMS UNIVERSITETS INSTITUTION
för
GEOLOGISKA VETENSKAPER
No 341

Oden Southern Ocean 0910
OSO 0910

Cruise Report

John Anderson, Martin Jakobsson and OSO 0910 Scientific Party

Table of contents

Summary

The Oden Southern Ocean cruise began on February 8 as the Oden departed McMurdo Station in route to Little America Trough in the western Ross Sea for the deployment of oceanographic moorings (Figure 1). We began collecting swath bathymetry and sub-bottom profiler records as soon as we left the ice dock, which included mapping some interesting recessional moraines in McMurdo Sounds. Calm seas were encountered during the transit allowing us to set up coring equipment on the back deck and prepare the labs. We reached Little American Trough on February 10 and conducted a small bathymetric survey needed to select the mooring sites. The two mooring deployments went smoothly and were completed on schedule. The next scientific objective was the deployment of another oceanographic mooring in the western part of Pine Island Bay for scientist from the University of Gothenburg. Again, the mooring went successfully but winch problems prevented us from completing the CTD cast at this station. After the oceanographic work was completed, we attempted our first Kasten core, intended mainly to test the system and coring methods prior to reaching our main study area in eastern Pine Island Bay. The coring went well, except there was minimal recovery in the stiff sediments that cover the bottom at this locality.

On February 17 our 1 600 nautical mile journey from McMurdo Sound to eastern Pine Island Bay was completed and we began conducting scientific operations. Satellite images had indicated that there was very little sea ice in the area, which indeed proved to be the case. In fact, 2010 proved to be a historical event in terms of the limited sea ice cover in Pine Island Bay. This allowed us to conduct a detailed multibeam survey of the bay without restriction. In addition, we were able to occupy 29 coring stations and 10 CTD stations in the eastern part of the bay and in Ferroro Bay, which is a fjord located in eastern Pine Island Bay (Fig. map of study areas showing track lines and CTD and core stations). The preliminary results of our work in the region are provided in the following sections. See also Appendix 1 for brief descriptions of individual research projects.

Participants

Dr. John Anderson, Co-Chief Scientist, Rice University
Dr. Martin Jakobsson, Co-Chief Scientist, Stockholm University
Dr. Frank Nitsche, PI, Lamont Doherty Geological Observatory
Dr. Lars-Anders Hansson, PI, Lund University
Dr. Samuel Hylander, Scientist, Lund University
Dr. Nina Kirchner, Scientist, Stockholm University
Dr. Richard Gyllencreutz, Scientist, Stockholm University
Dr. Rezwan Mohammad, Scientist, Stockholm University
Mr. Björn Eriksson, Multibeam Technician, Stockholm University
Dr. Matthew O'Regan, Scientist, Stockholm University
Dr. Wojciech Majewski, Scientist, Polish Academy of Sciences
Mr. Kyle Jero, Scientist
Mr. Matthias Danninger, Scientist
Ms. Christina Wiederwohl, Scientist, Texas A&M University
Ms. Alexandra Kirshner, Scientist, Rice University
Ms. Rebecca Minzoni, Scientist, Rice University
Mr. Rodgrigo Fernandez, Scientist, Rice University
Mr. Travis Stolldorf, Scientist, Rice University
Mr. Thomas Aidehag, Teacher
Mr. Ville Lenkkeri, Artist
Mr. Paul Clark, Oceanographic Technician, Texas A&M University
Mr. Markus Karasti, Coring Technician, Stockholm University
Mr. George Aukon, Science Technician, Raytheon Polar Services

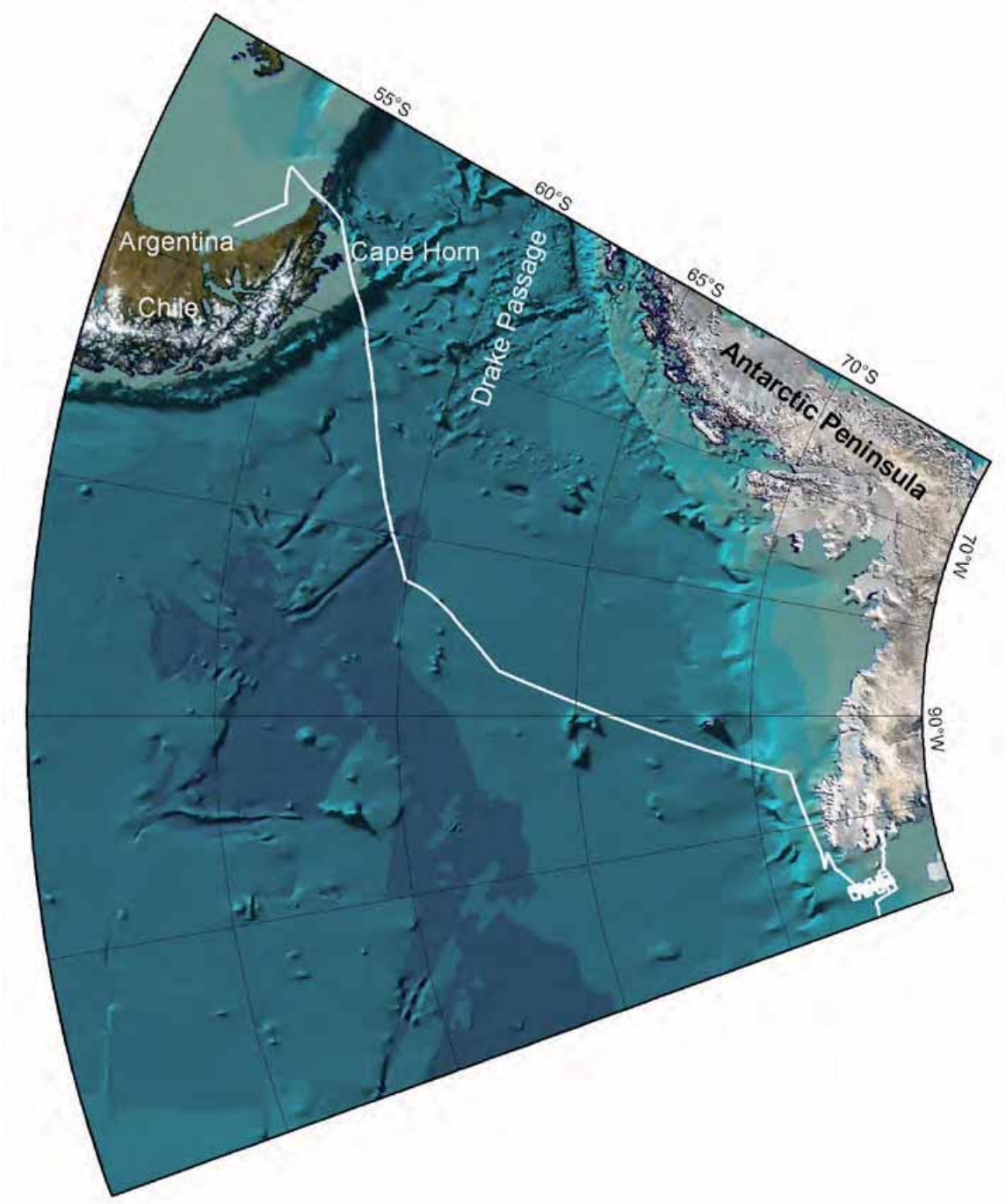

Figure 1. *b) Map showing the track for the crossing of the Drake Passage.*

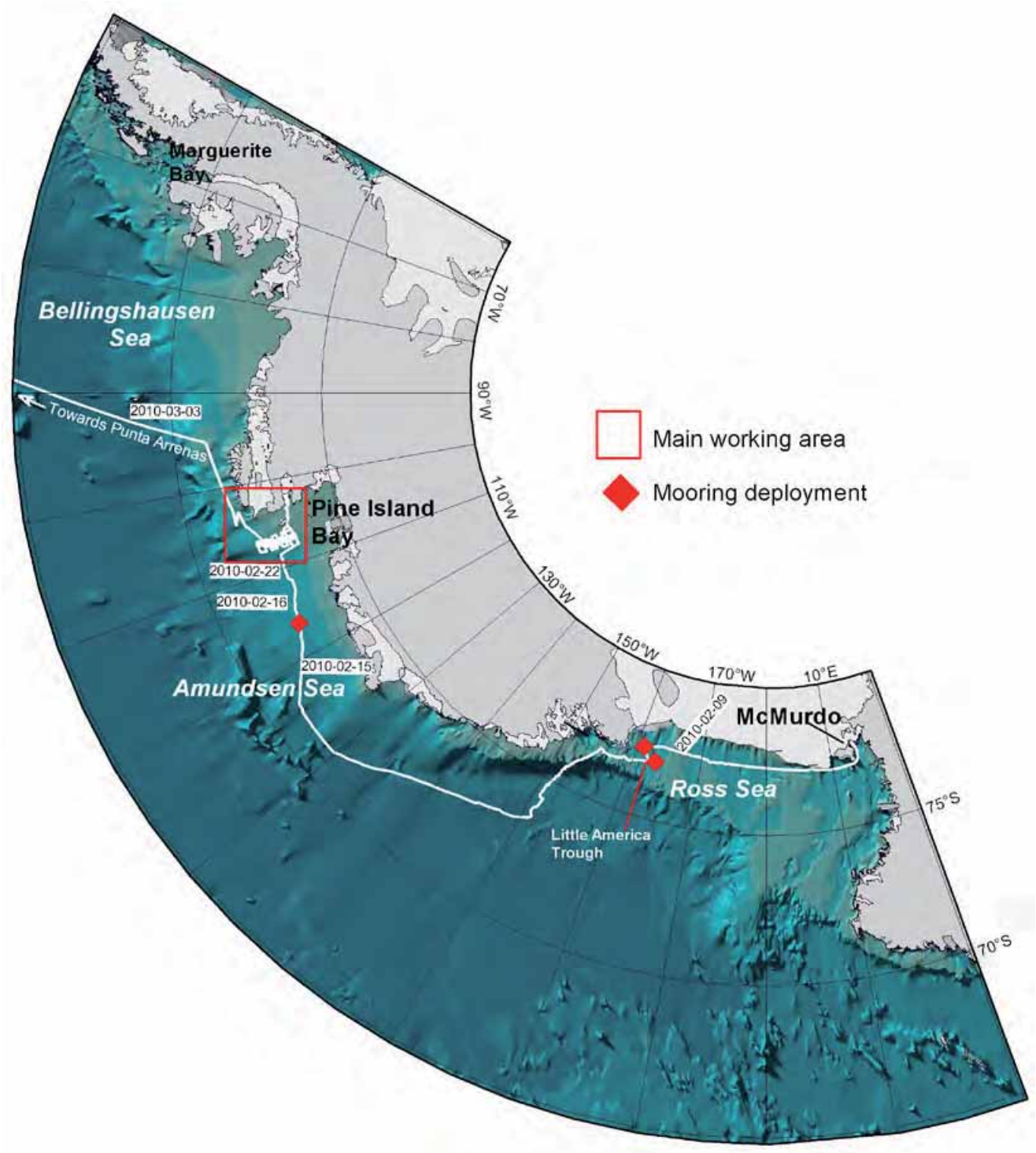

Figure 1. *a) Map showing the route (white line) of the OSO0910 expedition with icebreaker Oden. Coring, CTD and water sampling stations are shown in separate maps in the result sections of the included projects.*

Introduction and background

Marine geology and geophysics

One of the objectives of the 2010 *Oden* cruise was to investigate the history of Pine Island Ice Stream to see if it has a history of rapid change and to attempt to identify those factors that contributed to ice stream retreat in the past. Our first task was to map with *Oden*'s multibeam system a large trough on the continental shelf where Pine Island Ice Stream was located during and after the Last Glacial Maximum. The inner portion of the trough had been mapped in previous expeditions and is known to contain geomorphic features that are indicative of subglacial melt water drainage, possibly instantaneous discharge (Lowe and Anderson, 2002). The multibeam data acquired during our cruise revealed large lineations on the seafloor that are typical of other glacial troughs around Antarctica where ice streams flowed in the past. We also identified some large wedges of sediment that mark former grounding line positions and were successful in collecting cores on these features that yielded carbonate material for radiocarbon dating. These radiocarbon ages will hopefully allow us to study the history of ice stream retreat from the continental shelf, which is the first step in determining the cause of retreat. For example, we may find that the ice stream retreated from the shelf during times when sea level was rising rapidly. Other mechanisms for rapid ice stream retreat include under penning of the ice by subglacial melt water and, as previously mentioned, melting of the ice by warm deep water. We will study the cores for evidence of both mechanisms, evidence such as unique sediment types that might be generated by melt water discharge or unique fossil assemblages that might indicate periods of warm deep water incursion onto the continental shelf. Dr. Wojciech Majewski of the Polish Academy of Sciences will conduct analyses of foraminifera in the cores for assemblages that have been linked to Circumpolar deep water.

Swath bathymetry data acquired during OSO0910 will be integrated into a regional database that is being used to map and analyze the distribution of cross-shelf troughs and the related paleo ice flow pattern along the entire continental margin of the Bellingshausen and Amundsen Seas and thus significantly extend previous studies that focused mainly on two major trough systems in front of the Pine Island Glacier and in the central Bellingshausen Sea. Comparing location and shape of these cross-shelf troughs with present ice flow will lead to new insights into the different processes that created them and may indicate large-scale differences in ice sheet dynamics of today compared to previous glaciations. Building upon a previous bathymetric compilation of the Amundsen Sea (Nitsche et al., 2007) data colleted during OSO0910 will be used to generate the first bathymetric compilation of the entire margin. The new bathymetry compilation will be used to identify cross-shelf troughs, and determine their geometries, including width, depth, and orientation. Using information about present ice flow, such as balance velocity maps, we will compare the distribution of the cross-shelf troughs with present ice stream locations and identify troughs that can be linked to present ice streams or to smaller outlet glaciers. Cross-shelf troughs that correspond to neither of those, or appear too large to be formed by small outlet glaciers, will indicate the locations of previous ice streams that are different from present ones, and thus indicate major changes in ice flow pattern of the WAIS. Comparison with size and geometry of depositional features on the continental slope will provide additional indication if a trough drained large areas of the ice sheet or just a coastal glacier. The results will be integrated into a new conceptual model that describes the ice flow pattern during previous glaciations.

Oceanography

Oceanographic data collected during OSO0910 will be used to investigate processes controlling the flow of warm Cir-

cumpolar Deep Water onto the Antarctic continental shelf in the eastern Ross Sea. Two moorings were deployed to record current, temperature, salinity and pressure in the interior of Little America Troughs. High resolution conductivity/temperature/depth (CTD) measurements were taken to characterize the summer regional water mass stratification and circulation, the boundaries and spreading of water masses, and to infer mixing histories and interactions with the sea-ice and continental ice. The moorings will be left out for one year, with 2010 deployment and 2011 recovery.

Ecology

This project addresses how organisms in freshwater and marine ecosystems handle one of the most hostile environments on earth with respect to ultraviolet (UV) radiation. The project has a strong basic science profile by focusing on adaptations among a group of crustacean zooplankton that is able to adjust the photoprotective pigmentation in accordance with the present UV threat. We expect to find the strongest pigmented zooplankton on earth in Antarctic freshwaters, i.e. will be able to assess the potential reaction norm with respect to pigmentation. In addition to the basic science, the project will provide predictive knowledge regarding how organisms handle elevated UV levels, which are currently increasing also in temperate systems. Our study includes four parts 1) quantification of different pigments, 2) UV effects on community composition, 3) assessment of potential differences in the ecotoxicological fingerprints of marine and freshwater zooplankton, and 4) monitoring of Antarctic lakes in order to compare with an already existing database on Arctic systems. Studies will be performed both as monitoring of marine and freshwater habitats, as well as experimental studies of specific mechanisms. The general aim with the project is to connect large-scale global changes, biodiversity and evolutionary ecology, which has the potential to reveal intriguing predictions regarding the functioning and dynamics in present and, especially, future aquatic ecosystems.

Physics

Data collected during OSO0910 will be used to determine a complete set of cosmic ray response functions for the ice Cherenkov detector used in the surface air shower array that is part of the IceCube neutrino observatory now under construction at the South Pole. This will be accomplished by means of a latitude survey conducted with the detectors mounted in a portable freezer on the icebreaker *Oden*, recording data on the entire 2009–2010 voyage from Sweden to McMurdo and return. The project will advance understanding of the acceleration and transport of solar energetic particles by enhancing the ability of the IceTop air shower array to measure details of solar energetic particle spectra.

Specific objective of solar physics research with IceTop are to:

- Enable high resolution observations of the spectra of solar particles with momentum above 1 GV.
- Extend the sensitivity for detection of high energy particles by approximately two orders of magnitude to better understand the circumstances under which the sun can accelerate these particles.
- Examine the relationship between solar particle event size and spectral shape.

The geomagnetic field prevents cosmic ray particles from hitting the atmosphere below a “cut off” rigidity (momentum per unit charge) that is a calculable quantity for any location on Earth. By observing the change in signal of a detector on the surface of the earth with change in cut off one can deduce in some detail the response of the detector to the primary particles at the top of the atmosphere. Crudely speaking the cut off is high at the equator (few particles get in) and low near the magnetic poles (many particles get in).

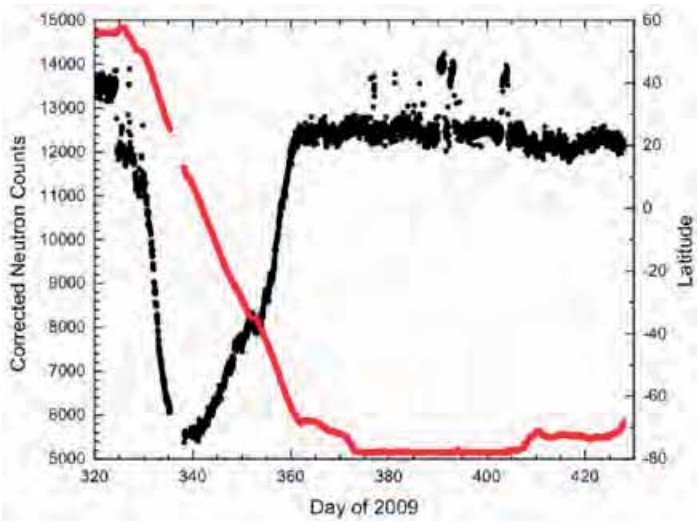

Figure 2. *Summary plot of barometric pressure corrected neutron counting rates for the voyage to date plotted together with geographic latitude. The occasional high values of the neutron intensity occur when the ship is docked – the extra neutrons are generated in the environment. This illustrates one important reason for doing a latitude survey on a ship – the water provides an nearly constant environment.*

Methods

Multibeam bathymetry

During the cruise the multibeam system was operated continuously, from McMurdo until we reached the economical zone of Chile, 200 nmi outside of the country's southern tip. In Pine Island Bay and Ferrero Bay systematic multibeam mapping was carried out along defined survey lines with 20 to >50% overlapping swaths (see Results). The multibeam and subbottom data acquisition was monitored around the clock during four hour shifts by one or two watchmen at each shift (Table 1). Post-processing of both the multibeam and subbottom profiling data was done during the watches (see below).

Equipment

Icebreaker *Oden* is equipped with a Kongsberg EM122 1° × 1° multibeam echo sounder including the capability of logging the acoustic properties of the water column (Figure 3). The system was upgraded in 2009 from an EM120. The EM122 multibeam can perform seabed mapping to full ocean depth (11 000 m). The nominal sonar frequency is 12 kHz with an angular coverage sector of up to 150 degrees and 432 beams per ping. Due to the ice protection of the transceivers, the useable angular coverage is reduced down to less than 2 × 65°; the width of the useable mapping data is typically three–four times the water depth. The transmit fan is split in several individual sectors with independent active steering according to vessel roll, pitch and yaw. This

Team 1 (0-4 & 12-16)	
Björn Eriksson	Stockholm University
Nina Kirchner	Stockholm University
Team 2 (4-8 & 16-22)	
Frank Nitsche	Lamont-Doherty Earth Observatory of Columbia University
Team 3 (8-12 & 20-24)	
Rezwan Mohammad	Stockholm University
Richard Gyllencreutz	Stockholm University

Table 1. *Multibeam watch standing.*

places all soundings on a "best fit" to a line perpendicular to the survey line, thus ensuring a uniform sampling of the bottom and possible 100% coverage. The EM122 transducers are linear arrays in a Mills cross configuration with separate units for transmit and receive.

A Seatex Seapath 200 motion sensor is used for roll, pitch and heave compensation of the Multibeam echo sounder. The Seapath 200 is also use to provide heading and position information.

System settings

The following system settings were usually used for EM122 multibeam surveys during the OSO0910 cruise:

(Runtime Parameters – Sounder Main)
Max. angle: 2 × 50…2 × 65 deg, depending on sea state
Max coverage: depending on water depth, usually higher than angular limit
Angular coverage mode: AUTO (MANUAL results in less beams being used)
Beam spacing: EQDIST
Ping mode: AUTO
Pitch stabilization: On
Heading filter: MEDIUM

Runtime Parameters – Sound Speed
Sound speed profile: .asvp file from CTD or XCTD/XBT/XSV
Abs. coeff. files, salinity: Automatically computed from SVP
Abs. coeff. files, CTD: D:\sisdata\common\svp_abscoeff\default
Sound speed at transducer: Sound velocity probe used. (In the Arctic where we have had more sea ice, we have instead used sound velocity from profile)

Runtime Parameters – Filter and Gains
Spike Filter Strength: OFF
Range Gate: NORMAL
Slope, Aeration, Sector Tracking, Interference: All off
Absorption Coefficient Source: Salinity, 35 ppt
Normal incidence sector: 6°

Runtime Parameters – Filter and Gains
Real Time Data Cleaning: None

Javad and Trimble: Off
ATH Logging: Off

Sound velocity correction

During the entire cruise regular XBT (eXpendable Bathy Thermograph), XSV (eXpendable Sound Velocimeter), and XCTD (eXpendable Conductivity Temperature Depth) casts were carried out. In total, 136 expendable probes were used and the data from most of them were used to calibrate the multibeam echo sounding data in terms of sound velocity. In addition, ten CTD stations were completed which also provided information for the sound velocity correction of the depth data from multibeam. The XSV is the only probe that directly provides a sound velocity profile of the water column. For all the other probes sound velocity has to be calculated from the water physical properties (pressure, temperature and salinity). The sound speed formula used is Coppens (1981, taken from the Simrad EM120 Operators Manual). A 12 000 m value of 1 666.81 (acquired previously from a deep CTD station) was added to the sound velocity profiles (the echo sounder operating

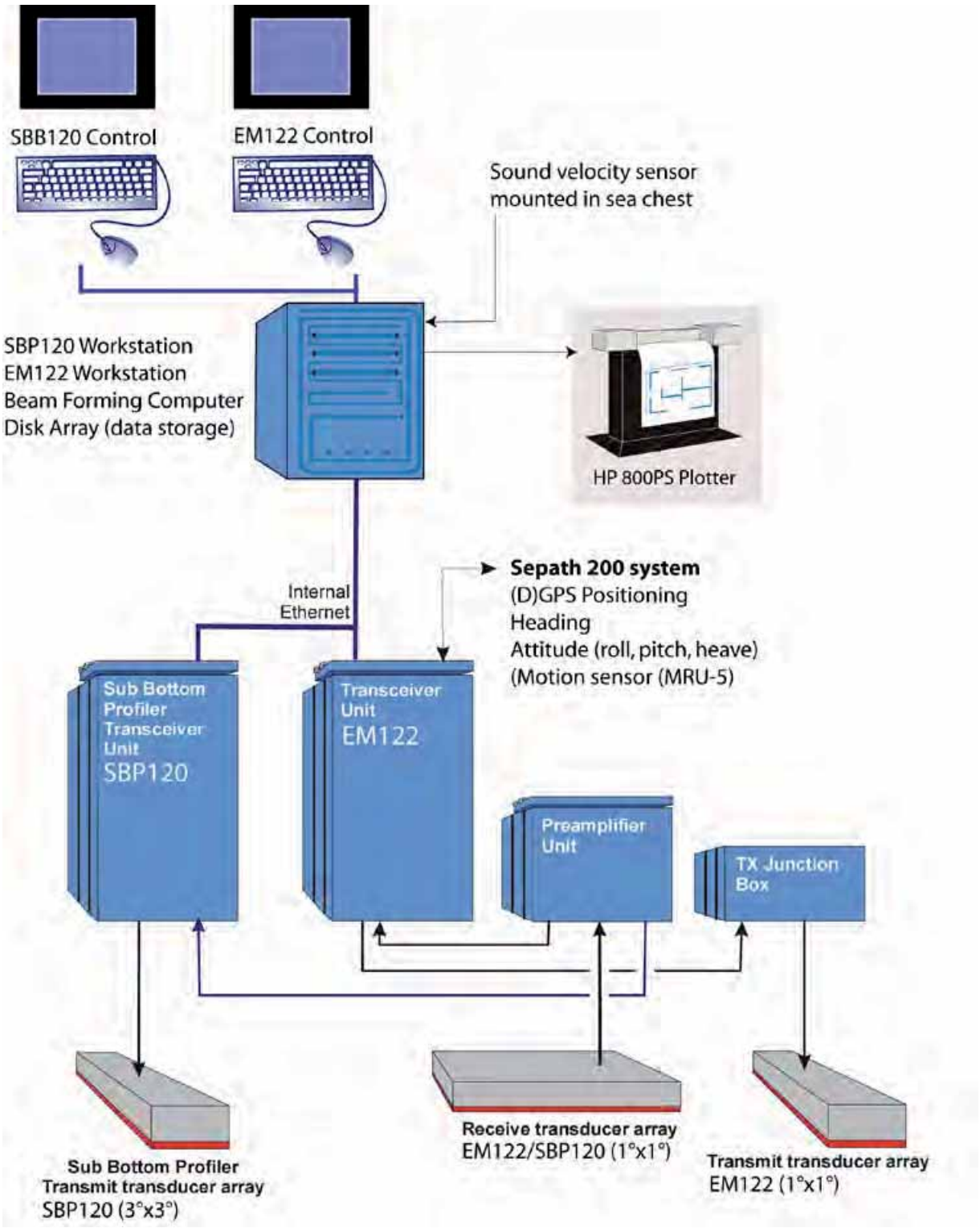

Figure 3. *Schematic illustration of the EM122/SBP120 system installed on the Oden. The drawings are modified versions of Kongsberg's original. The system was financed by the Knut and Allice Wallenberg foundation, Swedish Research council and Swedish Maritime Administration.*

software requires all profiles to extend to 12 000 m depth). Icebreaker *Oden* is equipped with a real-time sound velocity probe by Applied Micro System LDT for providing up-to-date sound speed values near the transducers needed for beam forming. This real time probe is situated within the sea-water intake in the ship's hull. Depending on re-circulation of water in the sea-water intake and probably other factors, the sound velocity reading can fluctuate within a range of up to several meters per second (usually some ±0.3 m/s). However, during the OSO0910 cruise the values provided by the real time probe were stable and usually in good agreement with the surface values from the expendable probes or CTD stations. Therefore, the real time probe data were used. During previous Arctic Ocean expeditions, the real time probe values have been of varying quality and not always possible to use. The sea ice free conditions in Pine Island Bay likely made this probe more reliable during the OSO0910 expedition.

Ship board processing

The acquired multibeam data were immediately processed onboard using the software Fledermaus, version 7.0.1 d. The surveyed areas were divided into several PFM projects (Figure 4). PFM, Pure File Magic, is the multibeam file structure of Fledermaus. The raw multibeam data (.all is Kongsberg's raw file format produced with the EM122 system) within a survey area are merged into a PFM with a defined grid size resolution. The grid resolution was set depending on the water depth in the survey area. In general, a grid cell size of 20 × 20 m was used for all the surveys on the ca 300–1 000 m deep continental shelf during the OSO0910 expedition. The deepest survey lines located in >3 000 m water depth were merged into PFMs with 80 × 80 m sized grid cells. The projection was set to Polar Stereographic with a true scale at 71°S and the horizontal datum to WGS 84. In general, the processing consisted of a first application of the "Cube" algorithm (Calder and Mayer, 2003) followed by manual inspection and editing using tools available in Fledermaus. The final edited cube surfaces were used for analysis of the seafloor morphology. However, in some cases the actual "clean" soundings were exported to allow higher resolution surfaces to be created than the preset PFM surfaces. The processing continued until we arrived at Punta Arenas when all of the data had gone through a first cleaning.

Chirp sonar profiling

Equipment

Icebreaker *Oden* is equipped with a Kongsberg SBP120 3° subbottom profiler. The SBP120 subbottom profiler is an extension to the EM122 multibeam echo sounder. The primary application of the SBP120 is the imaging of the topmost sediment layers under the sea floor. The SBP120 uses an extra transmit transducer unit, whereas one broadband receiver transducer of the EM122 multibeam echo sounder is used for both the EM122 and the SBP120 systems. A frequency splitter directly after the receiver staves divides the 12 kHz multibeam signal from the lower frequency (2.5 to 7 kHz) chirp sonar signal.

The normal transmit waveform is a chirp signal (which is an FM pulse where the frequency is swept linearly or hyperbolically). The outer limits for the start and stop frequencies of the chirp are 2.5 kHz and 7 kHz, providing a maximum vertical resolution of approximately 0.3 milliseconds. In addition to linear chirps, the system offers CW pulses, hyperbolic chirps and Ricker pulses. The system is capable of providing beam opening angles down to 3°, and up to 11 beams in a transect across the ship's keel direction with a spacing of usually 3°. The system is fully compensated for roll, pitch and heave movements of the ship by means of the Seatex Seapath 200 motion sensor used for the Multibeam echo sounder.

System settings

The initial system settings used for SBP120 chirp sonar were adopted from the Lomonosov Ridge off Greenland (LOMROG)

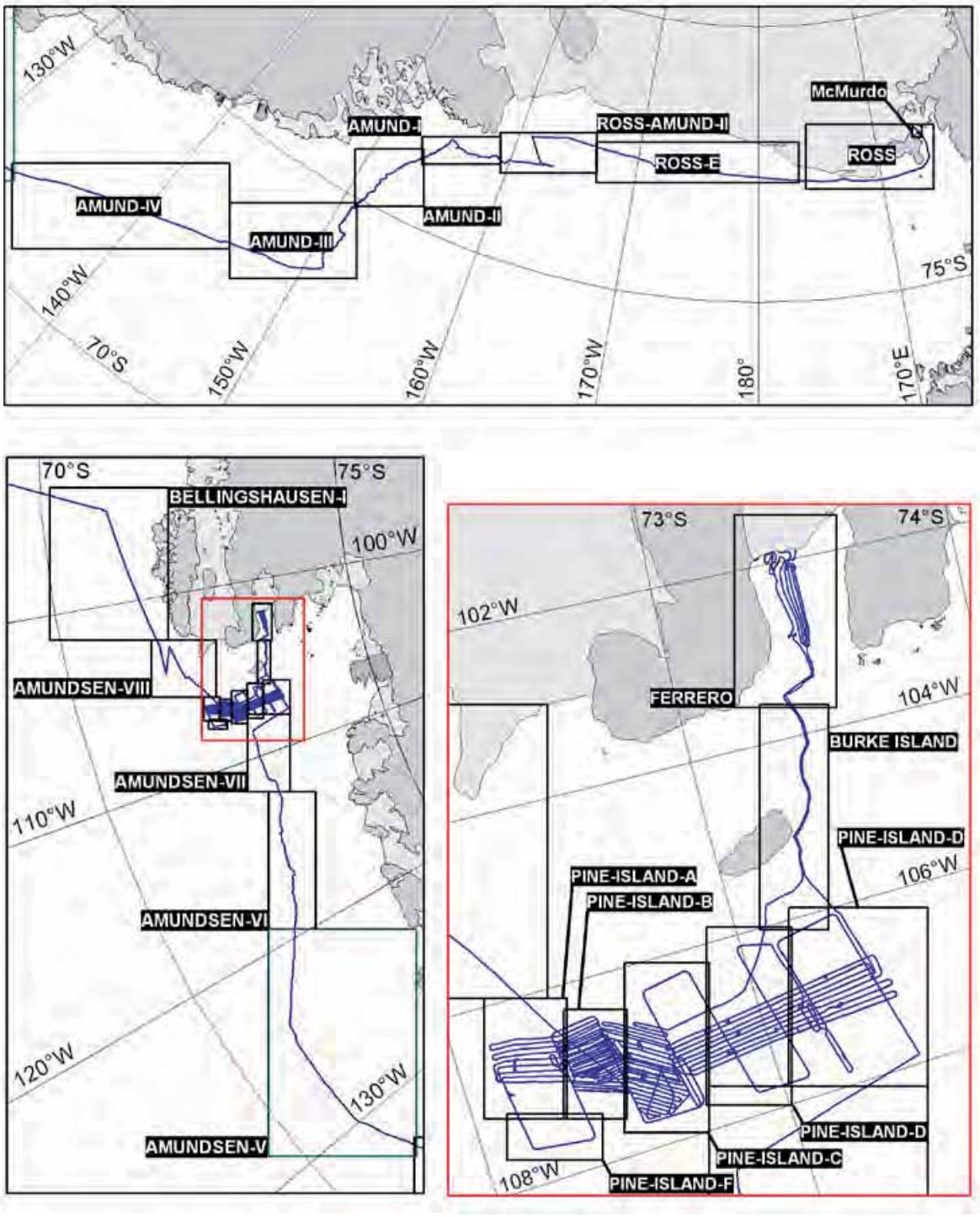

Figure 4. *Maps showing the extents of the PFM multibeam processing projects. The filename of each processing project is shown with letters in a black box.*

expeditions (Jakobsson et al., 2008). However, since there was very little sea ice during the OSO0910 expedition, some different settings were applied. In particular, it was possible to use the automatic adjustment of the acquisition delay. The most commonly applied settings are listed below and a screen dump of the acquisition window is shown in Figure 5.

Transmit mode: Normal
Synchronization: Fixed rate
Ping interval: 500 ms
Acquisition delay: Calculate delay from depth
Acquisition window: 200–250 ms. In steep terrain when it is hard to follow the seafloor reflection a larger window was sometimes used
Pulse form: Linear chirp down
Sweep frequencies: 2 500–7 000 Hz
Pulse shape: 5% (Simrad recommendation, 0% actually will not result in a non-tapered signal, but in an almost-not-documented slight tapering due to physical and electronics restrictions).
Pulse length: generally around 35 ms (seems to be a good trade-off between energy/penetration and resolution).
Source power: –1 dB
Beam width Tx/Rx: 3° ("focused" is not narrower than 3°, which is the physical limit of the transducers)
Number of beams: 5 beams
Beam spacing: 3°
Automatic slope correction: Off
Slope along/across: Usually 0.0° but can be changed when going along/across steep slopes (> 3°) *constantly*.
Slope quality: Parameter read from Multibeam data stream, do not set or change

Ship board processing

Since the main part of the work during the OSO0910 expedition was carried out in Pine Island Bay along pre-defined survey lines proper line breaks for the subbottom profiles were made. This greatly facilitated the data processing. The profiles were named according to the convention OSO0910-PI-##, where ## simply represent a line number that was incremented. Raster images of the chirp sonar profiles were created using the Kongsberg SBP120 software. The post-processing consisted of match filtering and in some cases Time Varied Gain (TVG) was applied. Some examples of chirp sonar profiles and a map of the named profiles in Pine Island Bay are shown in the result section.

Sediment coring and processing

Coring

A piston/gravity corer, which in piston core mode can be rigged up to 12 m, and a 3 meter long Kasten corer were brought to take sediment cores during the OSO0910 expedition. The result section provides further information on sediment cores collected during the expedition, including maps and tables of the core locations and sediment recovery. One attempt at collection of a gravity core loaded with a weight of 1 020 kg was unsuccessful due to a winch failure. The gravity corer was lost as the wire had to be cut. The main hydraulic coring winch was found to be un-repairable and heavy coring operations with the piston/gravity corer had to be terminated. A smaller electrical winch capable of pulling ca 1.5 ton had instead to be used for all coring operations. Thus, all 27 sediment cores collected during the cruise were collected with the 3 meter Kasten corer. Actually, the original plan for the cruise called for use of the Kasten corer as this method allows quick access to the core for onboard sampling. The main objective of the coring was to acquire suitable material for radiocarbon age dating and previous coring in the region had shown that carbonates are rare. Thus, our strategy was to collect and wash onboard large volumes of material, which in some cases involved collecting more than one core from the same location. The Kasten corer has a 3 meter long 15 × 15 cm barrel made out of stainless steel. The core head can be loaded with a maximum of 18 led

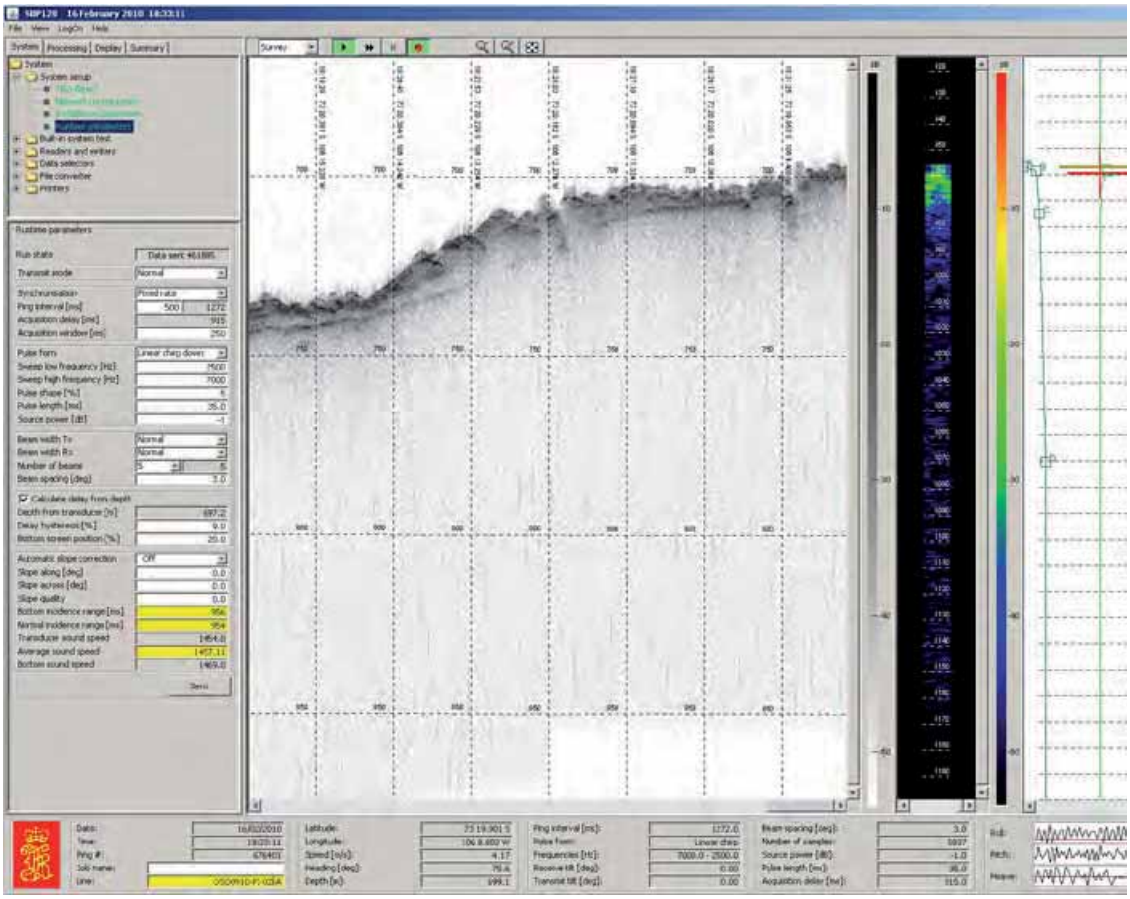

Figure 5. *Screen dump of Kongsberg's acquisition software for the SB120 chirp sonar profiler were the system settings listed above can be seen. This software was also used for post-processing of the multibeam data.*

weights of 32 kg/weight. Until coring station ten 14 weights were used while after this station the amount of weights were increased to 17.

Core locations were selected using a combination of swath bathymetry and sub-bottom profiler data. In general, Pine Island trough was found to contain relatively little post-LGM sediment, so most cores penetrated only a meter or two before terminating in stiff till or gravelly glacimarine sediments. No thick post-glacial sediments were identified within the trough.

As soon as the core was on deck it was transported into a tent that had been erected on the back deck with a large sink for washing samples (see photo of tent). The cores were described, photographed, and physical properties (shear strength) were measured. Lithological descriptions were based on sediment color (Munsell Color Chart), texture, and structures. Samples were also taken from the freshly opened cores for foraminiferal analysis. Next, two archive cores were taken from each Kasten core by inserting liner halves with inner diameter of 80 mm into the Kasten core and removing the smaller core halves using a piano wire and spatulas. The archive cores were delivered to the sedimentology lab where they were logged and later described in detail (Appendix I). The remaining sample in the Kasten core was sieved in a 2 mm and 0.5 mm sieve and examined for carbonate shell material. A separate sample was washed and examined for foraminifera. This approach proved highly successful and a total of 31 carbonate samples were recovered at 14 core locations, including a number of samples at the contact between subglacial

The 3 m long Kasten corer lowered into the water using the A-frame of the Oden.

Core processing in the tent setup on Oden's aft deck.

and glacimarine sediments that will allow us to determine the timing of retreat of the Pine Island ice stream.

Of the two archive core halves, one will be shipped to the Antarctic Marine Geology Research Facility in Tallahassee, Florida for permanent storage and the other will be transported to the Stockholm University.

Multi Sensor Core Logging

The Geotek Multi-Sensor Core logger (MSCL) from Stockholm University was set-up in the main lab on the foredeck of the *Oden*. Sensors were oriented in the vertical direction to allow for split-core logging. Measurements of the gamma ray derived density, compressional wave velocity (p-wave), magnetic susceptibility, sediment

Tent setup on the aft-deck for sampling and processing of the Kasten cores.

Washing and sieving of sediment samples taken from the Kasten corer.

thickness and temperature were acquired at a down core resolution of 1 cm. Each logged section was digitally scanned and the RGB values extracted from the image by averaging over a 1-cm moving window.

Gamma-ray attenuation was measured using a ^{137}Cs source with a 5 mm collimator and a 10 second count time. Calibration of the system was performed using a machined piece of aluminum that fits within a split core liner. There are 8 different thicknesses of aluminum on the calibration piece. Once filled with distilled water, the calibration piece and liner were placed under the ^{137}Cs source, and the number of gamma rays passing through each section over a course of 30 s was logged. The relationship between the measured counts per second [ln(cps)] and the known density of the aluminum/water mixture at each step is defined by either a 2nd order polynomial or a linear relationship. The difference between the two best-fit approaches is often minimal, and in this instance R^2 values for the polynomial fit and linear fit were 0.99973 and 0.99962 respectively. The simpler linear fit was used to convert cps to density where;

$$\ln(cps) = -0.063(Density * Thickness) + 9.7031$$

For p-wave velocity measurements, a pair of automated transducers sends a compressional wave through the sediment. The upper transducer is automatically lowered to a prescribed height, so that it is in contact with the sediment surface, and the travel time of the p-wave between the send and receive transducer is logged. Conversion of the travel time into a p-wave velocity requires calibration to account for delays introduced by the electronic circuitry and those associated with the passage of the p-wave through the liner. Calibration is performed by measuring the travel time through a section of split liner filled with distilled water at a known temperature. The temperature and thickness of the water is used to calculate a theoretical travel time, with the difference between the logged and theoretical travel time used to define a p-wave travel time offset (PTO). This was found to be 22.26 s. A 40 s gate and 30 s delay was used for calibration and logging.

Magnetic susceptibility was acquired with a Bartington point sensor. Magnetic susceptibility of whole cores is often collected using a loop sensor, which provides a spatially integrated susceptibility signal that encompasses the entire diameter of the core, with effective sensor lengths of generally 4–6 cm. The point sensor differs in that the area influencing the magnetic susceptibility measurement is much smaller, generally being constrained to the diameter of the sensor face (~2 cm), and a depth of only a few mm into the sediment. No mass or volume corrections were made to the Magnetic susceptibility measurements.

The ambient room temperature was recorded during logging of each section using a standard platinum resistance thermometer, placed on the bench beside the MSCL. All cores were allowed to equilibrate with room temperature overnight prior to logging.

Sediment thickness is a key parameter for calculating the density and p-wave velocity of sediments. The measurement of sediment thickness is achieved using two displacement transducers attached to the p-wave velocity housings. At the start of logging a reference height is set by manually lowering the p-wave transducers so that they are in contact with the sediment surface. This reference height becomes the maximum distance the transducers will travel in the vertical direction, and by default, the minimum sediment thickness recognized by the MSCL. In theory, intervals where the sediment thickness is larger than the reference height are recognized and recorded as the sediment surface stops the downward motion of the p-wave velocity transducers. However, in soft and easily deformable sediments, the resistance of the spring-loaded transducers is often higher than the sediment strength. In these instances, small deviations in down core thickness (i.e. 1–5 mm) are not recorded.

A reference height was set for each core and/or section at the beginning of logging.

The location of the reference height measurement was selected where the sediment thickness was minimal. The actual sediment thickness at this location was measured and recorded using a set of calipers, and subsequently used to process the data. Because of the uncertainty in the true sediment thickness (see below), processing was not done using the MSCL utilities program, but rather manually in Excel. Sediment thickness was calculated from,

$$Thickness_X = Thickness_R - \frac{CTD_X}{10} - \frac{CTD_R}{10}$$

where $Thickness_X$ (cm) is the sediment thickness (excluding the liner) at position 'X'; $Thickness_R$ (cm) is the caliper-measured thickness of the sediment where the p-wave velocity transducers were used to set the reference height; CTD (mm) is the logged '*core thickness deviation*'. Once the downcore sediment thickness was calculated, the bulk density and p-wave velocity of the sediments could be determined using the calibration data. Bulk density (ρ_B) was calculated from,

$$\rho_B = \frac{[\ln(cps) - 9.703]}{(-0.063 * Thickness_X)}$$

where *cps* were the logged *counts per second* for gamma rays passing through the sediment. Constants in this equation are from the linear relationship derived between the ln(cps) and the set of variable density standards used to calibrate the system.

The equation for calculating the p-wave velocity (Vp in m/s) was,

$$Vp = \frac{(10000 * Thickness_X)}{(TOT - PTO)}$$

where TOT is the logged total travel time of the p-wave passing through the sediments, and PTO the travel-time offset that accounts for delays in the electronic circuitry and the delay associated with the liner thickness. No temperature or salinity corrections were applied to the processed p-wave data.

Errors associated with the sediment thickness measurement impact the density and p-wave calculations oppositely, and both are sensitive to small (±1 mm) errors. For example, a 1 mm underestimate of the sediment thickness will cause the density to be ~0.05 g too high and the p-wave velocity ~41 m/s too low (Figure 6). In many instances, the derived sediment thickness was adjusted by a few mm to get reasonable agreement between the calculated density and velocity data (Table 2). For example, cores displaying very high bulk density (>2.0 g/cc) in intervals where the p-wave velocity was consistently below 1 400 m/s

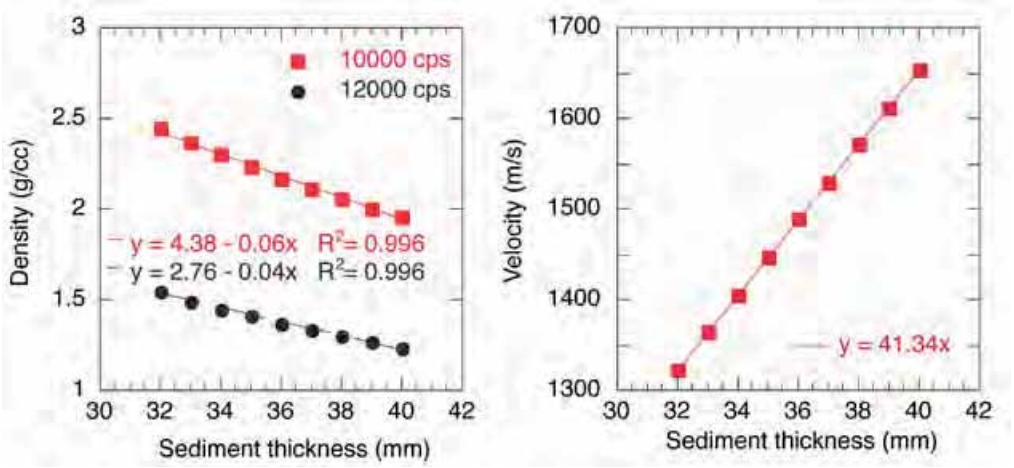

Figure 6. *Influence of core thickness deviations on the calculated bulk density and p-wave velocity. Error introduced into the calculated density is slightly non-linear, with larger errors associated with higher density (lower cps) sediments.*

Core	Sect.	Length (cm)	Depth of reference height (cm)	Measured thickness (cm)	Thickness in processing (cm)	Difference (cm)	General Comments
KC04	1	133	120.0	3.40	3.60	0.20	
KC04	2	80					
KC05	1	151	60.0	4.10	4.10	0.00	
KC05	2	94		3.70	3.70	0.00	
KC06-A	1	104	6.5	3.70	3.65	-0.05	
KC06-B	1	103	6.0	3.70	3.60	-0.10	
KC07	1	50	5.0	3.30	3.40	0.10	
KC08	1	40	6.0	4.10	4.20	0.10	MS sensor not in contact with core during logging run. Rerun with MS only, fixed in processed file.
KC09-A	1	21	4.0	3.40	3.70	0.30	
KC09-A	2	25					
KC09-B	1	21					
KC09-B	2	25	14.0	3.35	3.50	0.15	
KC10-B	1	74	60.0	3.70	3.70	0.00	KC10-A was run as KC10-B. Fixed in processed file.
KC10-B	2	10					MSCL records a large height difference beginning below 45-55 cm. This is not real, and arises from a change in liner height. Fixed in processed file.
KC10-A	1	74	36.0	3.50	3.40	-0.10	KC10-B was run as KC10-A. Fixed in processed file. No archived CC for KC10-B.
KC11-B	1	146	116.0	3.40	3.80	0.40	The screws on the vertical transducer mounting became loose and the stepper motor lost ability to track height changes. Section re-run. Original raw files overwritten.
KC11-A	1	146	9.0	3.30	3.45	0.15	
KC13-A	1	151	126.0	3.60	3.70	0.10	Footprint (i.e. someone stepped on the core) between 31-43 cm of section 1
KC13-A	2	76	14.0	3.45	3.65	0.20	Sections logged separately due to height difference
KC13-B	1	151	121.0	3.70	3.85	0.15	Sections logged separately due to height difference. RGB data avoids 2 large pebbles.
KC13-B	2	77	12.0	3.55	3.65	0.10	
KC14-A	1	72	41.0	3.80	3.80	0.00	
KC14-B	1	72	36.0	3.60	3.65	0.05	Two large pebbles (16-25 cm) and (50-60 cm) removed before logging.
KC15-A	1	131	115.0	3.40	3.80	0.40	
KC15-B	1	132	113.0	4.00	4.10	0.10	
KC16-A	1	39	13.0	3.40	3.40	0.00	

***Table 2**. Adjustment of derived sediment thickness in order to get reasonable agreement between the calculated density and velocity data.*

KC16-B	1	39	28.5	3.40	3.60	0.20	
KC17-A	1	146	39.0	3.85	3.85	0.00	
KC17-B	1	146	32.0	4.20	4.20	0.00	
KC18-A	1	148	129.0	4.00	3.90	-0.10	
KC18-B	1	148	112.5	3.20	3.60	0.40	
KC19-A	1	139	13.0	3.90	3.90	0.00	KC19-A was run as KC19-B. Also logged bottom-to-top. Both fixed in processed file.
KC19-B	1	139	8.0	3.70	3.90	0.20	KC19-B was run as KC19-A. Fixed in processed file.
KC22-A	1	115	84.0	3.50	3.50	0.00	Sediment surface too far below liner for accurate height measurements between 56-93 cm.
KC22-B	1	115	89.0	3.70	3.70	0.00	
KC23-A	1	36	36.0	3.50	3.50	0.00	
KC23-B	1	36	36.0	4.30	4.30	0.00	
KC24-A	1	137	18.5	3.60	3.80	0.20	Poor quality core, full of pebbles.
KC24-A	2	24.5					
KC24-B	1	137	26.0	3.50	3.80	0.30	
KC24-B	2	24.5					
KC25-A	1	78	12.5	4.00	4.00	0.00	
KC25-B	1	78	17.5	4.10	3.80	-0.30	
KC26	1	106	28.0	3.90	3.90	0.00	
KC27	1	52	16.0	3.80	3.80	0.00	

(the velocity of water) were rectified by increasing the sediment thickness by a few millimeters. Adjustments to the reference sediment thickness were facilitated by comparing downcore variations in density and p-wave between archived halves taken from the same Kasten core. Where necessary, further improvements to the adjusted sediment thickness can be achieved by directly measuring the sediment thickness every 1–2 cm.

The processed data files include all the raw data required to calculate the sediment thickness, density and p-wave velocity. For presentation purposes, the data was cleaned, providing two additional columns in the data files. Bulk density values of <1.15 g/cm^3 were replaced in the cleaned data column by a value of –999. Similarly, for p-wave velocity, only values >1 450 m/s and with a signal amplitude of >40% were retained.

Results from core logging (showing only the cleaned data) are presented for each archived half in Appendix II. The lithologic plots in I also contain MSCL data (magnetic susceptibility and bulk density). Where two archived halves exist from a single Kasten Core, the measurements are overlain. Large variations between the two archived halves from the same core sometimes exist. Differences in magnetic susceptibility generally arise from non-uniform distribution of pebbles/rock fragments, or significant anomalies in sediment thickness (holes/dropstones) while differences in bulk density give a relative indication of sample disturbance and/or core thickness logging errors.

Index properties

Index property samples, commonly used to directly determine the bulk density, porosity, water content and grain density of sediments, were taken using two 9.8 cm^3 stainless steel rings. The sample bulk density was calculated shipboard by measuring the wet mass of the sample and dividing this by the volume. However, motion of the ship, even during coring operations, resulted in a digital balance accuracy that was, at best, within ±1 g of the true sample weight. Sample weights ranged between 29 and 40 g for the wet samples, indicating a ±2.5–3.5% error. Additional errors can arise from incomplete filling of the constant volume sampler or overfilling the ring by compressing the sediment during sampling.

Shorebased analysis of the dried samples using a helium displacement pycnometer will provide accurate data on the grain density of sediments from different lithologic units, and is independent of sampling and shipboard measurement errors for the bulk density measurement. The grain density is used in conjunction with either direct or MSCL derived measurements of sediment bulk density to determine sediment porosity from basic phase relationships,

$$\phi = (\rho_G - \rho_B)/(\rho_G - \rho_F)$$

where ϕ is the porosity, ρ_G is the grain density, ρ_B the bulk density and ρ_F the pore fluid density.

Shear strength

The undrained shear strength (Su) and unconfined compressive strength (UCS) were measured on the scraped surface of each Kasten core using a hand-held shear vane and pocket penetrometer respectively. Measurements were made prior to sampling of the archived halves, and approximately every 10–20 cm downcore. Measurements near the base of the Kasten core and in the core catcher material were sometimes omitted due to clear sample disturbance.

The hand held vane shear is equipped with three different diameter blades. The largest was used for the majority of measurements, as it is most sensitive for low strength sediments. The force required to reach failure is read directly from the instrument face, and is given in kg/cm^2. One full rotation of the standard (medium) blade is equal to 1 kg/cm^2, while a full rotation of the large blade is equal to 0.2 kg/cm^2 (where 1 kg/cm^2 = 98.067 kPa).

The pocket penetrometer measures the unconfined compressive strength, which is equal to twice the undrained shear strength. A 25 mm diameter (1.23 cm^2) foot was

used on the penetrometer, and the dial reading (in kg) after the foot was pressed into the core surface was used to calculate UCS (kg/cm^2). In many instances, the presence of pebbles in the sediment made acquiring reliable vane shear measurement difficult. In such instances the smaller area of influence exerted by the penetrometer provided more accurate strength readings. Where both penetrometer and vane shear measurements are taken on the same core, there is generally good overall agreement between the measured and derived shear strengths, but generally, the penetrometer readings provide a slightly higher strength estimate. Shear strength measurements are displayed alongside the lithologic columns in Appendix I.

Oceanography

Moorings

Two moorings were deployed in the Little America Trough of the eastern Ross Sea. The moorings are identical in design and each consists of dual Benthos acoustic release, 3 Sea-Bird SBE-37 Microcats, and 2 Nortek Aquadopps 3000 (Figure 7). The acoustic releases were tested and armed using a Benthos Universal Deck Box UDB-9000M provided by the University of Gothenburg.

CTD/LADCP measurements

Profiles of temperature, conductivity, dissolved oxygen, and currents were measured using equipment property of Texas A&M University. The basic CTD package consisted of a Sea-Bird Electronics SBE911+ CTD body and deck unit system fitted with dual ducted conductivity-temperature sensors paired with pumps, and a single SBE-43 dissolved oxygen sensor. A downward-looking Teledyne RD Instruments 300 kHz Workhorse Sentinel Lowered ADCP was used to profile currents. This instrument comes with its own internal compass and tilt sensors and was calibrated in McMurdo with the same battery pack used during the cruise. Water samples were drawn from 12 10-liter Niskin bottles using a 24-position SBE-32 Carousel sampler triggered through the Sea-Bird 11+ deck unit. To guide the approach to the ocean floor a Teledyne Benthos 200 kHz sonar altimeter was mounted on the lower frame of the rosette. Most profiles reached to within 10 m of the bottom.

CTD data were acquired and processed using Sea-Bird Seasave software, version 7.18 c on a laptop computer running Windows XP Professional. Immediately after each cast all CTD/LADCP raw data outputs were copied over to the ships network. Processed CTD data files were made available to all science staff generally within an hour of each cast completion.

The surface pressure readings from CTD sensor was recorded on the log sheet before each deployment. The rosette was initially lowered to 10 meters for approximately 2 minutes to soak the CTD sensors, and after the pumps turned on and the oxygen sensor signal stabilized, it was returned to the surface before starting the actual cast. To best accommodate LADCP and CTD descent rates, the winch payout and hauling rate was 60 m/min for most of the down cast. On approaching within ~25 m off the bottom, as determined from altimeter, the winch was slowed to 30 m/min. On the way up, the rosette was stopped to close the Niskin bottles at depths selected during the down-cast to resolved main water column features. E.g. target levels included extreme values in T and S, regions with homogeneous layers for salt control, and layers near the sea surface and sea floor. Once on deck, water samples were collected from the Niskin bottles for salinity and oxygen-18 isotopes measurements. Salinity analysis was done primarily to standardize conductivity measurements derived from the CTD sensors. Analysis of oxygen-18 samples will be carried out at TAMU.

Salinity calibration:

118 water samples were drawn from the rosette for onboard analyses of salinity. Autosal Model 8400B provided by the University of Gothenburg located in highly a

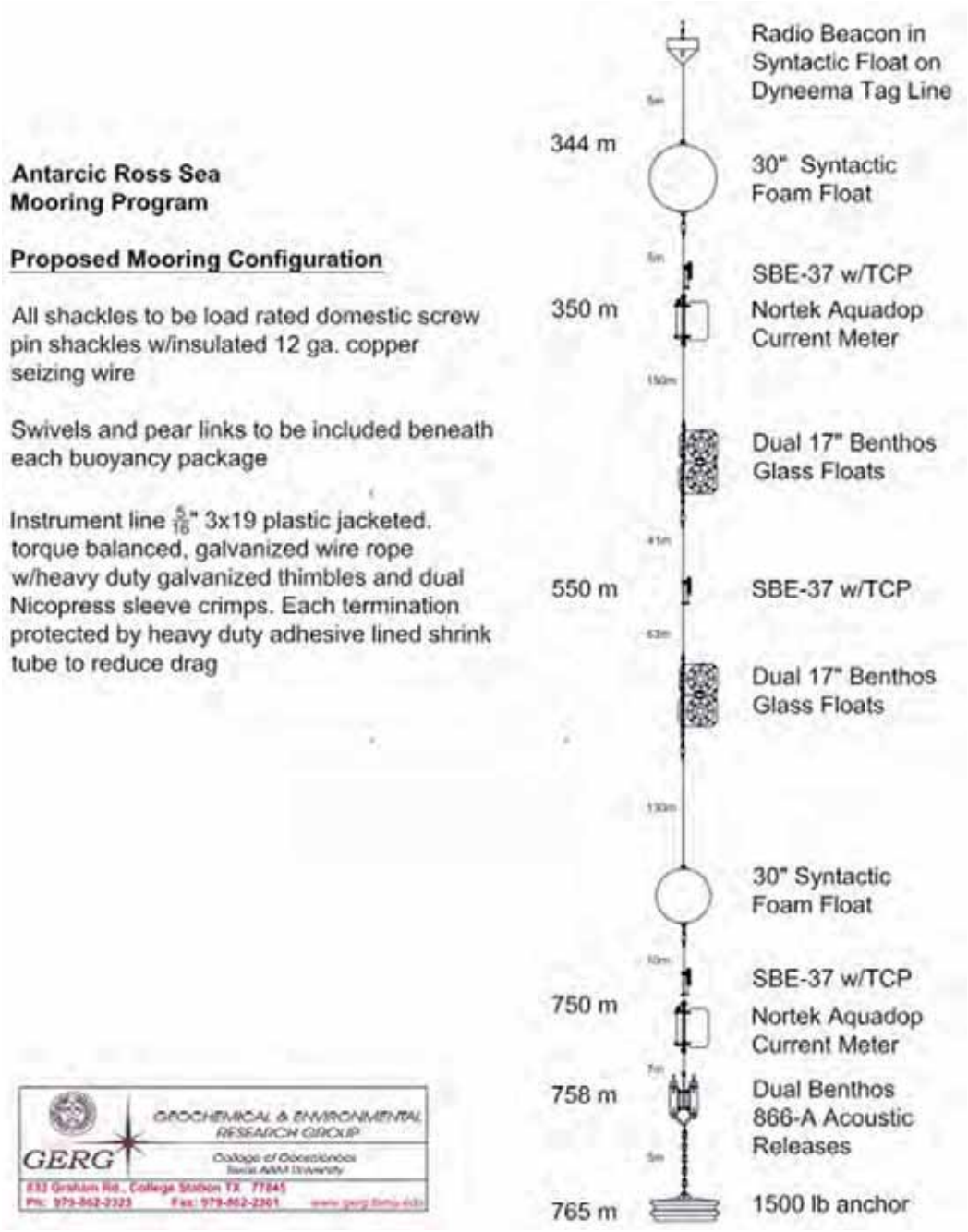

Figure 7. *Schematic of mooring design.*

stable air-conditioned lab, was used for salinity measurements. Calibration was performed at the beginning of each run with batch P149 of IAPSO Standard Seawater from October 2007.

Error in salinity remained constant throughout the cruise (Figure 8). Salinity error, denoted as DeltaS, is reported as rosette salinity minus CTD salinity. Mean Delta S was ~0.0099 with a standard deviation of 0.0066. For the estimation of this error, 112 points out of 118 (95%) were used. Points excluded were greater than 2 times the standard deviation of the mean error.

Ecology

Water sampling for ecological studies
We sampled 10 sites along the East Antarctic coast from McMurdo (S77045.2´; E163008.8) to Ferrero Bay (S73023.4; W102048.9´). Sampling was performed with a 20 L Niskin sampler at 2, 10, 20, 40, 80 and 120 m depth. From each level the water was analyzed for nutrient and chlorophyll levels, as well as zooplankton and algal taxonomy and numbers. A light and temperature profile was also taken at each site with a light meter (Biospherical Instruments, San Diego, USA).

Experimental study on marine animals
In order to test if the animals change strategy when not allowed to migrate and when released from predator cues, we performed a mechanistic experiment onboard *Oden* using copepods gathered in Pine Island Bay. The experiment consisted of 12 aquaria with seawater and copepods put under UV

Sensor	Serial number	Calibration date
Pressure (on SBE9 body)	40371	27-Feb-95
Temperature (SBE3)	783, 800	6-Jan-06
Conductivity (SBE4)	101, 382	6-Jan-06
Dissolved Oxygen (SBE 43)	431498	9-Sept-08

***Table 3**. Details of the CTD 911+ sensor set.*

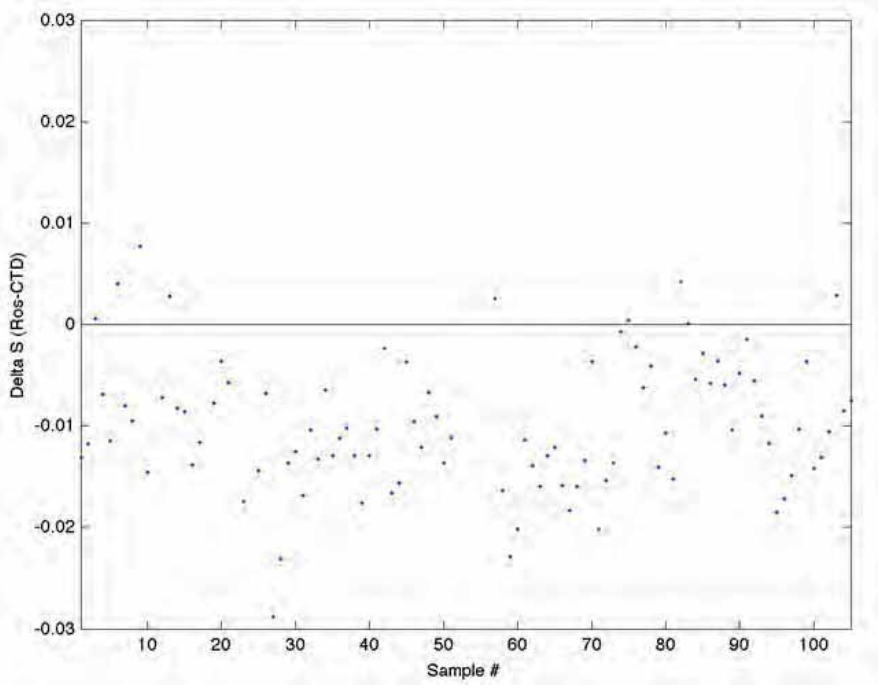

***Figure 8.** Salinity difference, DeltaS (Rosette-CTD), vs. Sample number for conductivity sensor.*

lamps. Each aquarium was covered with Plexiglas allowing, or not allowing UV to penetrate. The experiment was run for ten days and each treatment was replicated six times.

Lake studies

Our freshwater study was performed 1–2 February 2010 in Lakes Fryxell and Hoare and we used a Jiffy drill to enlarge holes previously drilled by the LTER project above the deep site of the lakes positioned at S770 36,620´; E163 0 08,755' and S77 0 37,661'; E162 0 54.574', in Lakes Fryxell and Hoare respectively. All sampling equipment were kept dry for at least a month and rinsed in alcohol (70%) prior to sampling and also between lakes, in order to reduce the risk of spreading organisms to these pristine systems. From the hole in the ice we sampled along a depth profiles at 1, 4, 9 and 15 m depths. In Lake Hoare the profile was taken once, whereas in Lake Fryxell we performed a diurnal study (at the times: 16, 22, 04 and 10). With a water sampler (Limnos TM) 20 L of water were taken up from each depth, put into buckets. From the 20 L sample we took sub-samples for phytoplankton enumeration (preserved in Lugol´s solution), conductivity and temperature (Ecoscan Con 6, Eutech Instruments, Vernon Hills, USA). Then the 20 L sample was filtered through a 50 µm net and zooplankton larger than that size were retrieved on the net. These were rinsed into a 50 ml centrifuge tubes and preserved in Lugol´s solution for later enumeration using a dissecting microscope. From the 50 µm filtered water, sub-samples for seston nutrient composition (carbon, nitrogen and phosphorus) were taken out with a syringe and filtered through a GF/F filter (25 mm, Whatman). Prior to the sampling syringes, filter holders and filters for P analysis were acid washed and all filters were combusted at 550 °C. The sample sizes for N, P and C analyses ranged between 80 and 150 ml. Sub-samples for analysis of chlorophyll a (range 0.2–1.5 L) were then taken out and filtered through GF/F filters. Filters were stored at –20 °C until analysis onboard *Oden*. Light and temperature profiles were taken from surface to 18 m depth with a light meter (Biospherical Instruments, San Diego, USA), measuring at wavelengths

Niskin sampler deployed from the starboard side of Oden

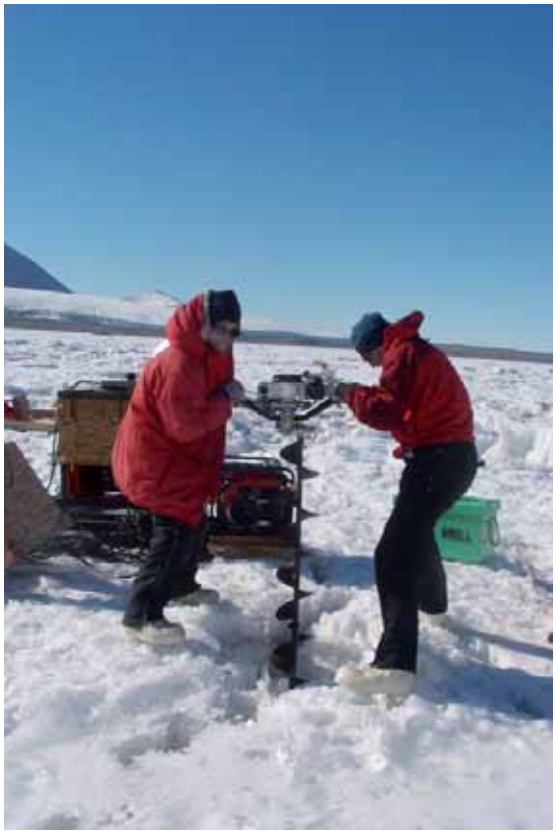

Drilling a hole through several meters of ice is challenging. With logistical support from NSF we were able to sample two lakes in the Dry Valleys.

400–700 (PAR) and 340 nm (UV-A) and 320 nm (at the border between UV-A and UV-B).

Preliminary Results

Marine geology and geophysics

Multibeam bathymetry

The first area that was multibeam surveyed was McMurdo Sound since *Oden* was going back and forth clearing the passage from ice to the US base located on Ross Island. Several passes over the same track allowed gridding at a resolution of 15 × 15 m grid cells in water depths even deeper than 500 m (Figure 9a and b). The data revealed so-called recessional moraines, a sign of that the ice sheet retreated. These moraines are developed perpendicular to the ice flow direction (Figure 10).

After *Oden* finished the mission of clearing a passage to McMurdo and escorted the US cargo ship American Tern into relatively safe waters beyond the worst pack ice, we began our journey towards Pine Island Bay. The multibeam was operated continuously along this transit with an opening angle set between 65 and 60°. The reason for narrowing the swath is that the outer beams are noisy and generally suffer from an offset making the outer parts of the swath appear like a "railroad track". It is clearly seen in figure 11 how the noisy outer part is excluded when narrowing the beam, however, on the cost of narrower swath width. The route towards Little America Trough, where two moorings were going to be deployed before we could go to Pine Island Bay, took us along the front of the Ross Ice Shelf, where catabatic winds had cleared the sea ice. The weather was calm implying that high quality swath bathymetry could be collected. In fact, the swath bathymetry from this transect required a minimum of post-processing. The routine of throwing XBTs for sound velocity correction of the multibeam data had begun already in McMurdo Sound (see the oceanographic section for a map with XBT/XSV/XCTD/CTD locations). Glaciogenic features dominates the seafloor morphology in front of the Ross Ice Shelf, in particular Mega Scale Glacial Lineations (MSGL) (Figure 11). In the area of Little America trough we mapped regular undulating features with relief of about 1 m and constrained to some MSGL (Figure 11). These undulating features make the seafloor appear with a corrugated pattern. Identical features have been mapped previously in the western Ross Sea (Anderson, 1999) and they will be the subject for our further analysis.

Pine Island Bay was reached February 17. The wind was calm and there were practically no sea ice at all in the bay allowing us to map along pre-defined survey lines. Some multibeam swaths had previously been collected in our area of interest. These provided a general idea of the extension of the Pine Island Trough. The inner part of the trough is rather well mapped while the

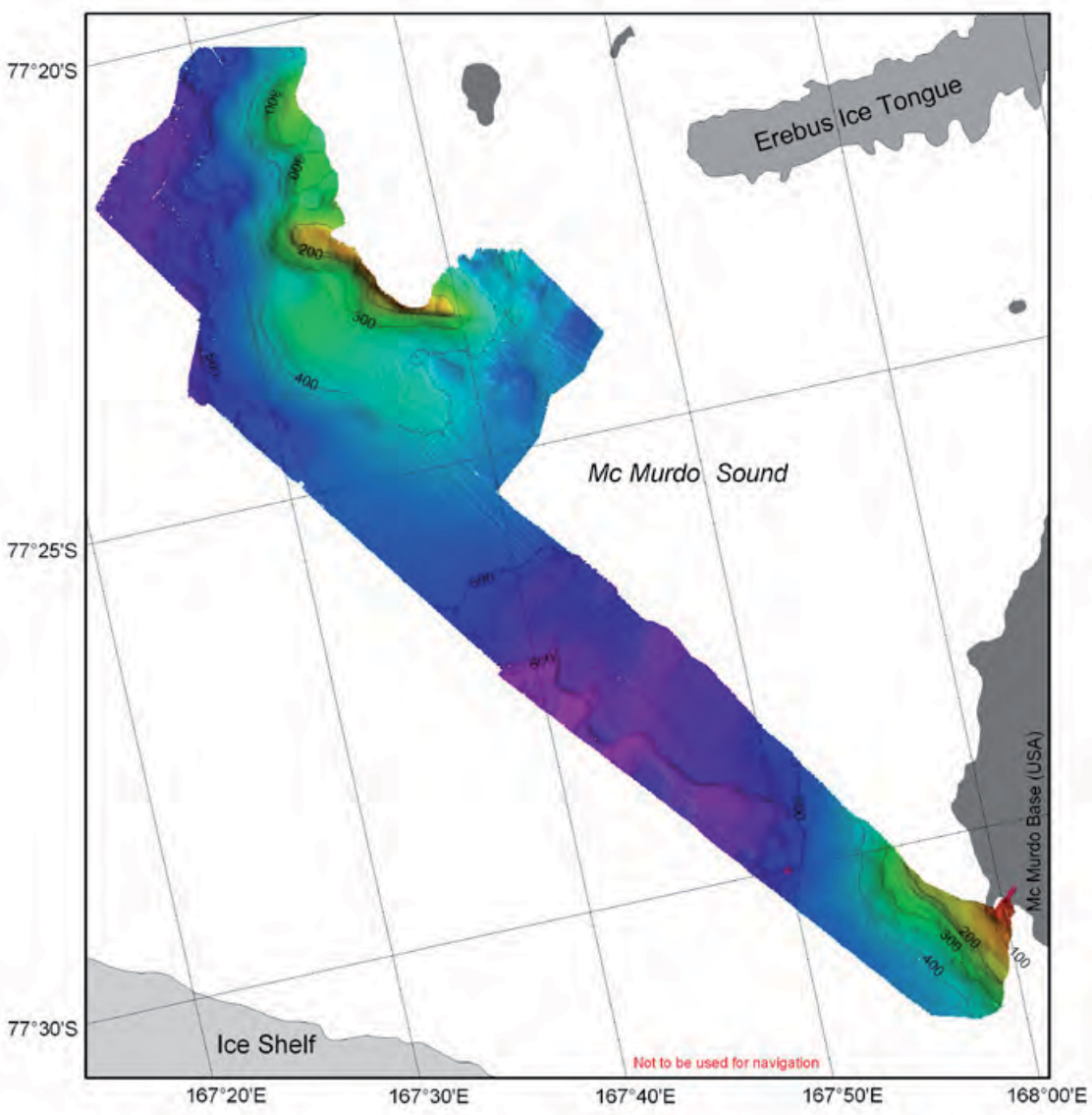

Figure 9a. *Swath bathymetry of McMurdo Sound collected while Oden was clearing the passage from ice to McMurdo Station.*

outer seaward part, which was our main area of interest, is poorly mapped. Our survey began with some overview lines crossing the trough. This was necessary in order to gather information to begin the coring program which aimed to identify ice stream grounding line wedges in the trough and core in front, on, and behind them to derive a chronology of the deglaciation. After the overview lines we completed a full survey could begin where mapping was done with 20–50% overlapping swaths. The area of interest was divided into four subareas, the first three were defined in between the crossing overview tracks and the last along the trough axis since we realized that we not were going to be able to fill the all the areas between the trough crossing lines (Figure 12). The final result is shown in figure 13 in the form of shaded relief derived from a 50 × 50 m resolution grid. The data is, however, processed to a higher resolution (mostly 20 × 20 m) allowing more detailed maps to be generated.

MSGL are prominent in the mapped

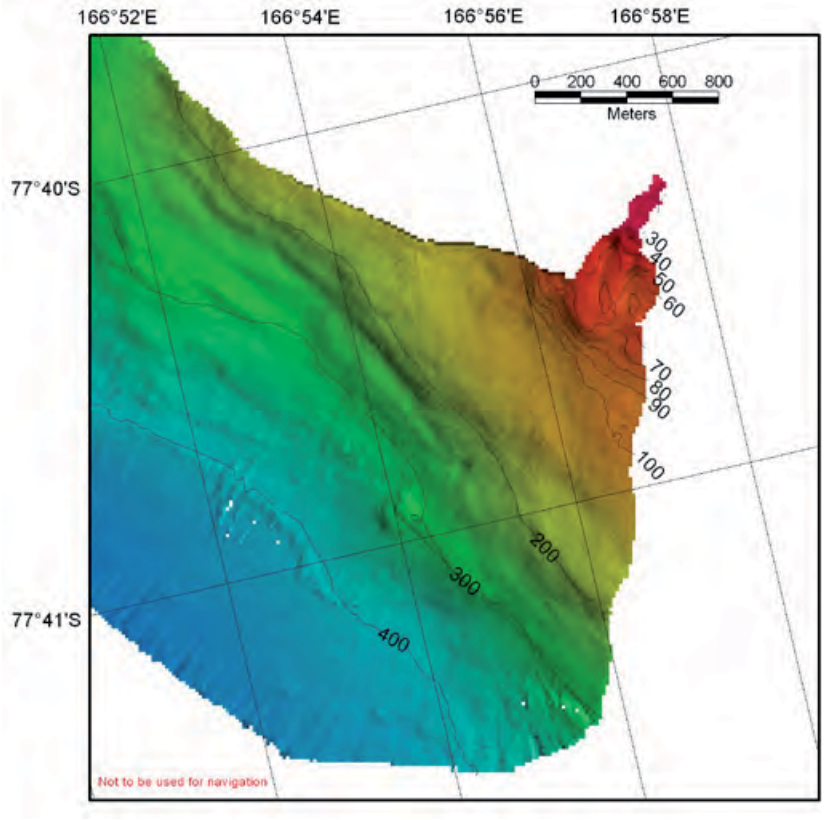

Figure 9b. *Detailed map of the mapped area closest to McMurdo ice pier.*

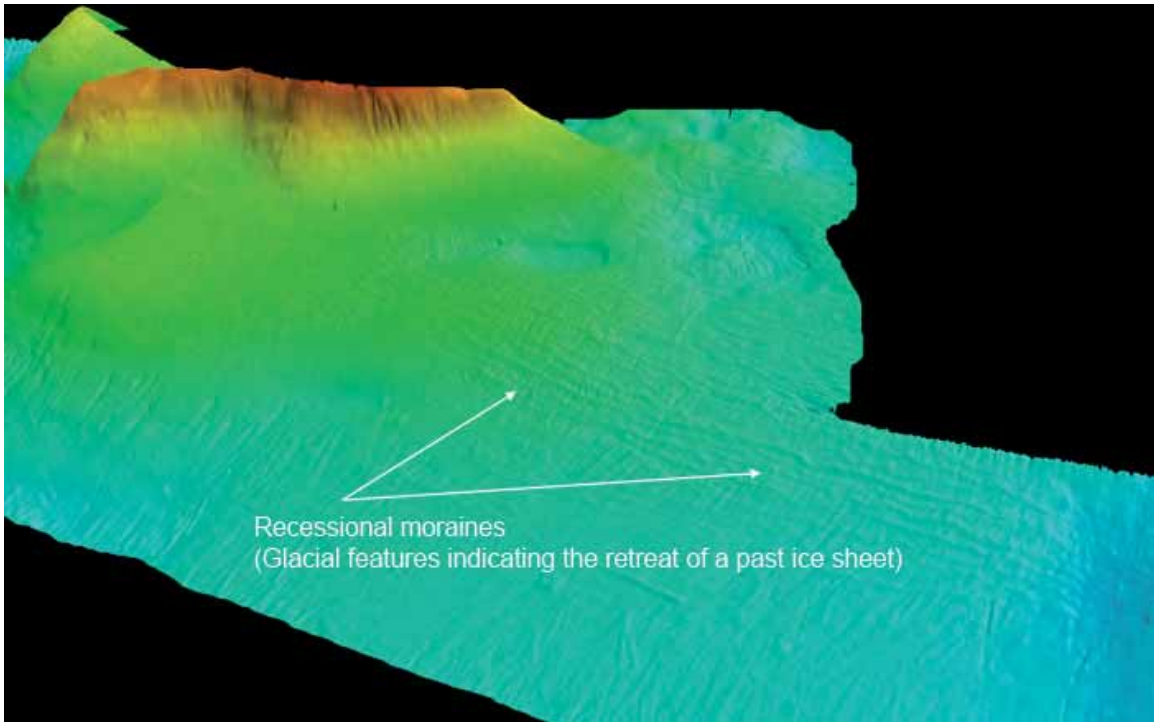

Figure 10. *3D view of the swath bathymetry collected in McMurdo Sound. The image shows recessional moraines.*

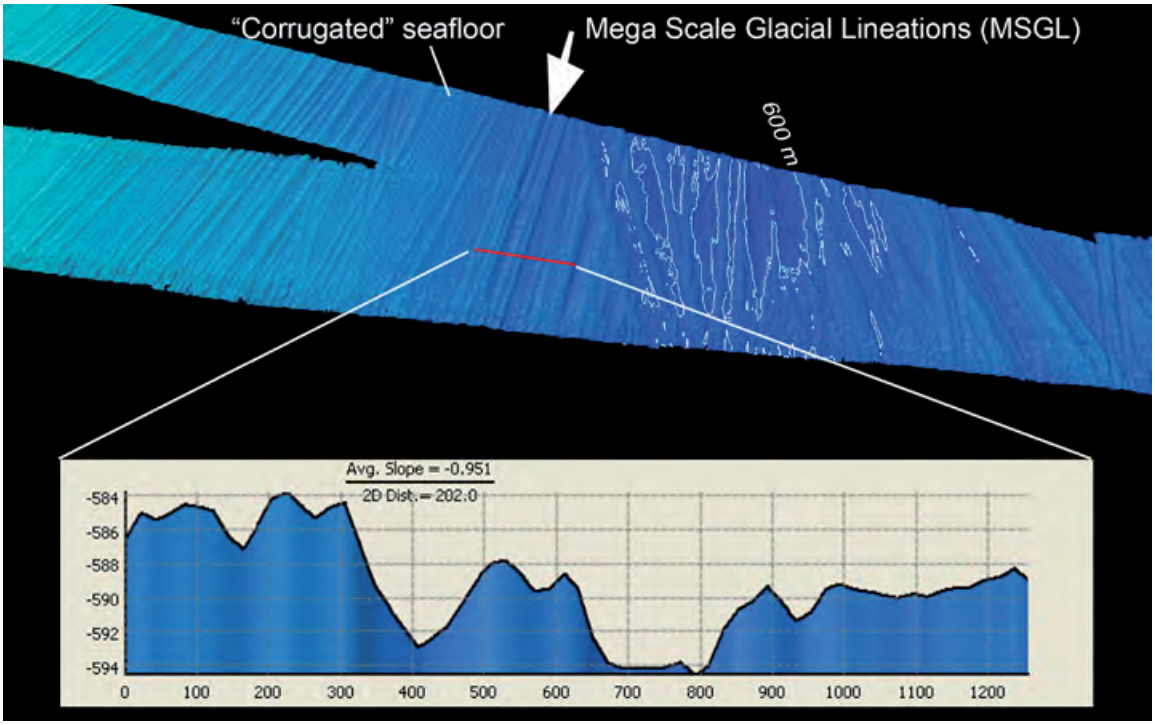

***Figure 11**. Swath bathymetry from the area of Little America Trough. The shown part is from processing tile ROSS-AMUND-II shown in figure 2. The upper swath is acquired with an opening of 60° while the lower is acquired with 65°. Note the somewhat rougher appearance of the outermost part of both the port and starboard side of the swath when an opening of 65° is used. This problem is vastly accentuated in bad weather conditions. Up is south and thus towards the Ross Ice Shelf.*

area at water depths below approximately 670–700 m. There is a pronounced grounding line wedge at about 72°50'S that rises more than 50 m in the topography. The surface of the wedge located shallower than 670 m is completely obliterated by iceberg scours (Figure 13). Similar features to those mapped in the eastern Ross Sea that gives the seafloor a corrugated appearance are also mapped here.

The wind picked up very rapidly the 24th of February and waves built up almost instantly. We decided to head for Burke Island located in Pine Island Bay to map and potentially core some areas of interest. However, the area off the southwestern shores of Burke Island did not provide enough protection for the swell so we decided to instead go to another target area; Ferrero Bay. This bay forms an over-deepened fjord and there are traces in the sea floor suggesting that an ice stream extended out from the bay in the past and possibly joined up with the large Pine Island ice stream. There is also a possibility that the inner part of the fjord could contain sediment records for higher resolution climate studies. There exist, to our knowledge, one multibeam track leading in and out of Ferraro Bay. Mapping was carried out along this existing track for two reasons: 1) To successively build upon the existing bathymetric database, and 2) by following the outer edge of the existing multibeam swath into Ferraro Bay unknown potential hazardous shallow areas could be avoided. Figure 14 shows a map compiled from the multibeam data collected in Ferrero Bay. These data have only been subjected to a first rough cleaning and will be further processed. However, since there were practically no sea ice or wave motion in Ferraro Bay, the collected data was of high quality.

Chirp sonar profiling

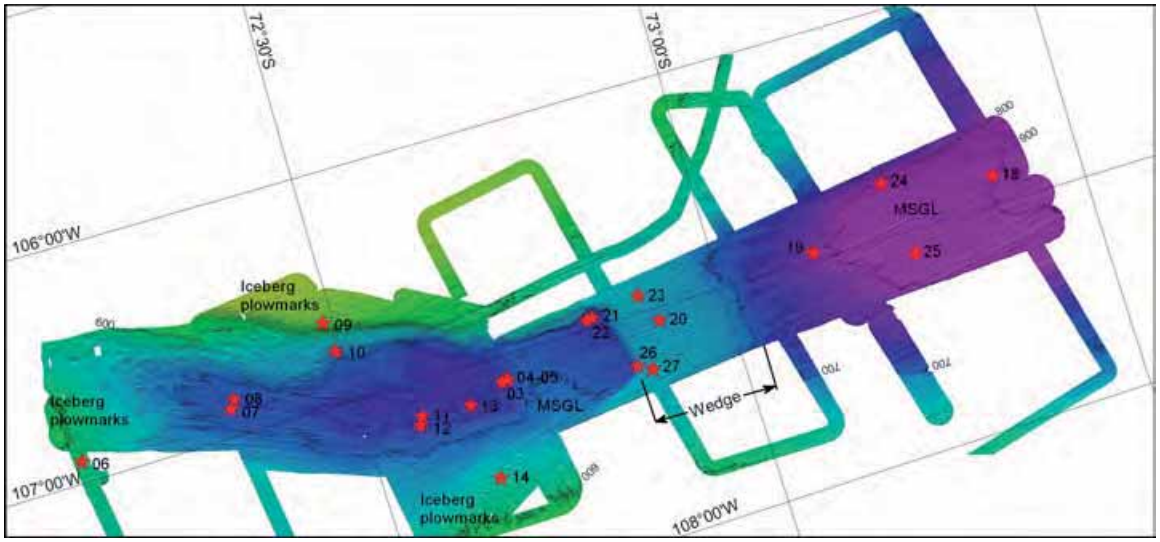

Figure 13. *Swath bathymetric image derived from the Pine Island Bay survey. The most prominent morphological provinces are labeled. The red stars are core locations (see coring results below).*

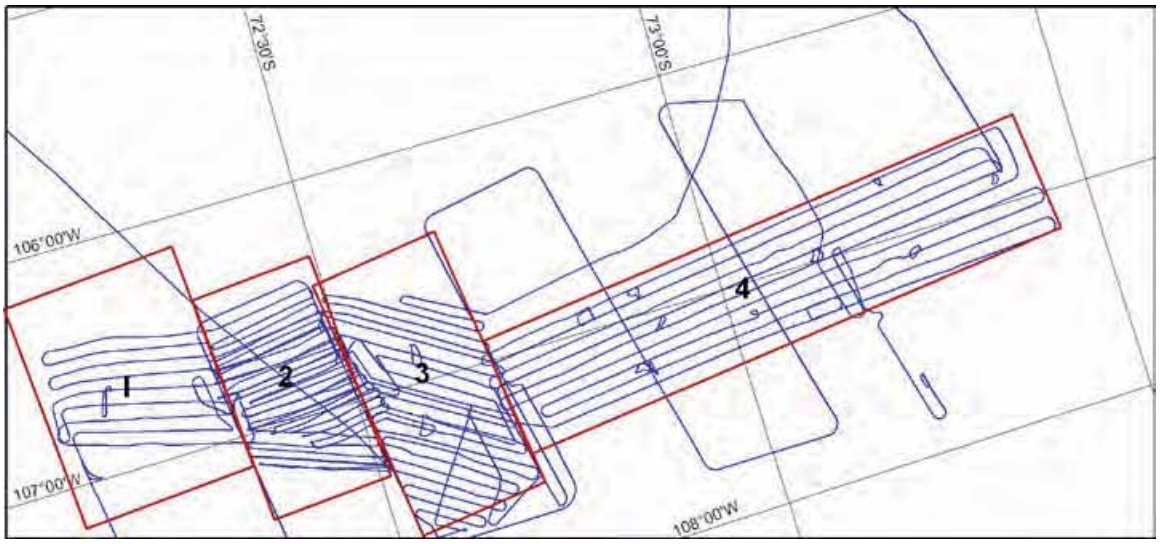

Figure 12. *Survey of the outer part of the Pine Island Bay Trough. The survey was divided into four sub-surveys represented by the labeled boxes in red. Box number 2 was surveyed in bad weather with heavy seas why several lines had to be run twice.*

The SBP120 chirp sonar system was run along with the multibeam continuously during the entire cruise. The transit from McMurdo to Pine Island Bay took mainly place over the continental shelf, which generally is characterized by a thin drape, sometimes less than 1 m thick, of unconsolidated sediment overlying diamicton. Typical profiles of the Pine Island Bay Trough are shown in Figures 15 and 16. The locations of the profiles are shown in Figure 17. As soon as we left the continental shelf the chirp sonar provided sometimes more than 100 ms TWT penetration in the sediment stratigraphy. Figure 18 shows a profile acquired at about 129°W off the continental slope. Appendix III contains subbottom profiles near all the coring sites.

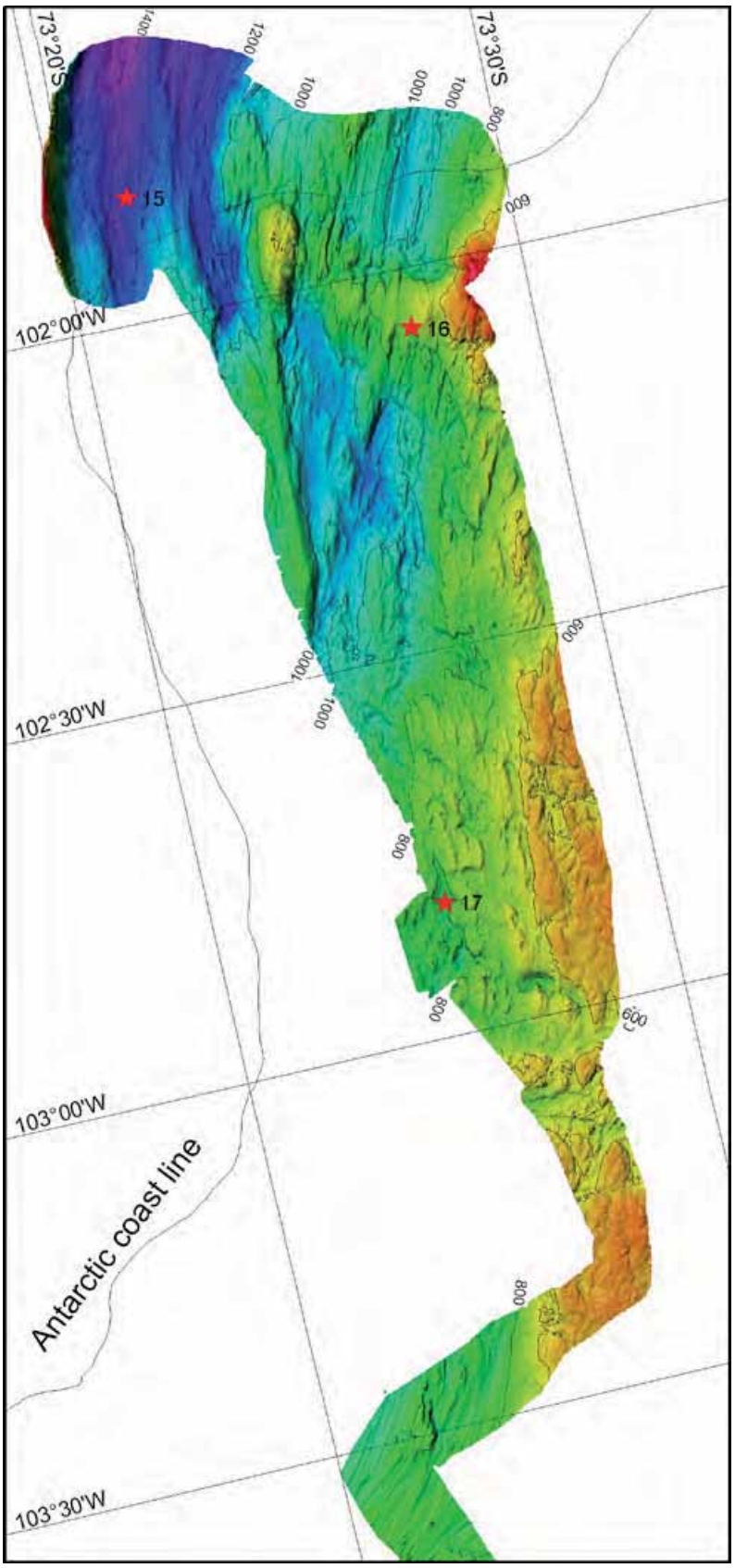

Figure 14. *Mulitbeam bathymetry collected in Ferrero Bay. The red stars are coring locations.*

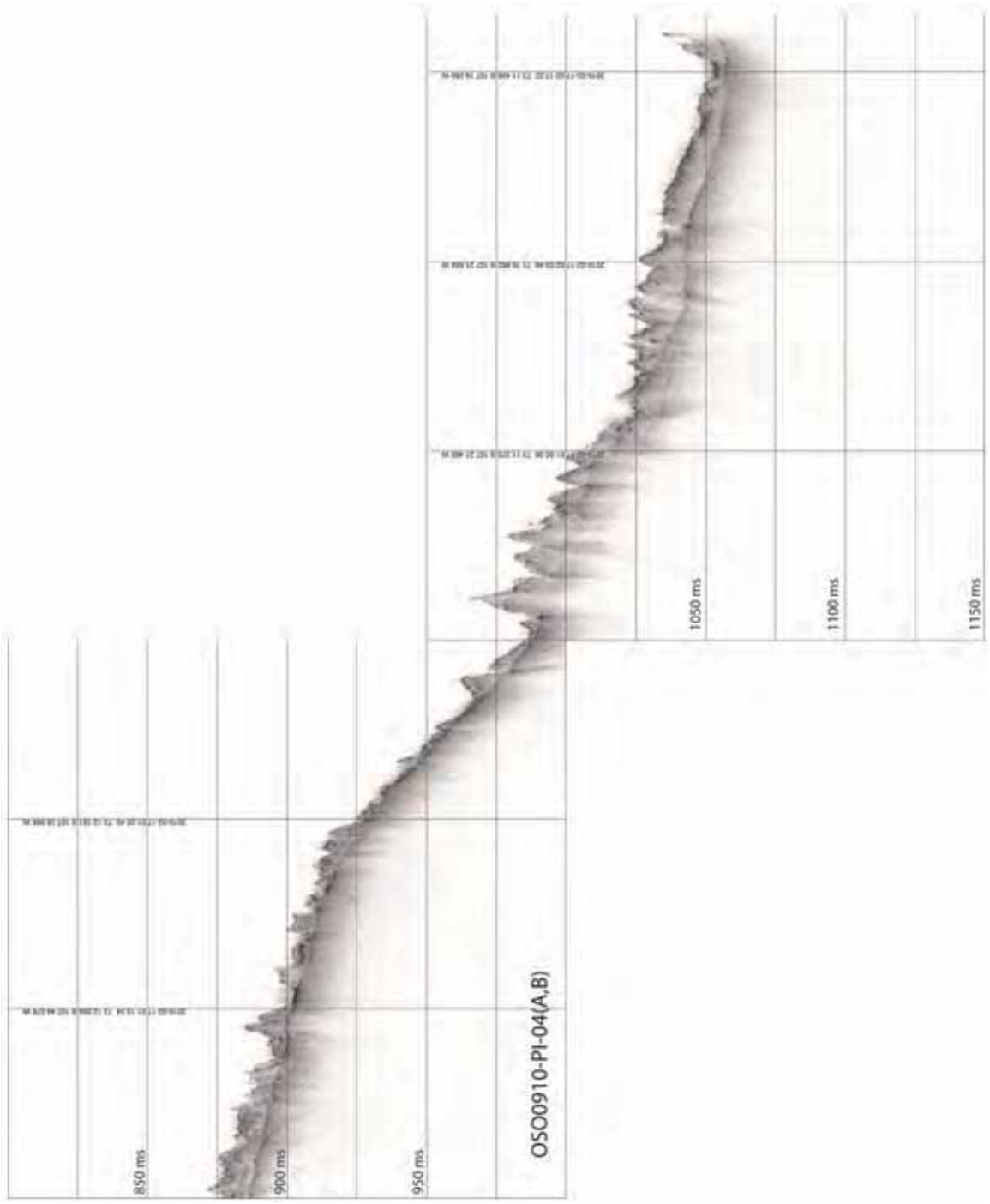

Figure 15. *Profiles OSO0910-PI4 A and B spliced together. The profile location is shown in Figure 17.*

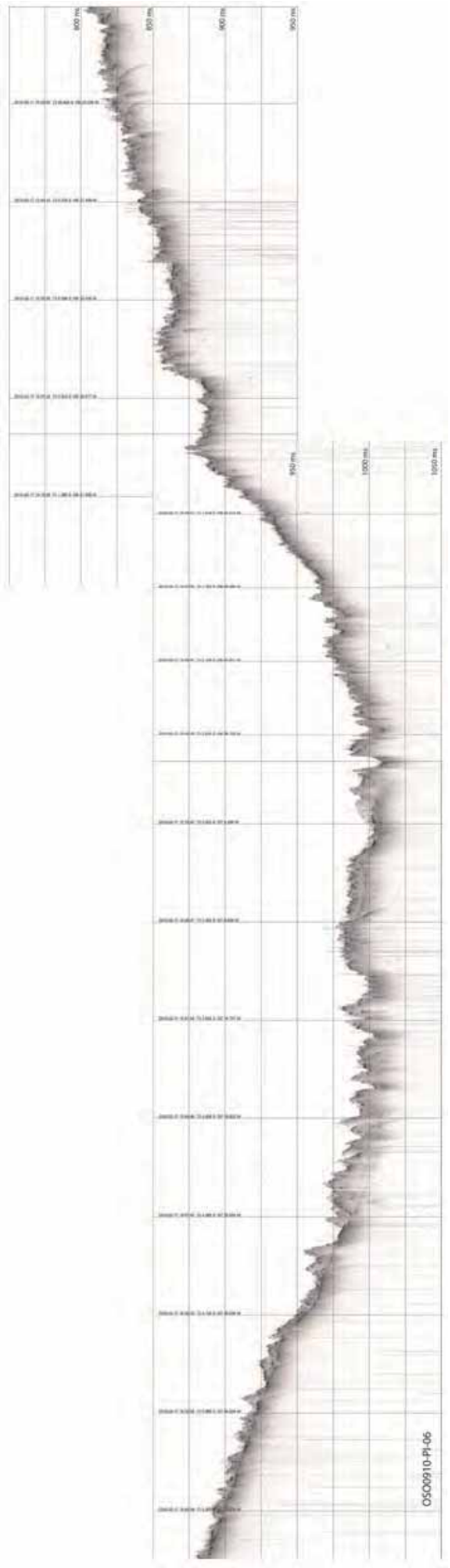

Figure 16. *Profile OSO0910-PI-06 across the entire Pine Island Trough. The profile location is shown in Figure 18.*

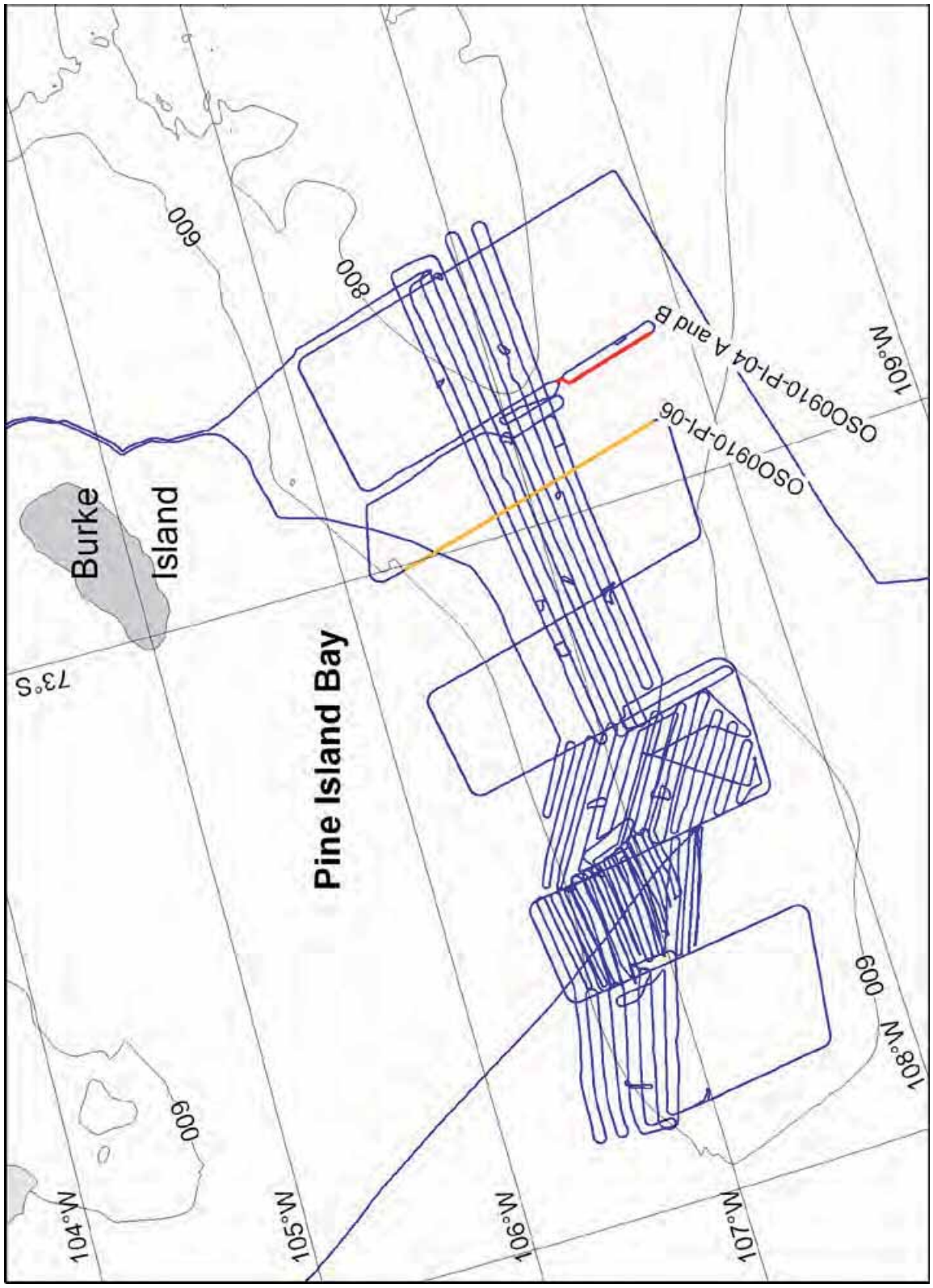

Figure 17. *Locations of the chirp sonar profiles shown in Figures 16 and 17.*

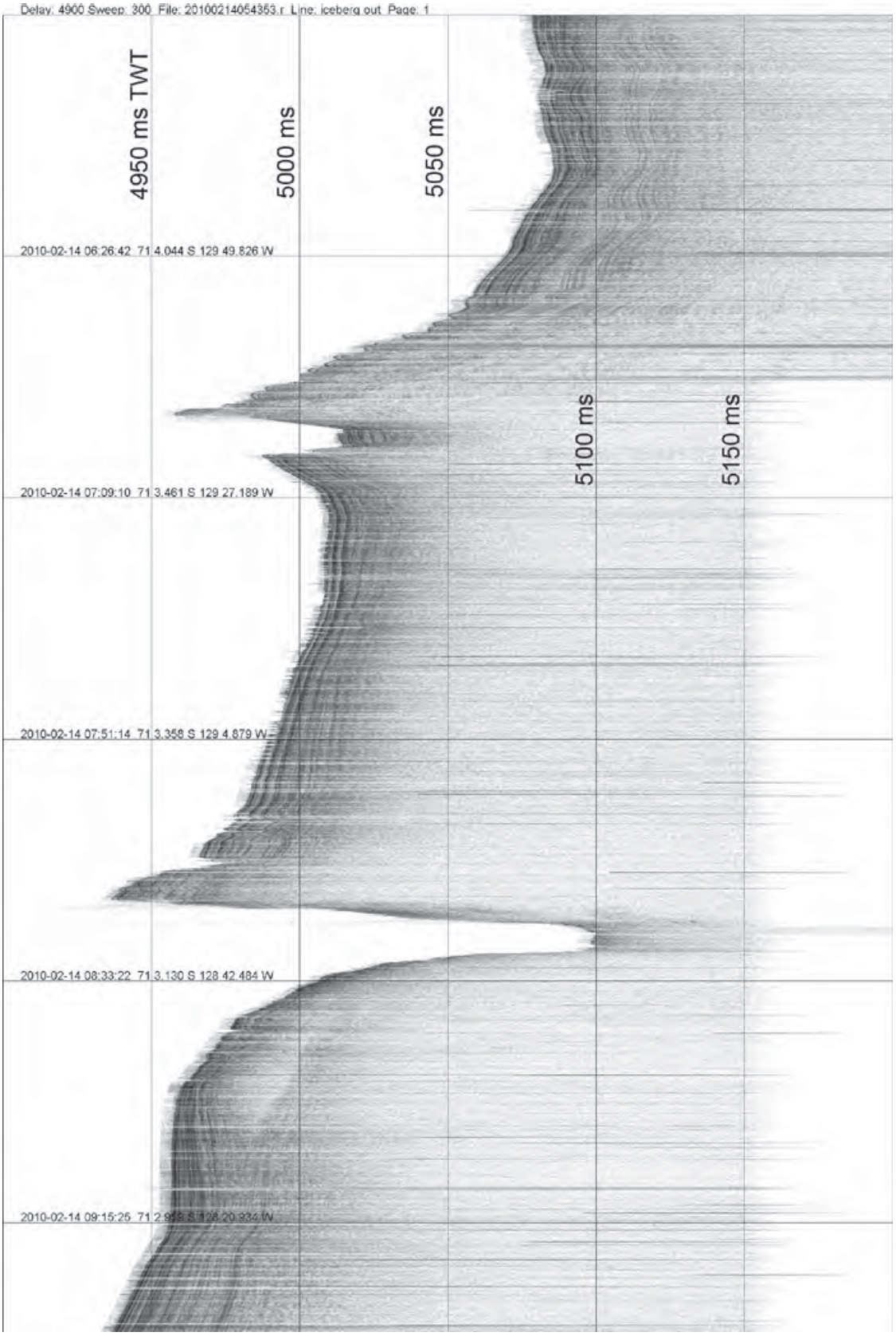

Figure 17. *Locations of the chirp sonar profiles shown in Figures 16 and 17.*

Sediment coring

In total 27 coring stations were occupied and of these 23 were successful in retrieving sediments (Figure 19). In general, post-LGM sediments are quite thin in the central and outer Pine Island trough. Previous coring operations have revealed thicker sediments in the inner trough, but these are confined to deep basins and are mainly composed of a single sediment facies consisting of brown clay with rare dropstones (Lowe and Anderson, 2003). The generalized stratigraphy of the central and outer trough consists of, from bottom to top, dark gray till and/or proximal glacimarine sediments, brown glacimarine sediments with an ice-rafted component that decreases upwards in the unit, and an upper unit consisting of brown clay with minor ice-rafted material. A few cores exhibit alternation between the upper two units, but all cores have surface brown clay units. This stratigraphic progression clearly reflects increasing distance from the grounding line as the ice sheet retreated from the continental shelf. Contacts tend to be relatively sharp, which implies that the grounding line of the ice sheet may have back-stepped across the trough. Future work will focus on the nature and timing of ice stream retreat in the bay.

Samples for foraminifera were taken every 10 cm from all cores except KC-5, where they were taken every 20 cm. Surface samples were taken at all sampling sites. In general, the core tops are rich in foraminifera, with benthic agglutinated forms dominating at sites from greater water depth. In

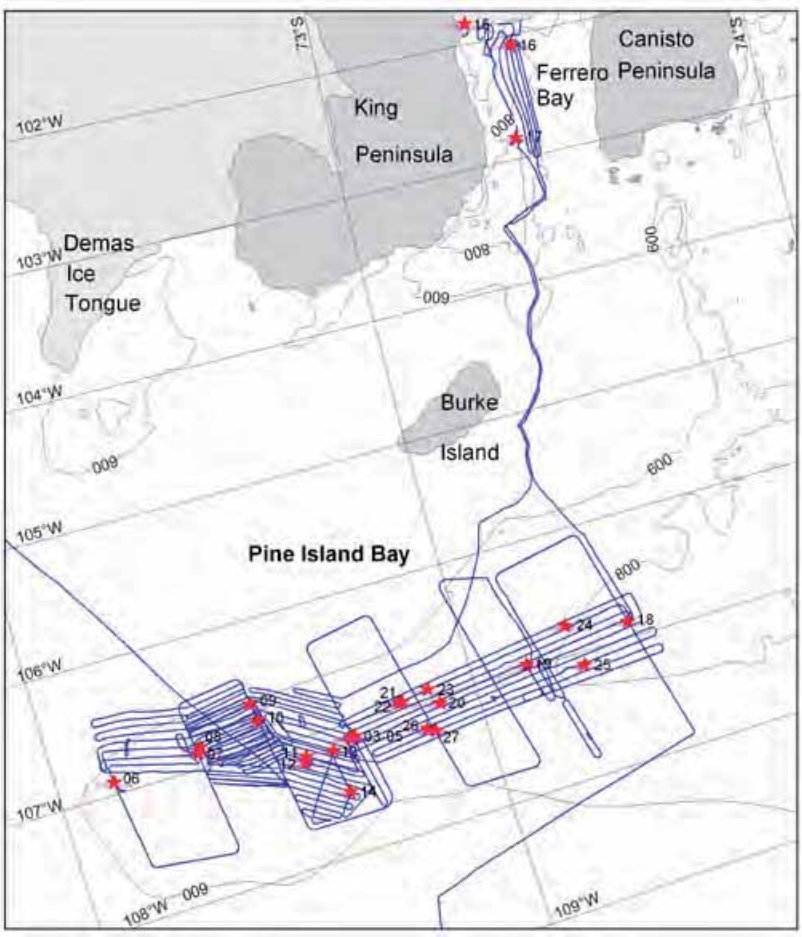

Figure 19. *Coring stations. Only the number of each coring station is shown. The full names follow the convention OSO0910-KC-##, where ## is the unique number plotted on the map for each station beginning with 1 for the first. KC means Kasten Corer. Note that even the stations were we did not recovered any sediments are plotted.*

the shallowest-water samples calcareous benthic and planktonic species are present. Foraminiferal diversity and abundances decrease sharply down core. From ~30 cm down, many samples are barren or contain few specimens only. However, in several horizons rich foraminiferal assemblages were encountered. They are strongly dominated by calcareous forms, especially the only planktonic Neogloboquadrina pachyderma. Environmental and stratigraphic significance of those events will be investigated.

Appendix IV contains relevant information on samples taken for radiocarbon age dating.

Multi Sensor Core Logging, index properties and shear strength

The results from the sediment physical property measurement are plotted in Appendix II and the shear strength measurements are displayed alongside the lithologic columns in Appendix I. The index samples are listed in Table 4.

Oceanography

Moorings

During this cruise we deployed 2 moorings in the Little America Trough of the eastern Ross Sea (Figure 20). The final location of each mooring was established at the ship GPS position when the anchor weight was slipped at the end of the deployment. XCTDs were launched within a mile of each

Core	Sec	Depth (cm)	Sample Ring #	Ring Mass	Ring Volume	Wet Mass (Sample + Ring)	Bulk Density (estimate)	Error in Weights (+1g)
OSO0910-KC05	1	105.0	2	17.2	9.8	36.0	1.92	2.02
OSO0910-KC05	1	200.0	1	17.2	9.8	38.0	2.12	2.22
OSO0910-KC06	1	70.0	2	17.2	9.8	35.2	1.84	1.94
OSO0910-KC06	CC	87.5	1	17.2	9.8	35.6	1.88	1.98
OSO0910-KC07	1	38.0	1	17.2	9.8	34.2	1.73	1.84
OSO0910-KC08	1	33.0	2	17.2	9.8	35.4	1.86	1.96
OSO0910-KC10	1	30.0	2	17.2	9.8	32.7	1.58	1.68
OSO0910-KC10	1	70.0	1	17.2	9.8	35.0	1.82	1.92
OSO0910-KC15	1	45.0	2	17.2	9.8	31.5	1.46	1.56
OSO0910-KC15	1	80.0	1	17.2	9.8	32.0	1.51	1.61
OSO0910-KC19	1	57.0	1	17.2	9.8	37.0	2.02	2.12
OSO0910-KC19	1	87.0	2	17.2	9.8	33.0	1.61	1.71
OSO0910-KC23	CC	25.0	2	17.2	9.8	38.8	2.20	2.31
OSO0910-KC23	CC	35.0	1	17.2	9.8	39.6	2.29	2.39
OSO0910-KC25	1	25.0	2	17.2	9.8	32.5	1.56	1.66
OSO0910-KC25	CC	10.0	1	17.2	9.8	29.2	1.22	1.33

Table 4. *Index samples taken using two 9.8 cm³ stainless steel rings.*

Mooring	Location	*Location*	*Longitude*	Date	Water Depth
A	Mid Little America Trough	-77.3169	-161.0682	10 Feb 10	656 m
B	Outer Little America Trough	-76.9347	-163.3263	10 Feb 10	602 m

Table 5. *Mooring locations and details.*

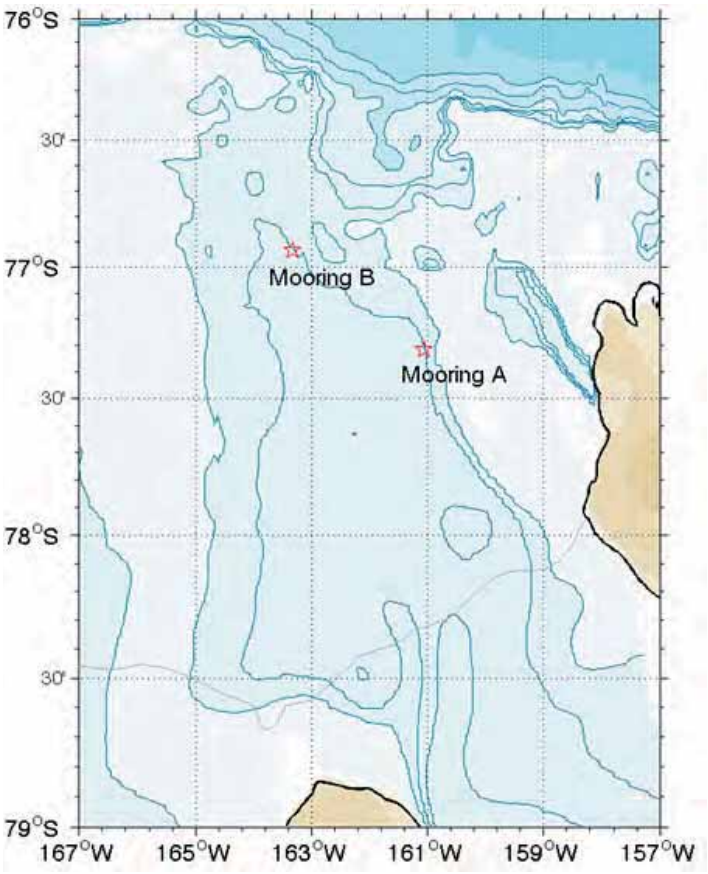

Figure 20. *Locations of the two moorings in the Little America Trough.*

mooring site. The moorings are to be retrieved in February 2011.

CTD and water sampling

CTD/LADCP

A total 10 CTD cast were occupied (Table 6, Figure 21) during this cruise in the main trough leading to Pine Island Glacier. CTD data from these casts confirm the inflow of relative warm and saline bottom water along this trough, as well as in Ferrero Bay.

While the rosette was at the sea surface during the first 3 casts, the pressure sensor on the CTD was reading –9 m. Because of this, the pressure offset in the configuration settings was increased by +9 m after station s003c1 to force the pressure at the sea surface to be approximately 0 m. The pressure sensor will be sent off for calibration upon immediate arrival at TAMU to investigate this offset.

Serious problems with the CTD winch reoccurred throughout the cruise. This resulted in multiple missed opportunities to collect key hydrographic (CTD/LADCP) data, in particular a broken winch prevented us from taking CTD stations at the mooring locations. Other missed opportunities were due to regular servicing of the CTD winch and the breaking of the hydraulics on the A-frame.

XBTs/XCTDs

XBTs/XCTDs were launched at sites where CTD stations were originally planned, or unobtainable due to weather, winch problems, and time constraints. In total, 127 XBT and 5 XCTD probes were launched (Appendix V). XBTs were provided by TAMU, Stockholm University, and Lamont Doherty Earth Observatory and XCTDs provided by Stockholm University.

Ecology

Station	Location	Latitude	Longitude	Date	Depth m	CTD depth m
s001c1	UGOT mooring	-72.4480	-116.4179	15 Feb 10	557	311
s002c1	Pine Island	-72.6980	-107.1167	18 Feb 10	706	697
s003c1	Pine Island	-72.1346	-106.9356	18 Feb 10	596	586
s004c1	Pine Island	-72.5756	-107.1596	22 Feb 10	728	717
s005c1	Pine Island	-72.6397	-107.1743	22 Feb 10	738	728
s006c1	Pine Island	-72.6502	-107.5140	22 Feb 10	637	627
s007c1	Pine Island	-72.5873	-106.8324	23 Feb 10	702	694
s008c1	Pine Island	-73.3643	-101.8568	24 Feb 10	1186	1177
s009c1	Pine Island	-73.2363	-106.7478	27 Feb 10	790	781
s010c1	Pine Island	-72.8800	-107.2280	28 Feb 10	663	653

Table 6. *CTD stations.*

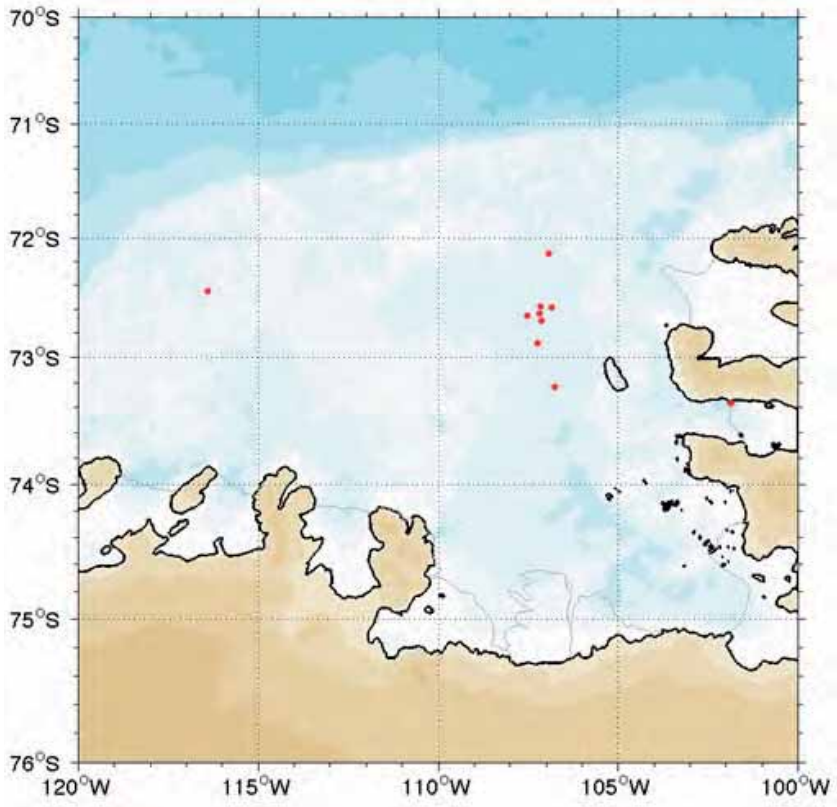

Figure 21. *Locations of the CTD stations.*

The ozone hole above Antarctica has during the last decades increased considerably allowing higher doses of ultraviolet (UV) radiation to reach the biota. Also aquatic organisms in the sea and in freshwater systems are strongly affected by UV and some, such as zooplankton, have evolved photoprotective pigmentation that can be adjusted to the present UV environment. The very high UV radiation and the long summer day lengths at the high latitudes of polar regions put a strong pressure on these organisms, probably the strongest on earth. Hence, studies in Antarctic systems offer a rare opportunity to study photoprotective adaptations when they are at their maximum and to address how these extreme levels of UV radiation may affect induction of different pigments, and shape communities in freshwater and marine systems. A main aim with our project has also been to compare responses among organisms in temperate and Antarctic systems. Such comparisons has the potential to improve our understanding of how ecosystem function and community composition may change as UV radiation increases also in temperate regions, as is currently the case in e.g. northern Scandinavia.

Handling simultaneous UV and predation threats in marine systems

As specific study organism we have chosen crustacean copepods (Figure 22), which are common in most fresh and marine waters on earth. Copepods at high latitudes are often pigmented bright red as a result of the carotenoid astaxanthin that is effective in protecting the animal against harmful UV-radiation, but also makes the animals more visible and thereby vulnerable to predation. In addition to red carotenoids, many crustaceans are able to incorporate mycosporine-like amino acids (MAAs) that are invisible, UV protective compounds. Preliminary results from temperate regions indicate that if predation is high, the animals prefer using MAAs instead of carotenoids, i.e. there is an inverse relation between the amount of these photoprotective pigments. A third opportunity to avoid high UV exposure during day is to migrate to deeper waters and then return to the surface during night, a phenomenon known as diel vertical migration (DVM).

We expected that Antarctic marine systems, where UV penetration is high, the amount of red photoprotective pigmentation would be very low, since predation from visually hunting predators, such as fish, is also high. Our studies along the East Antarctic coast confirmed this hypothesis showing almost undetectable amounts of visible photoprotective carotenoids (astaxanthins). However, the amounts of invisible photoprotective MAA´s were high (Figure 23) and the copepods performed considerable diel vertical migration (Figure 24). Hence, these small animals made the best of a bad situation: avoided the strongest UV

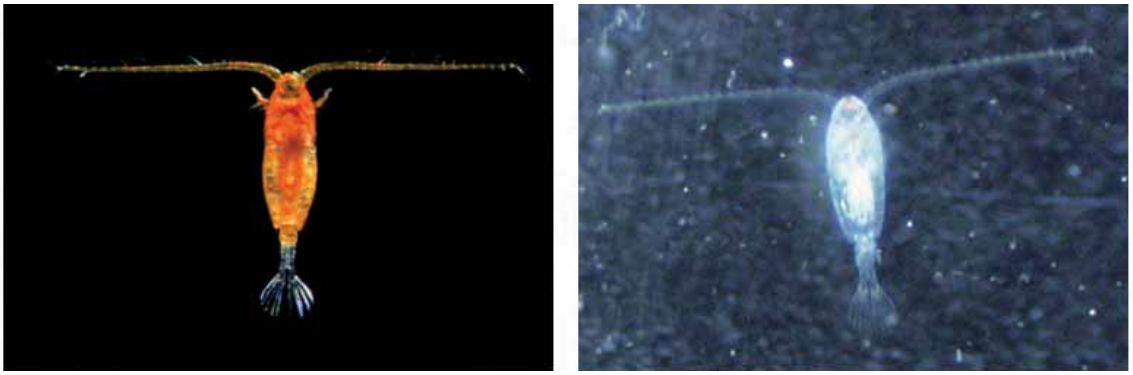

***Figure 22**. Copepods display large differences in pigmentation. The copepod to the left is from a system with low predation pressure and high UV exposure. The right one resembles the transparent, marine copepods in Antarctica.*

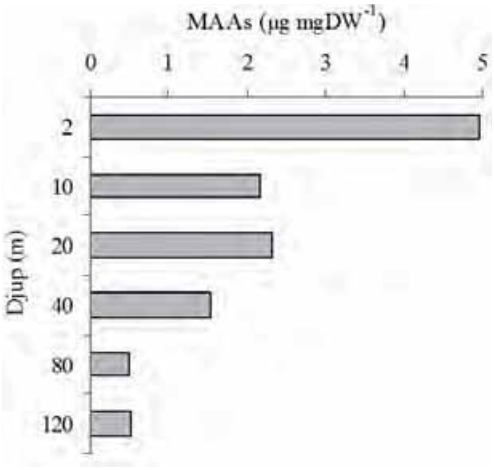

Figure 23. Contents of MAAs (mycosporine-like amino acids) were generally high compared with carotenoids, and individuals at the surface generally had higher MAA content than individuals dwelling deeper down where UV is less of a problem.

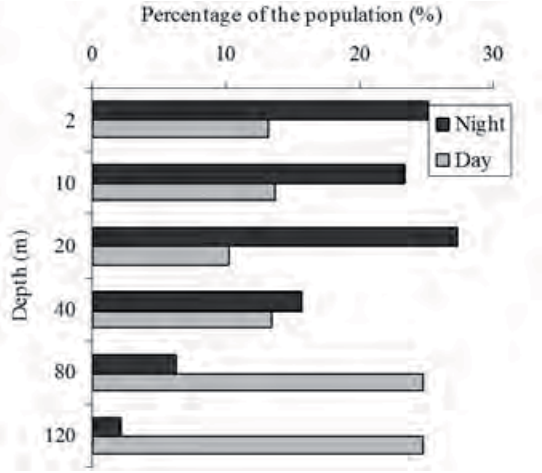

Figure 24. An example of copepod vertical distribution at day and night, showing that a main part of the population occur at the surface during night, but migrates to below 40 m during day.

radiation at the surface and were transparent in order to reduce the risk of being seen by predators, such as fish.

We expected the copepods in the UV treatment to increase their carotenoid and MAA concentration as protection against UV, whereas the copepods receiving only visible light were expected to reduce their photoprotective pigmentation. Interestingly, this hypothesis was corroborated by the data and already after 10 days the copepods in the UV treatment had about 66% higher MAA and 26% higher carotenoid concentrations than the ones receiving only visible light. Hence this experiment showed that copepods rapidly adjust their level of pigmentation to the current threat situation, i.e. pigmentation is a plastic trait.

Diel changes in the vertical distribution of lake zooplankton

Our original plan included studies also in freshwater systems, which turned out to be impossible at a later stage of the cruise planning. However, we were offered an opportunity to visit two lakes of the Dry Valleys near McMurdo prior to entering *Oden*. The two lakes studied were Lakes Fryxell and Hoare which are situated in Taylor Valley. The Dry Valley´s receive less than 50 mm precipitation per year and has a mean temperature of –180 °C, making them one of the driest, coldest and harshest aquatic environments on Earth. The lakes are ice-covered year around, although in late summer a fringe of water opens up close to the shore. Due to the low precipitation the only inflow to the lakes is from glacier melt water and they lack surface outflow. The surface areas of the lakes are about 7.1 and 1.9 km^2, and maximum depths 20 and 34 m in L. Fryxell and Hoare, respectively. The ice thickness in summer has been estimated to between 3.7 and 5.5 m, although we could only confirm a thickness of 1–2 m, not including the about 1 m thick porous, partly melted snow/ice cover on top of the regular ice.

We also performed a diel study on the vertical distribution of zooplankton in one of he lakes (L. Fryxell). Since very little UV is penetrating through the permanent ice-cover of the lakes and no predators exist, we expected that the zooplankton should be positioned where the food is, i.e. have the same vertical distribution as the algae. Interestingly, we found no such pattern, but instead the dominant taxa of rotifers (Philodinia sp.) generally showed a maximum close to the surface, whereas algal maxima

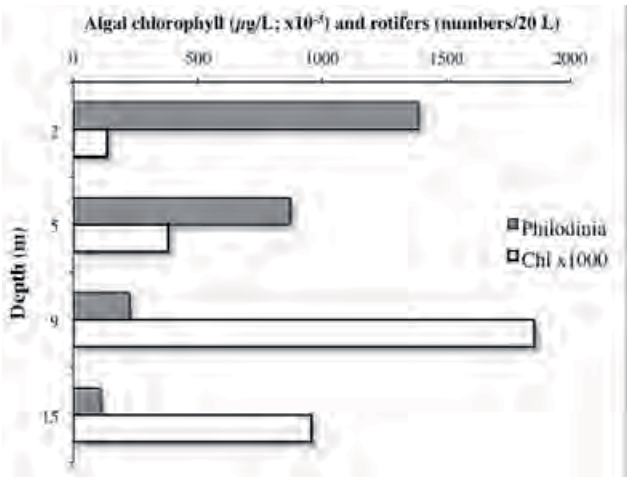

Figure 25.Depth distribution of the rotifer genus Philodinia and the concentration of chlorophyll a in Lake Fryxell showing that the rotifers are most abundant at the surface, while their algal food gather at the bottom of the lake.

were generally close to the bottom of the lake (Figure 25). Explanations to this inverted distribution may be either that Philodinia feeds on other organisms than algae or that rotifers at the surface has actually eaten the alga there.

Prior to our visit to the Dry Valley lakes we were informed that the biodiversity of the lakes should be extremely low and we should be prepared to find only a few species of rotifers and no crustacean zooplankton. Although the diversity was low, we found several species of rotifers that have never been recorded in this region (J. Laybourn-Parry, pers. comm), including Felinia sp., Kellicottia sp., Keratella quadrata and Brachionus sp. Moreover, we found three (3!) individuals of copepods in a total volume of 400 L water, suggesting that large crustacean are indeed rare. The reasons we were the first to recognize these organisms were our large sampling volumes and that the lakes are rarely sampled.

Acknowledgements

We thank the Captain and crew of icebreaker Oden for their great work. The Swedish Polar Research Secretariat, the National Science Foundation (NSF) and the Swedish Research Council (VR) organized and financed the expedition through a collaboration program. The ecology team from Lund University would like to express a specific thanks to Sven Lidström and Addie Coyac for making the Dry Valley sampling possible. The newly upgraded multibeam system on the Oden was financed by the Knut and Alice Wallenberg Foundation, VR and the Swedish Maritime Administration.

References

Anderson, J.B., 1999. Antarctic Marine Geology. Cambridge University Press, Cambridge.

Calder, B.R., Mayer, L.A., 2003. Automatic processing of high-rate, high-density multibeam echosounder data. Geochemistry Geophysics Geosystems 4, 1-22.

Jakobsson, M., Marcussen, C., LOMROG, S.P., 2008. Lomonosov Ridge Off Greenland 2007 (LOMROG) - Cruise Report, Special Publication Geological Survey of Denmark and Greenland. Geological Survey of Denmark and Greenland, Copenhagen, p. 122.

Lowe, A.L., Anderson, J.B., 2002. Reconstruction of the West Antarctic ice sheet in Pine Island Bay during the Last Glacial Maximum and its subsequent retreat history. Quaternary Science Reviews 21, 1879-1897.

Lowe, A.L., Anderson, J.B., 2003. Evidence for abundant subglacial meltwater beneath the paleo-ice sheet in Pine Island Bay, Antarctica. Journal of Glaciology 49, 125-138.

Nitsche, F.O., Jacobs, S.S., Larter, R.D., Gohl, K., 2007. Bathymetry of the Amundsen Sea continental shelf: Implications for geology, oceanography, and glaciology. Gechemistry Geophysics Geosystems 8, Q10009.


U.S. AIR FORCE
1106

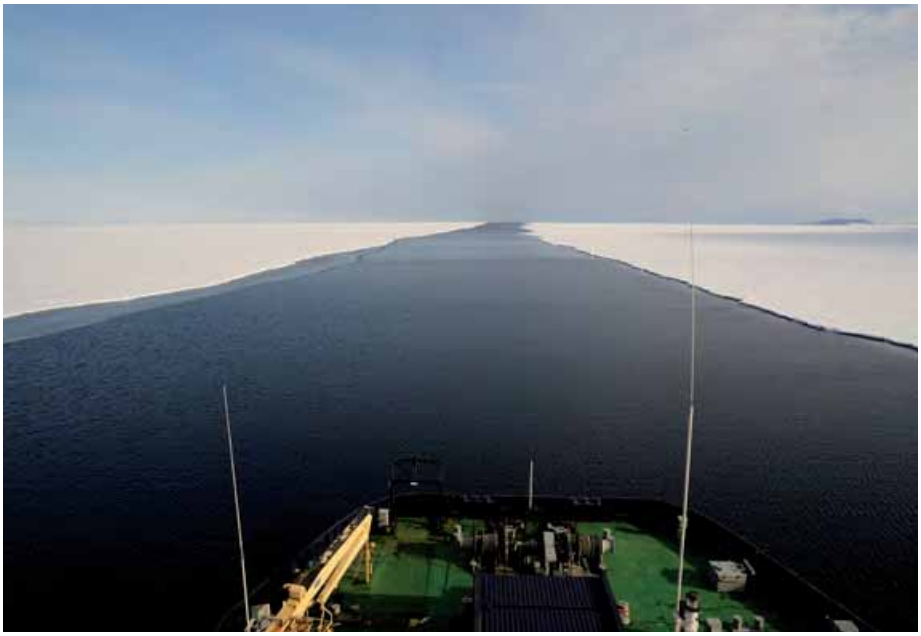

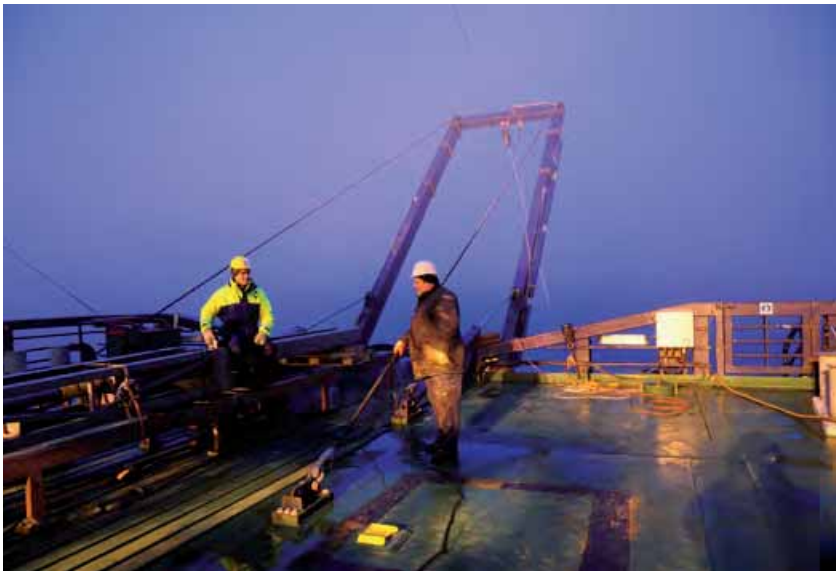

Appendix I

CORE: **KC04** LAT/LON: 72°41.8277'S, 107°6.6311'W DEPTH (mbsl): 729

KC length (cm): 204 Archive length (cm): 208 CC length (cm): 12.8

OSO0910

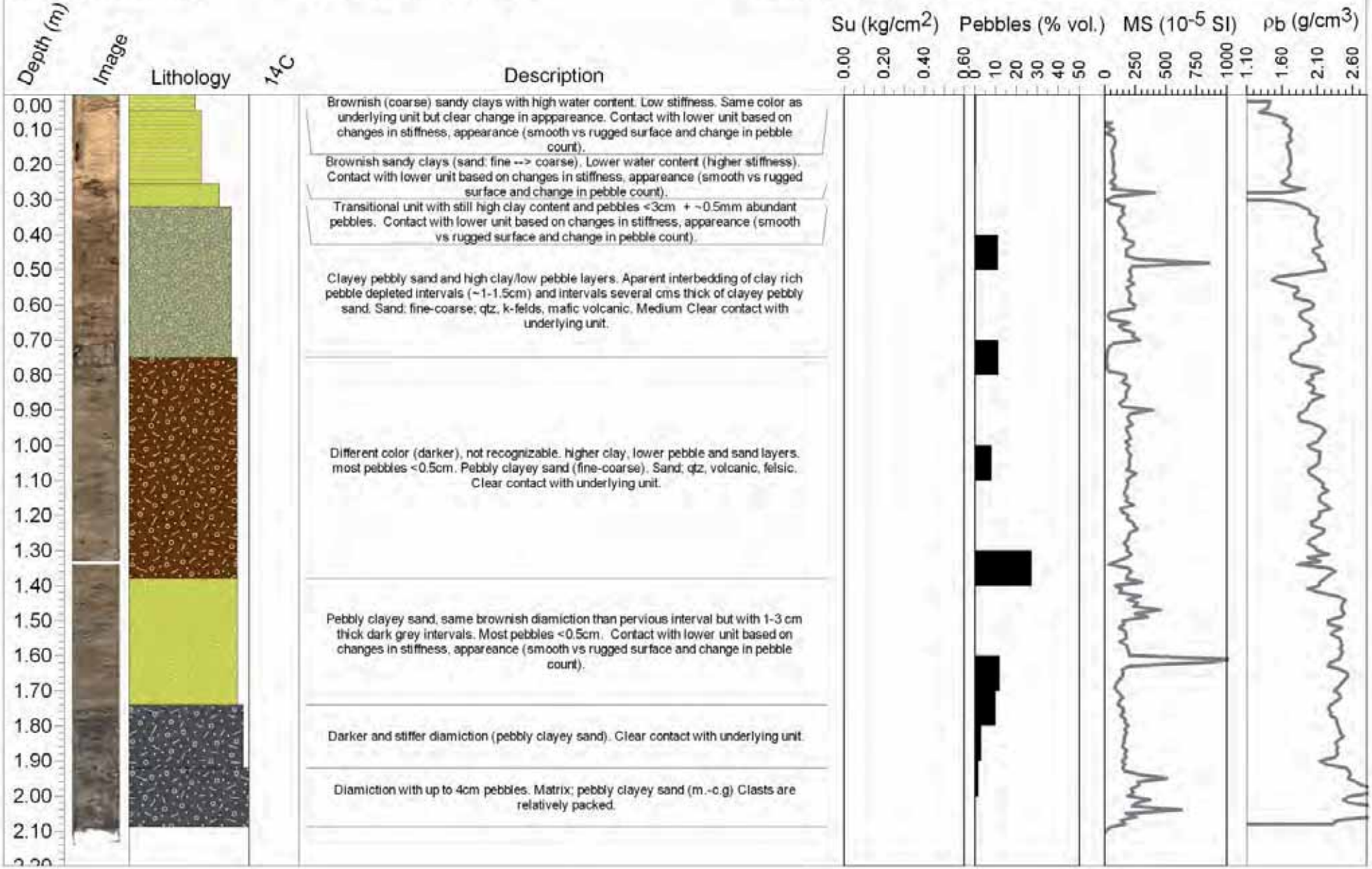

CORE: **KC05** LAT/LON: 72°41.8277'S, 107°6.6311'W DEPTH (mbsl): 729

KC length (cm): 249 Archive length (cm): 245 CC length (cm): 28

OSO0910

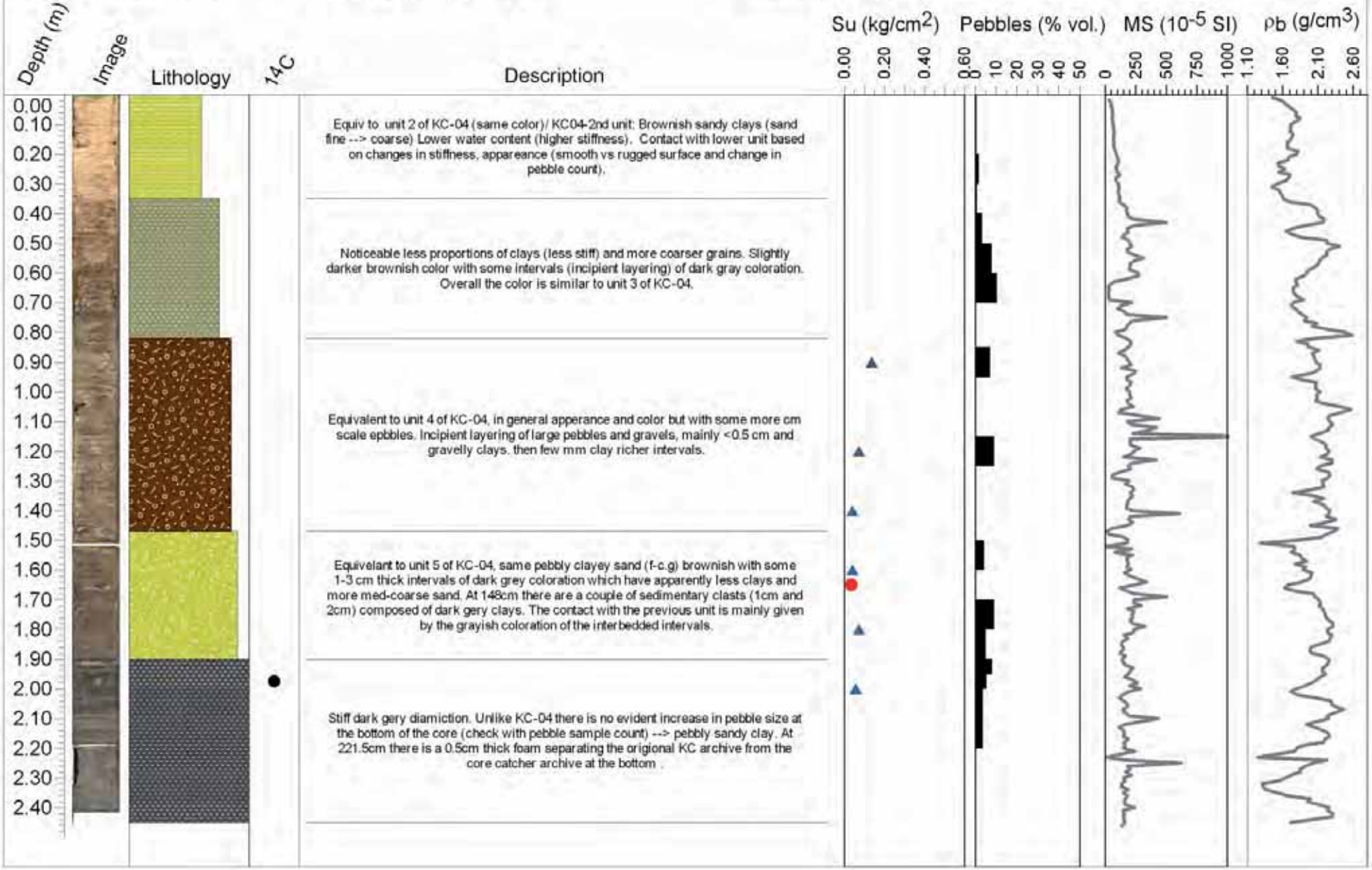

CORE: **KC06** LAT/LON: 72°7.95'S, 106°54.60'W DEPTH (mbsl): 614

KC length (cm): 104 Archive length (cm): 104 CC length (cm): 22

OSO0910

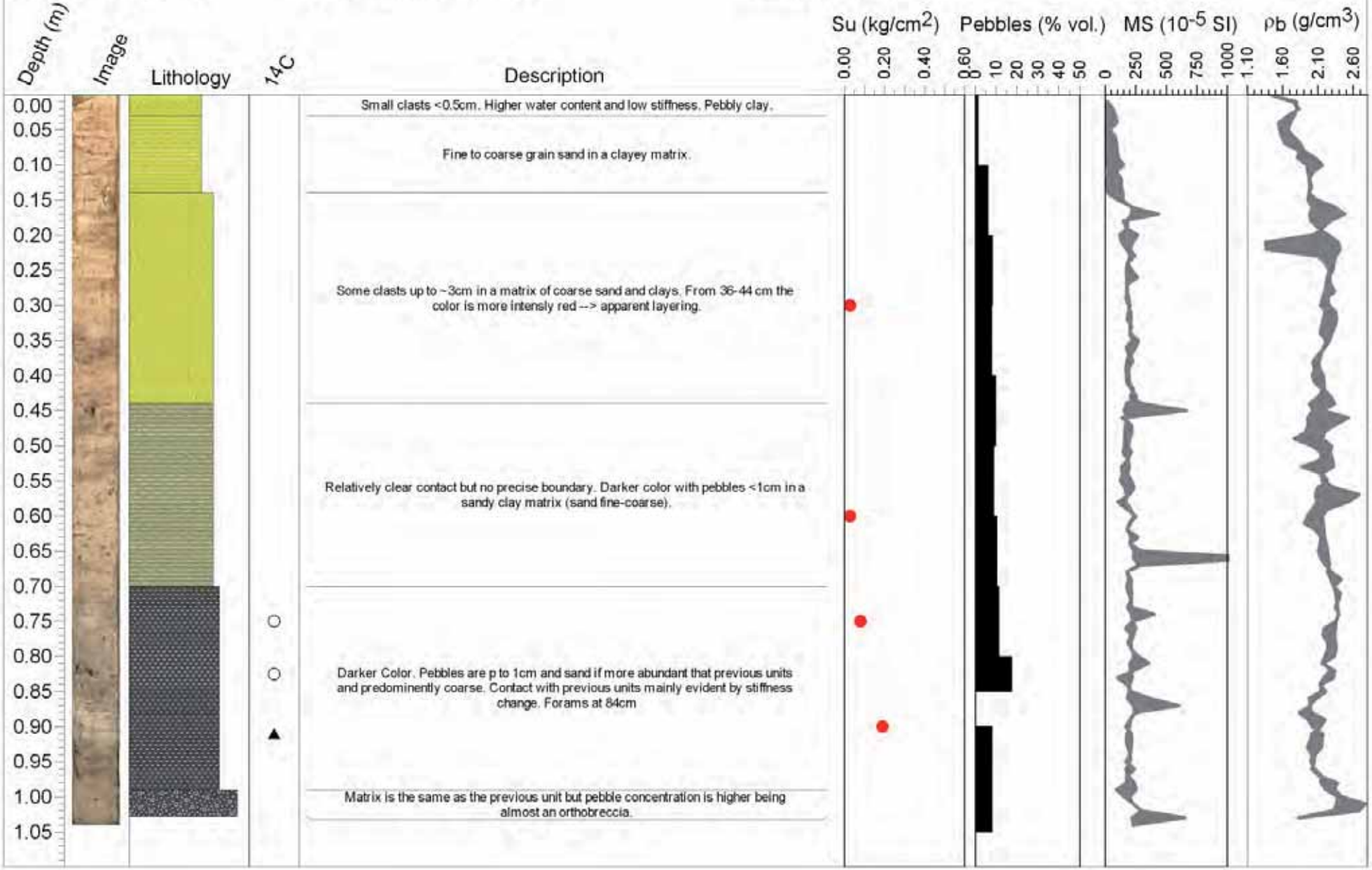

CORE: **KC07** LAT/LON: 72°20.3635'S, 106°52.9350'W DEPTH (mbsl): 707

KC length (cm): 63 Archive length (cm): 50 CC length (cm): 13

OSO0910

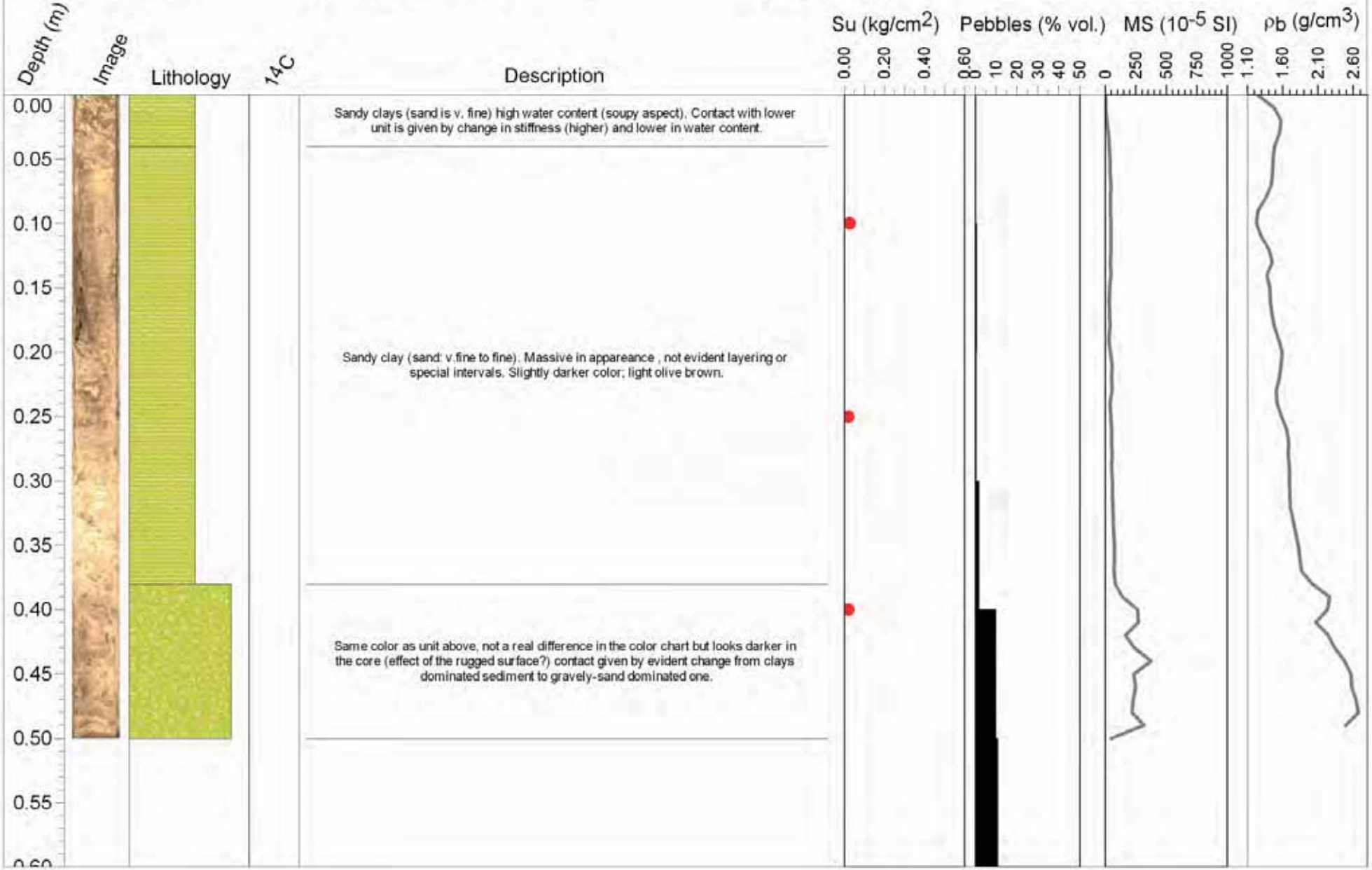

CORE: **KC08** LAT/LON: 72°20.8110'S, 106°52.6320'W DEPTH (mbsl): 711

KC length (cm): 60 Archive length (cm): 40 CC length (cm): 20

OSO0910

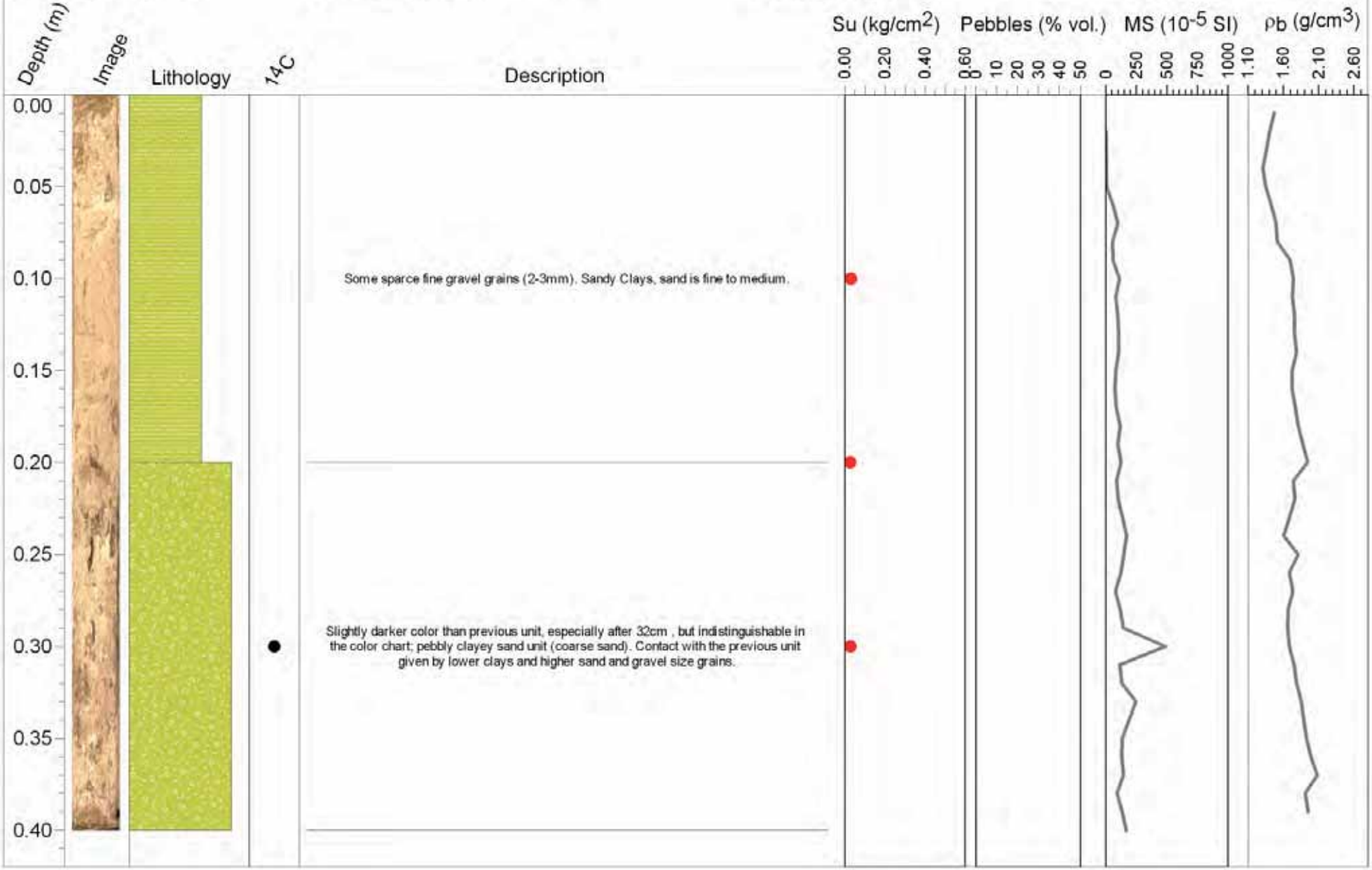

CORE: **KC09** LAT/LON: 72°29.2000'S, 106°38.3400'W DEPTH (mbsl): 548

KC length (cm): 45 Archive length (cm): 46 CC length (cm): 24

OSO0910

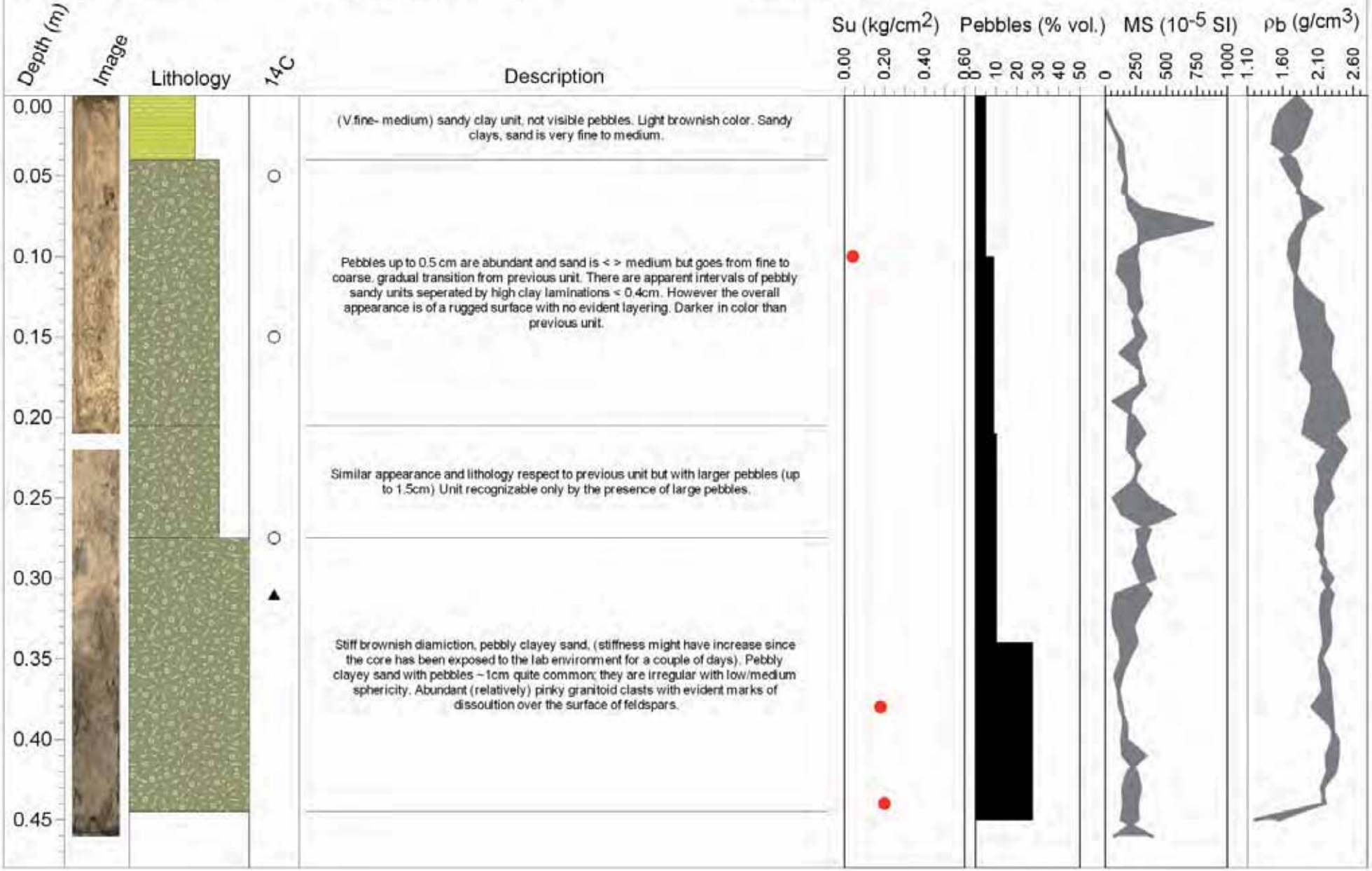

CORE: **KC10** LAT/LON: 72°29.5404'S, 106°46.4141'W DEPTH (mbsl): 687

KC length (cm): 88 Archive length (cm): 88 CC length (cm): 13

OSO0910

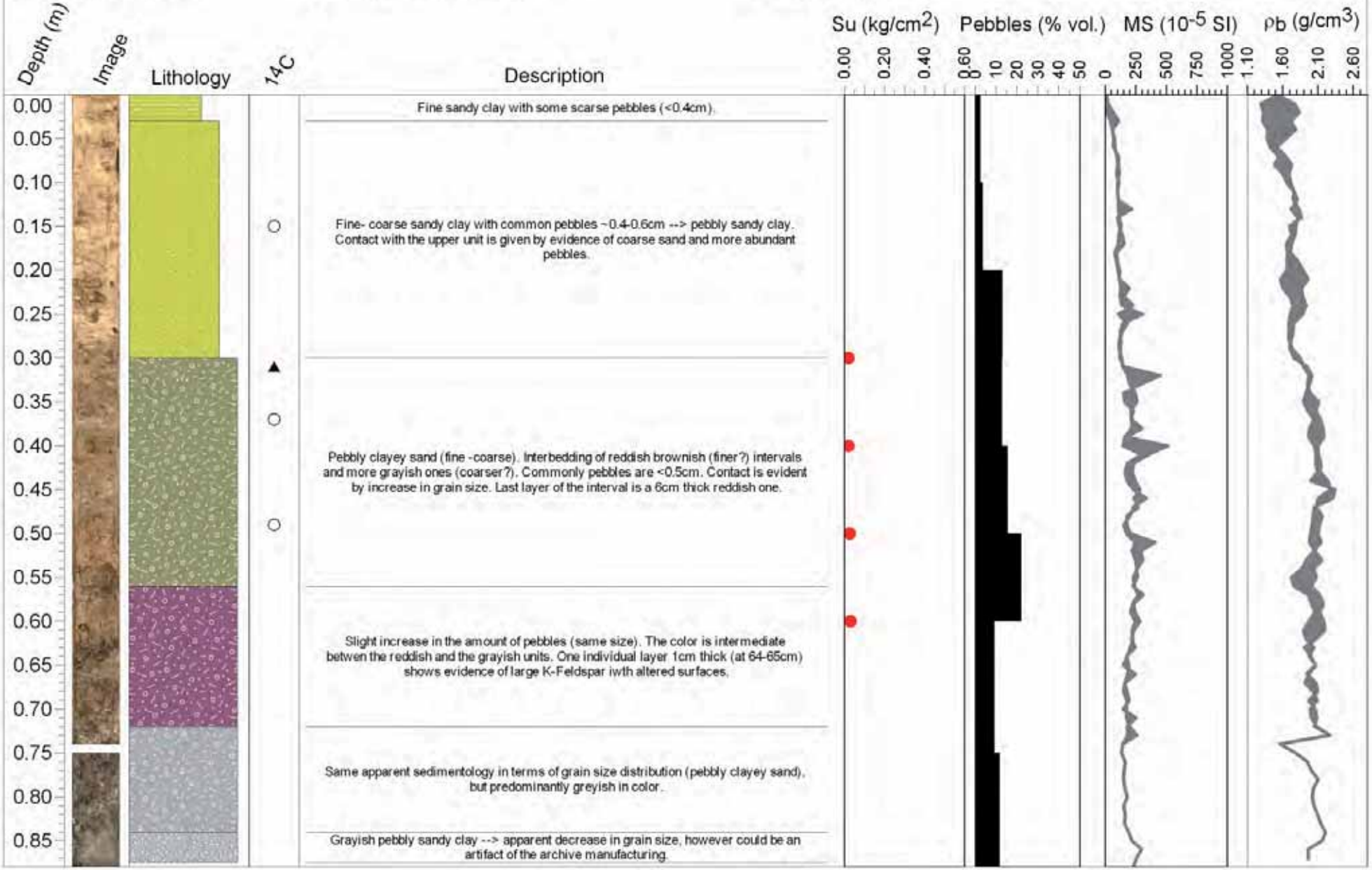

CORE: **KC11** LAT/LON: 72°34.57'S, 107°09.11'W DEPTH (mbsl): 733

KC length (cm): 150 Archive length (cm): 146 CC length (cm): 16

OSO0910

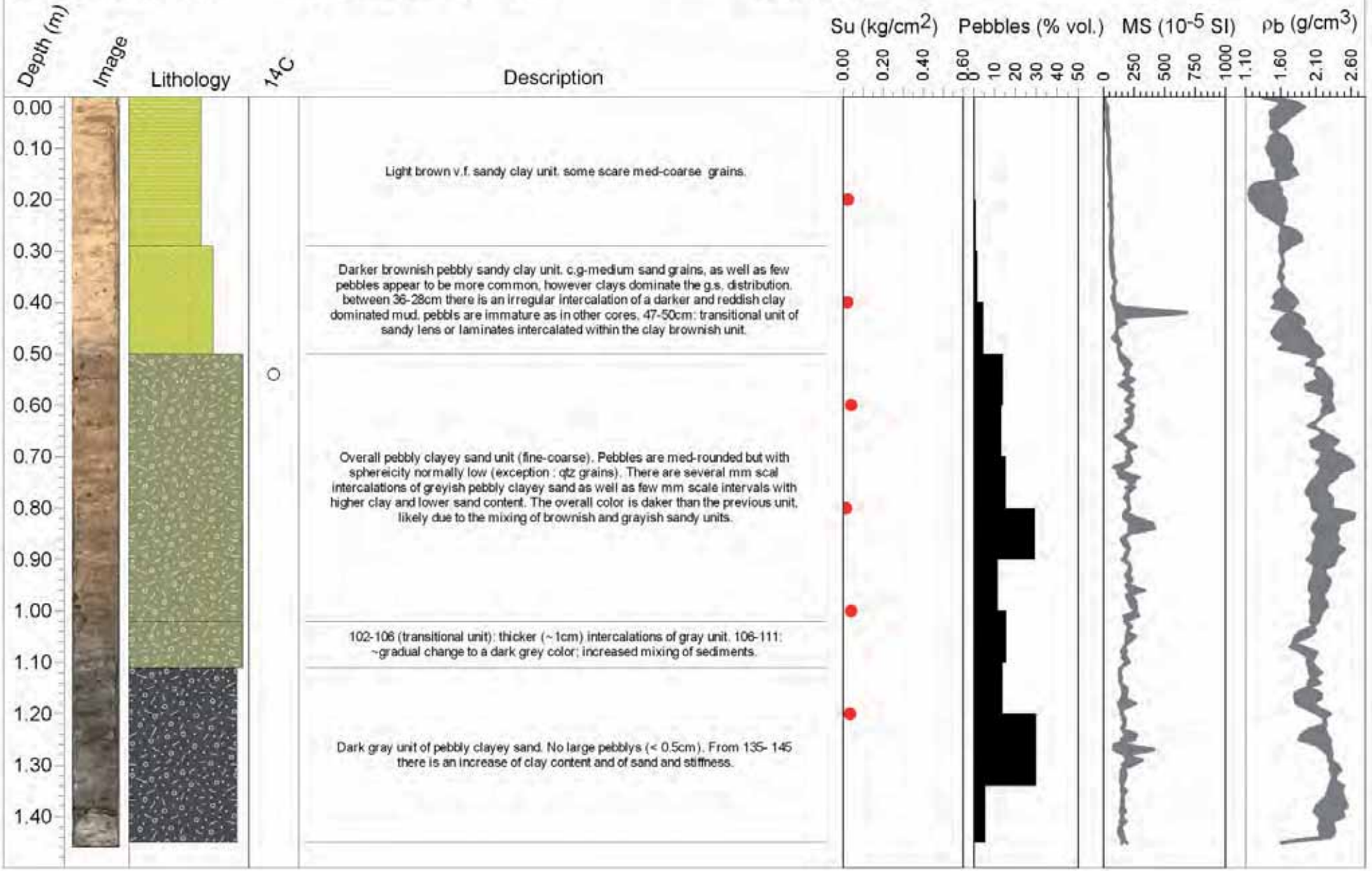

CORE: **KC12** LAT/LON: 72°34.23'S, 107°11.45'W DEPTH (mbsl): 735

KC length (cm): 104.5 Archive length (cm): 0 CC length (cm): 18

OSO0910

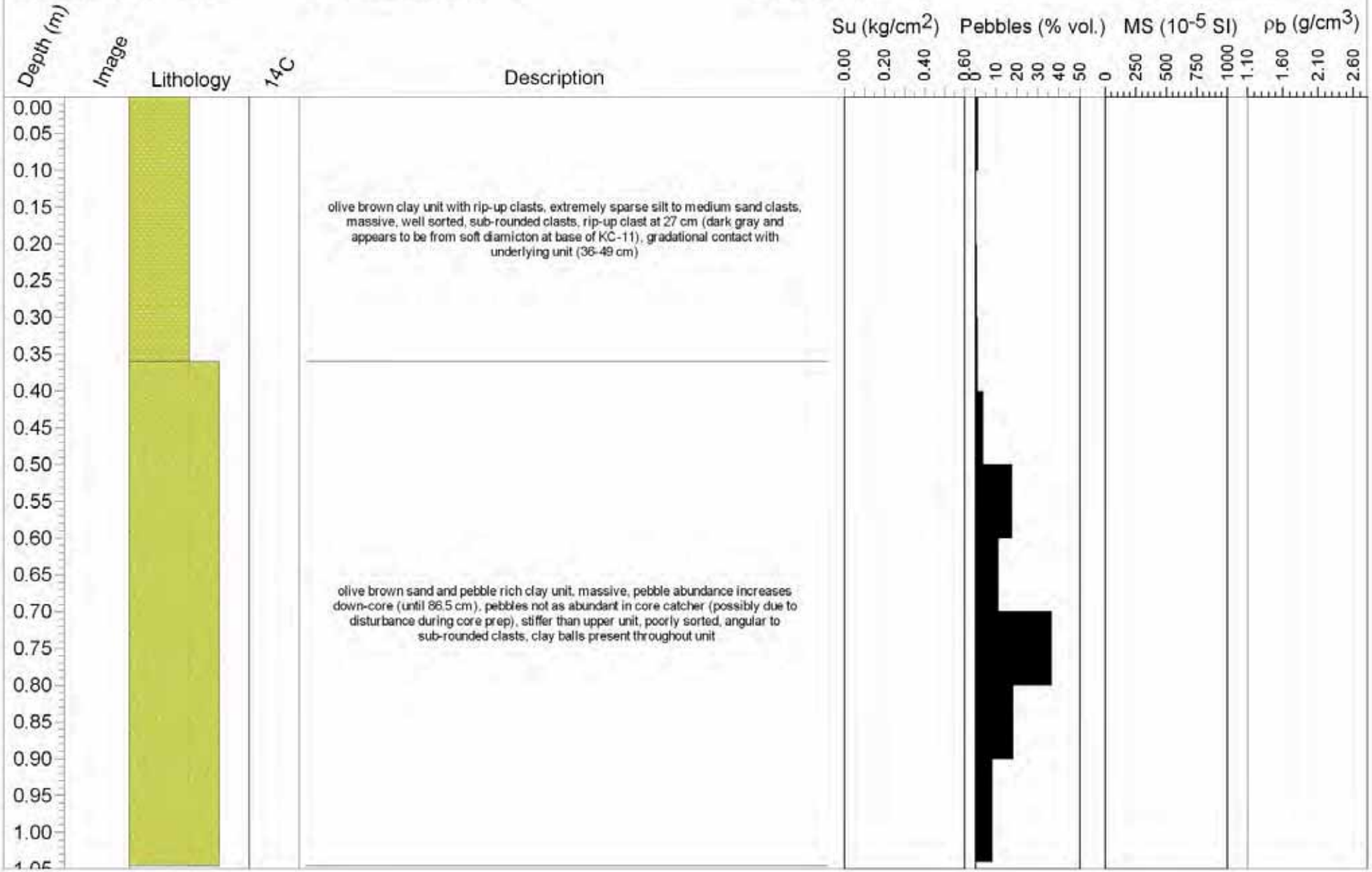

CORE: **KC13** LAT/LON: 72°38.44'S, 107°10.12'W DEPTH (mbsl): 742

KC length (cm): 226 Archive length (cm): 227 CC length (cm): 20

OSO0910

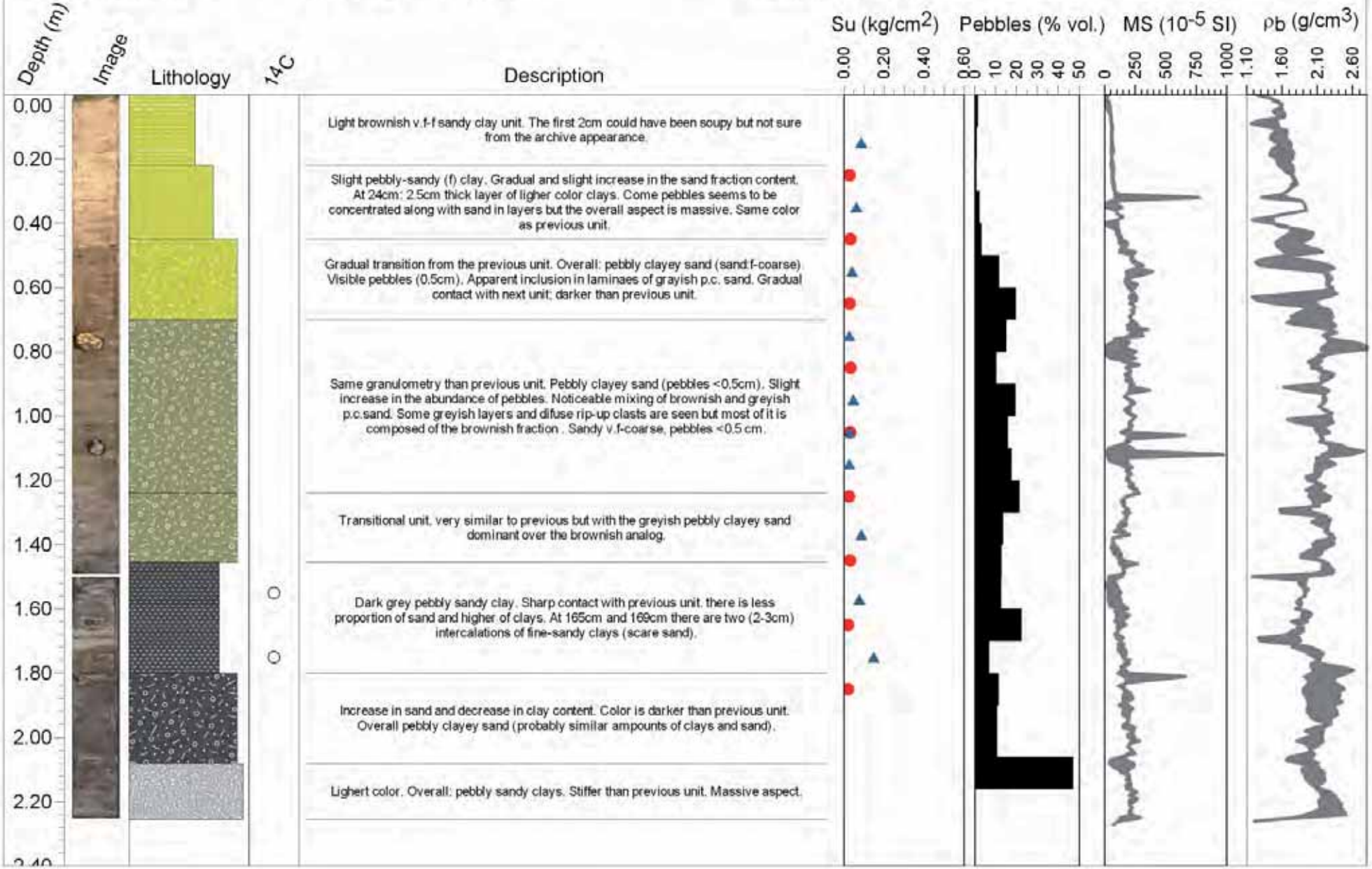

CORE: **KC14** LAT/LON: 72°39.02'S, 107°30.78'W DEPTH (mbsl): 639

KC length (cm): 72 Archive length (cm): 72 CC length (cm): 16

OSO0910

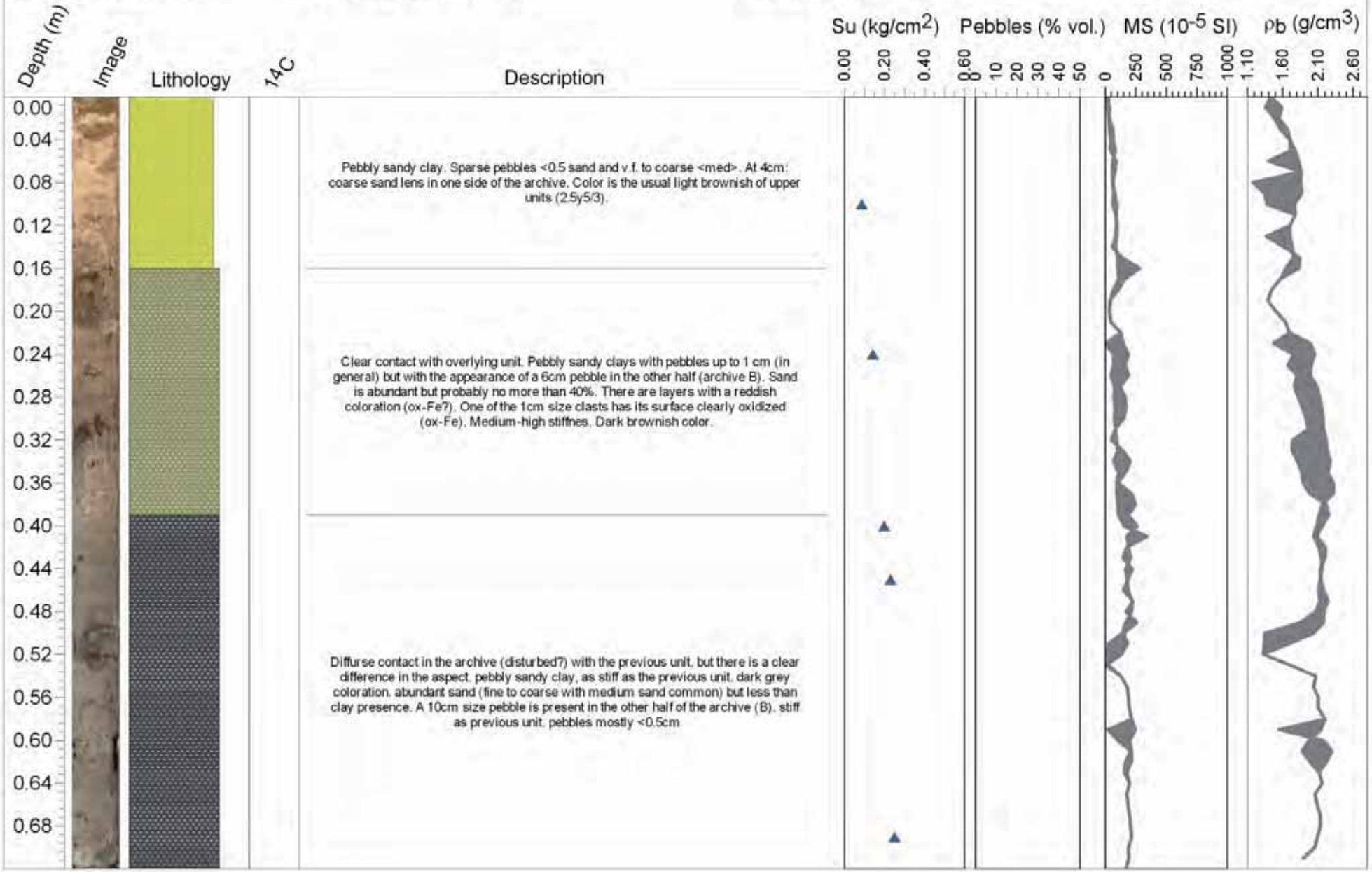

CORE: **KC15** LAT/LON: 73°21.62'S, 101°50.17'W DEPTH (mbsl): 1257

KC length (cm): 130 Archive length (cm): 131 CC length (cm): 14

OSO0910

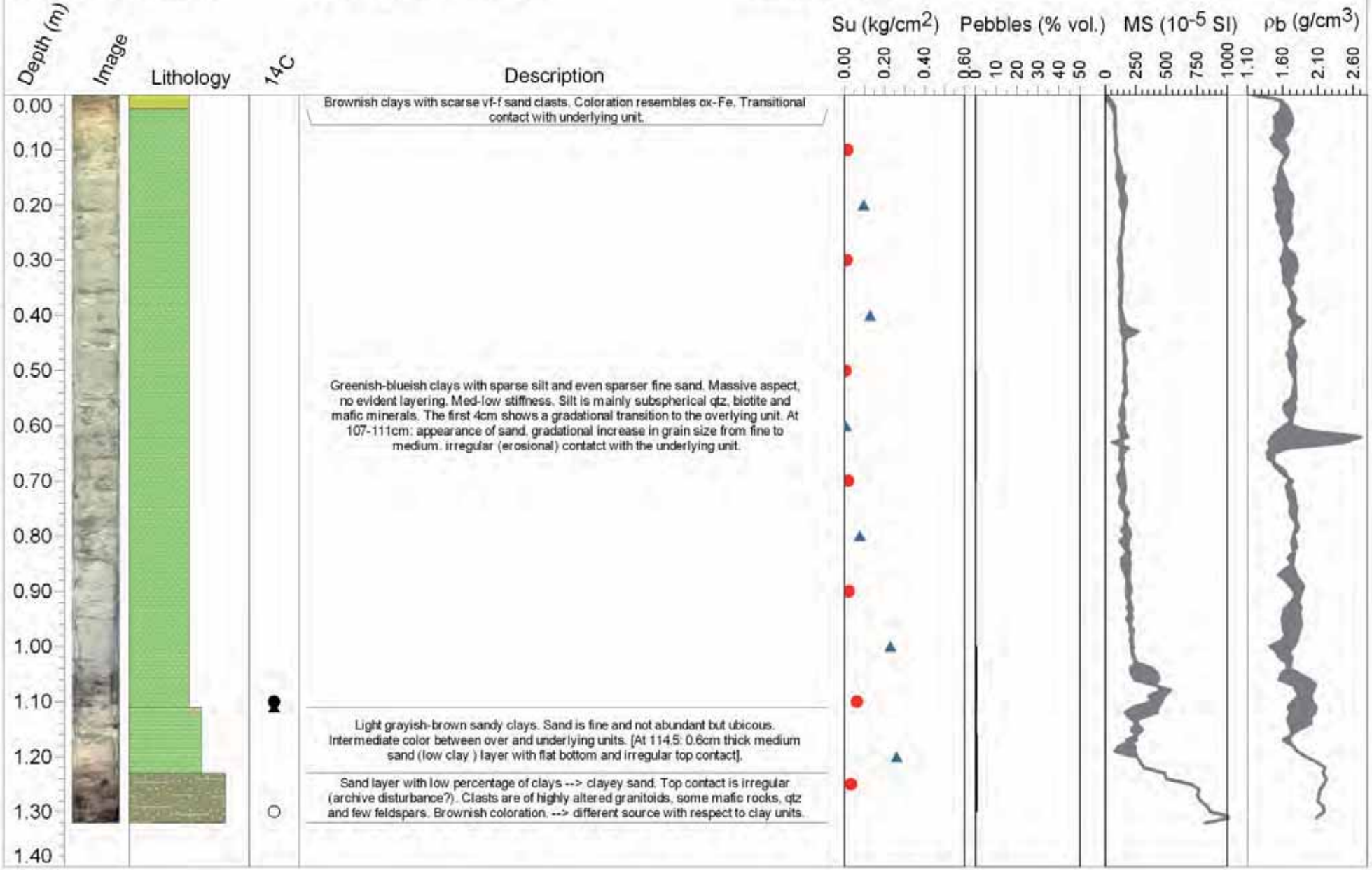

CORE: **KC16** LAT/LON: 73°27.24'S, 102°4.75'W DEPTH (mbsl): 706

KC length (cm): 38 Archive length (cm): 39 CC length (cm): 12

OSO0910

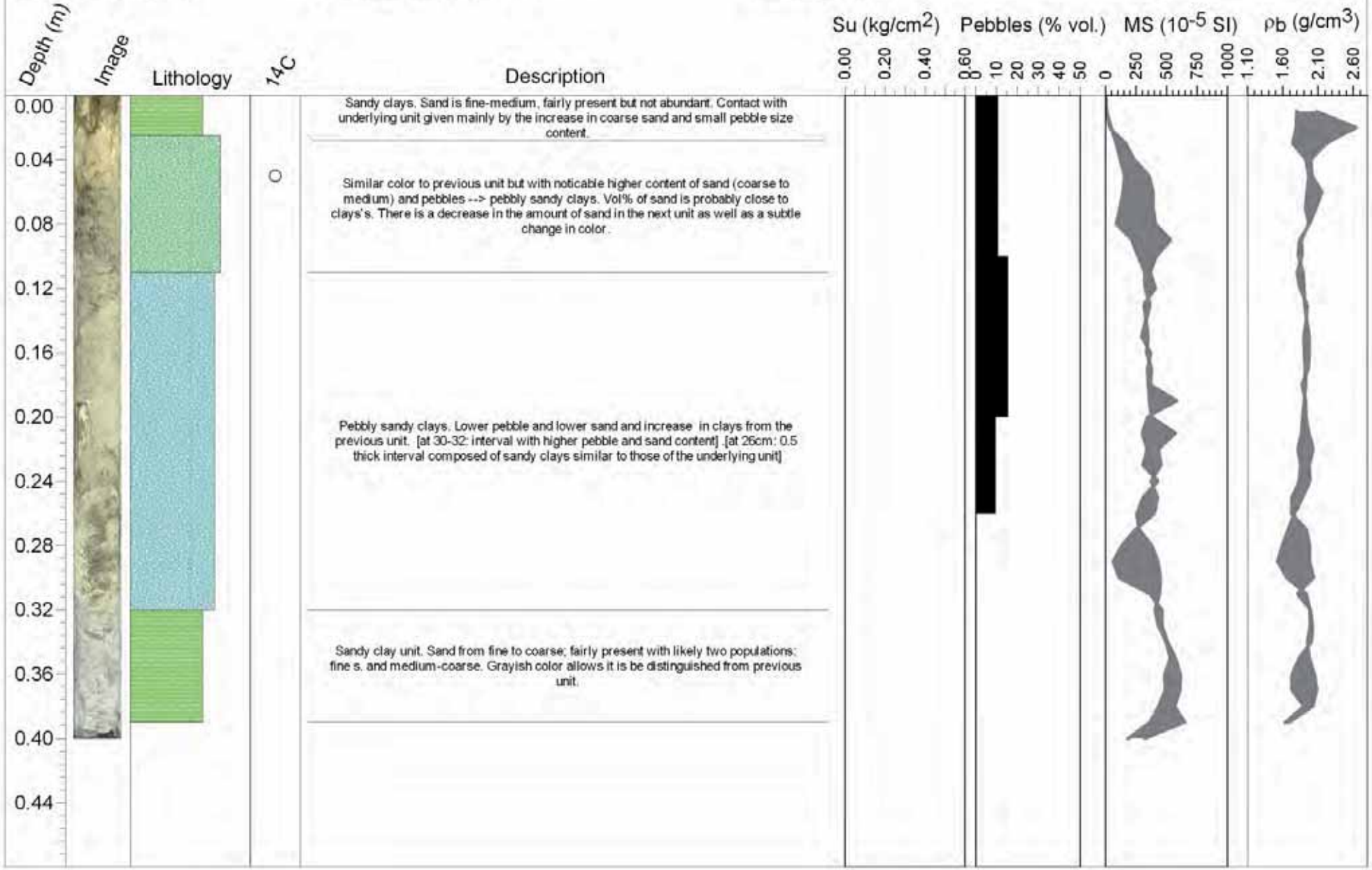

CORE: **KC17** LAT/LON: 73°25.18'S, 102°49.60'W DEPTH (mbsl): 855

KC length (cm): 147 Archive length (cm): 147 CC length (cm): 21

OSO0910

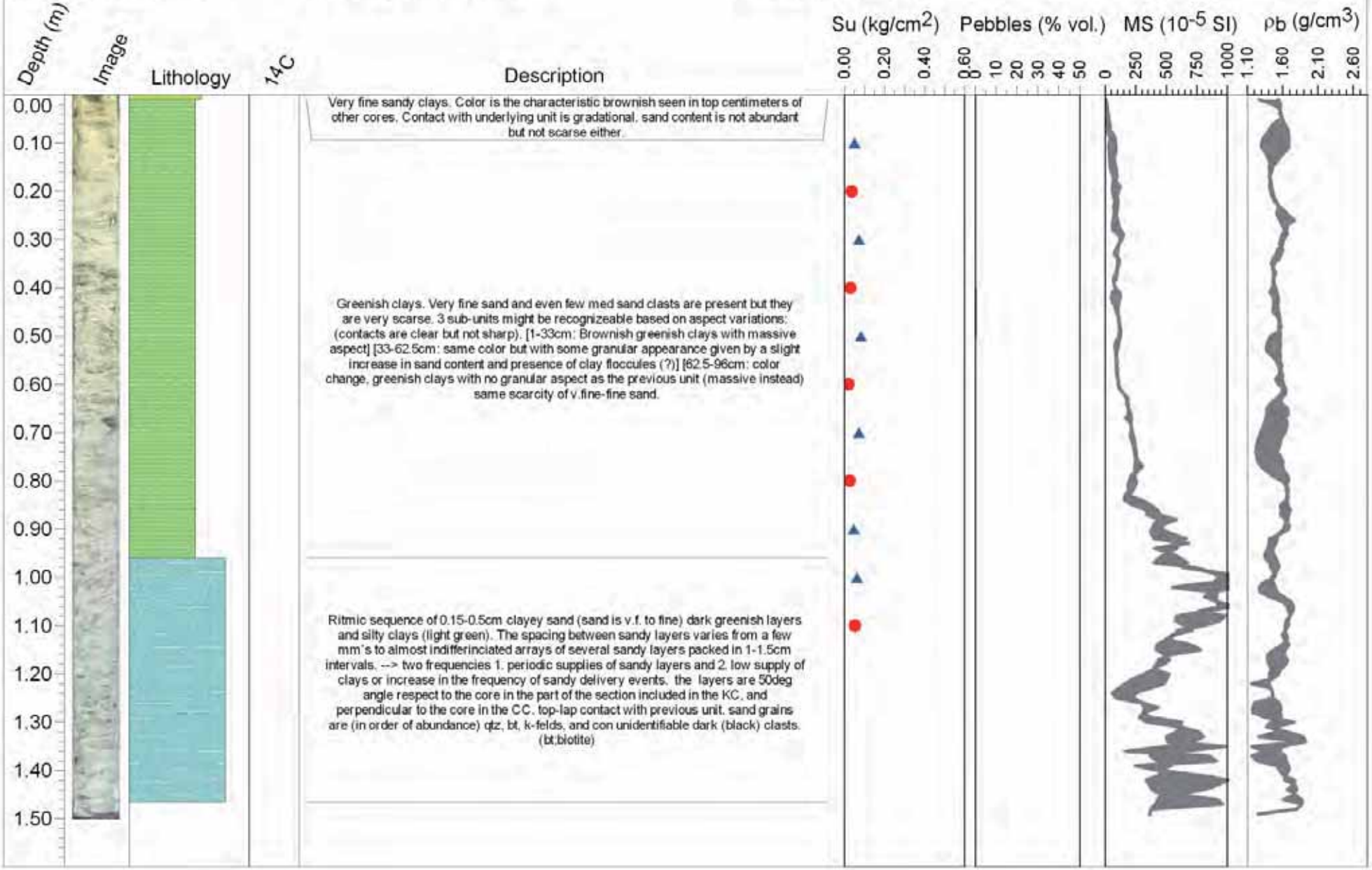

CORE: **KC18** LAT/LON: 73°23.01'S, 106°52.26'W DEPTH (mbsl): 894

KC length (cm): 148.5 Archive length (cm): 148 CC length (cm): 29.5

OSO0910

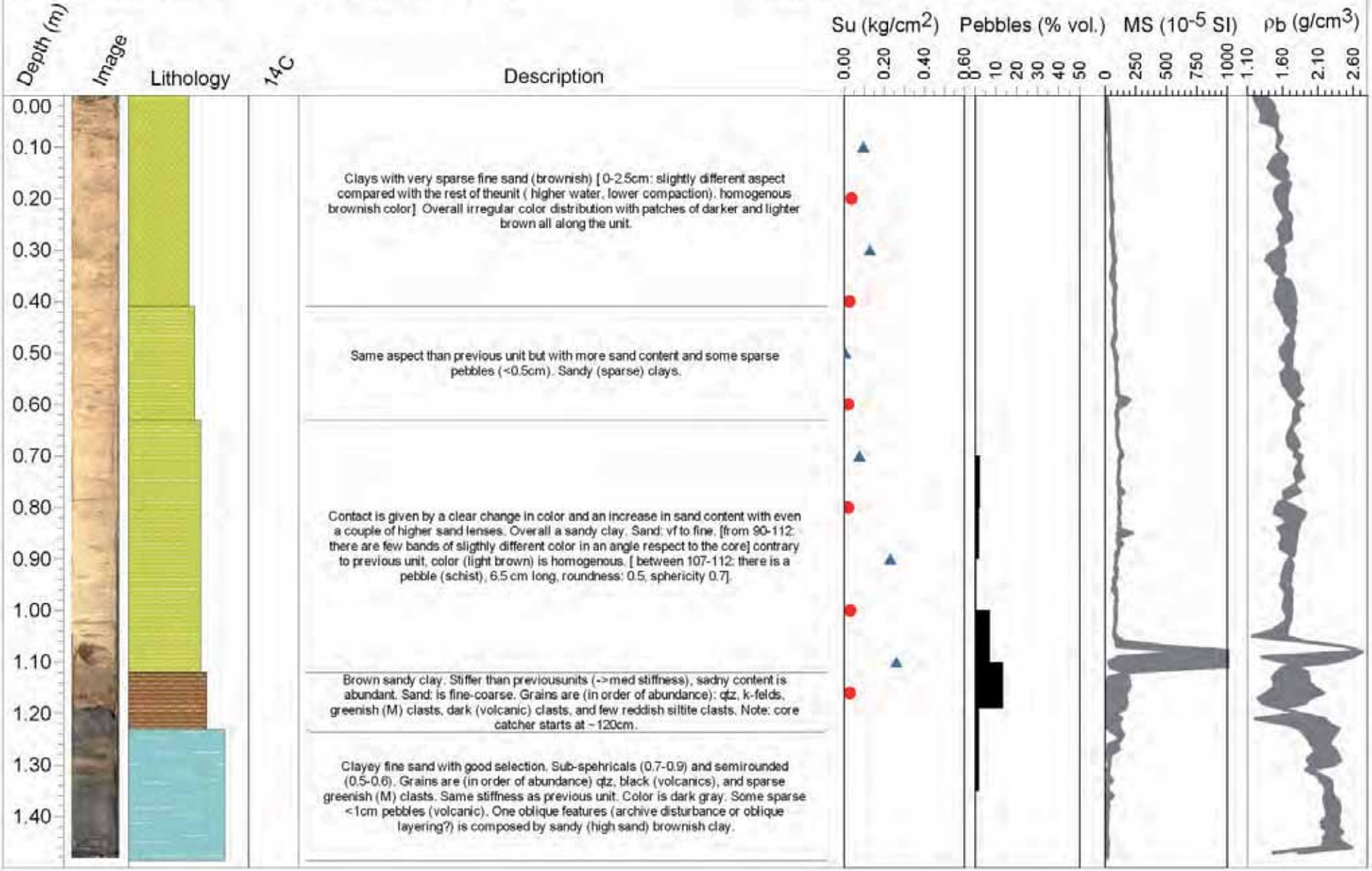

CORE: **KC19** LAT/LON: 73°7.71'S, 106°58.13'W DEPTH (mbsl): 782

KC length (cm): 139 Archive length (cm): 139 CC length (cm): 17

OSO0910

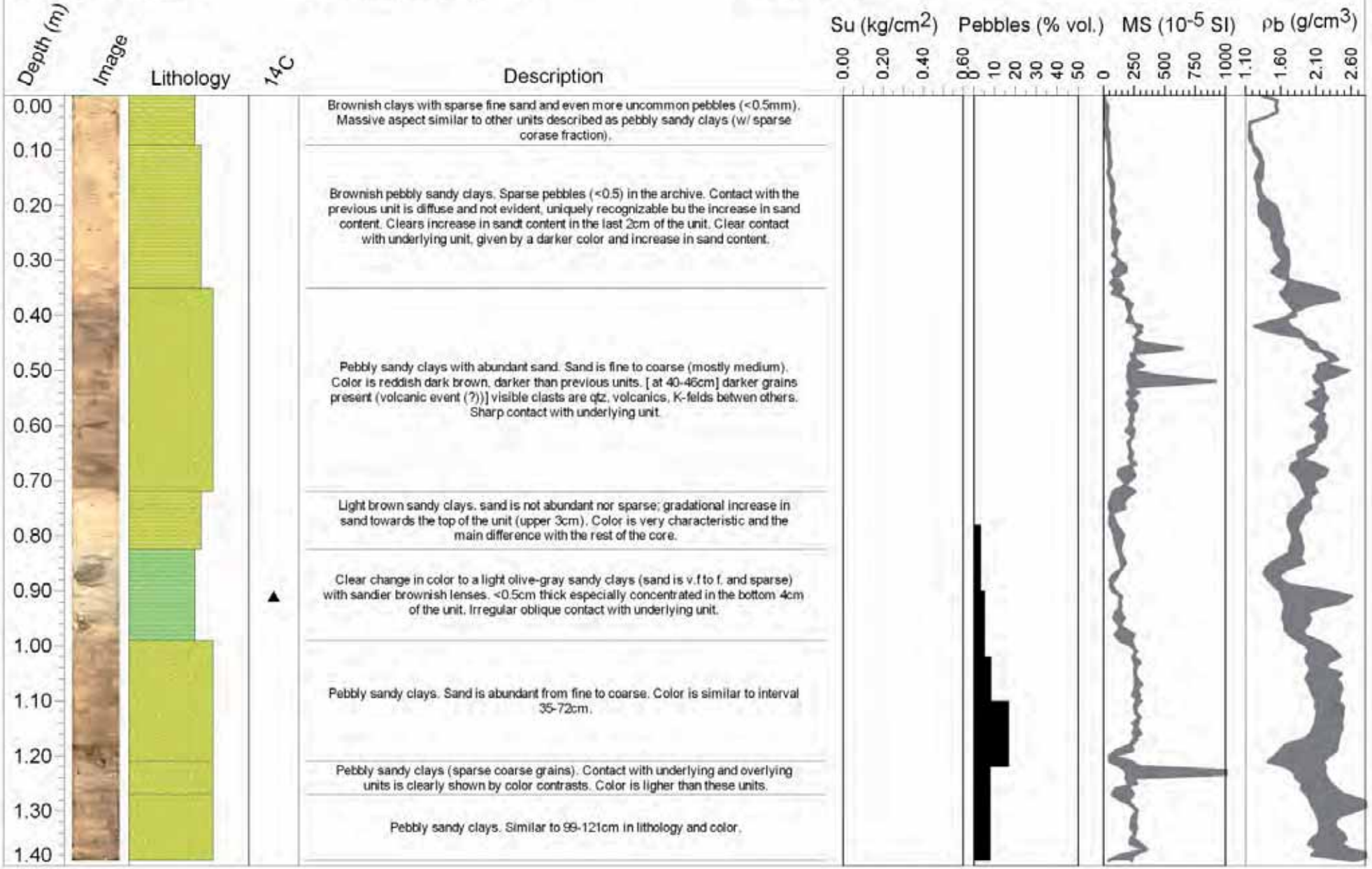

CORE: **KC20** LAT/LON: 72°54.61'S, 107°3.4'W DEPTH (mbsl): 671

KC length (cm): 15 Archive length (cm): 0 CC length (cm): 15

OSO0910

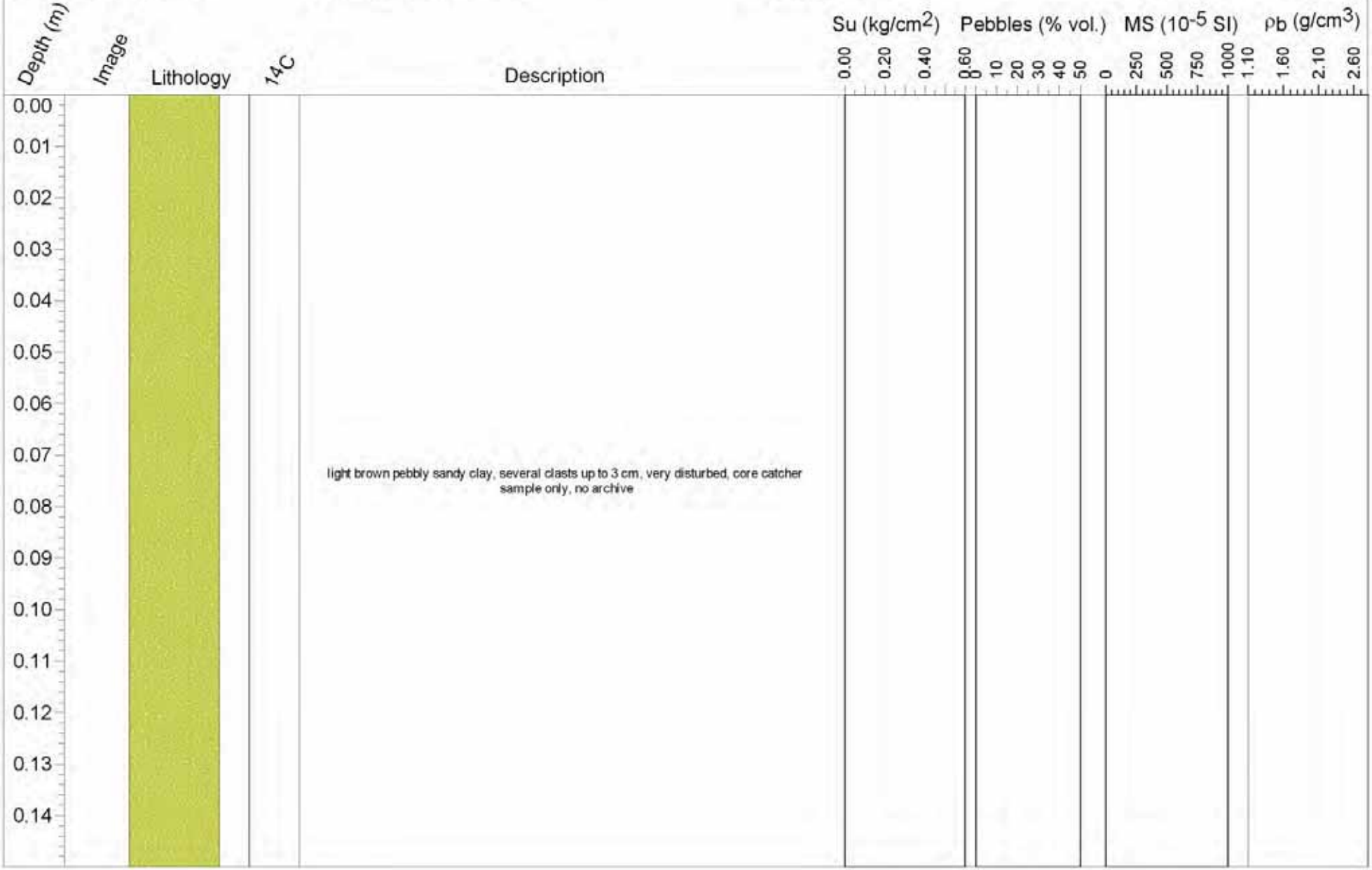

CORE: **KC21** LAT/LON: 72°49.61'S, 106°57.38'W DEPTH (mbsl): 728

KC length (cm): 70 Archive length (cm): 0 CC length (cm): 10

OSO0910

CORE: **KC22** LAT/LON: 72°49.12'S, 106°57.80'W DEPTH (mbsl): 724

KC length (cm): 115 Archive length (cm): 115 CC length (cm): 18

OSO0910

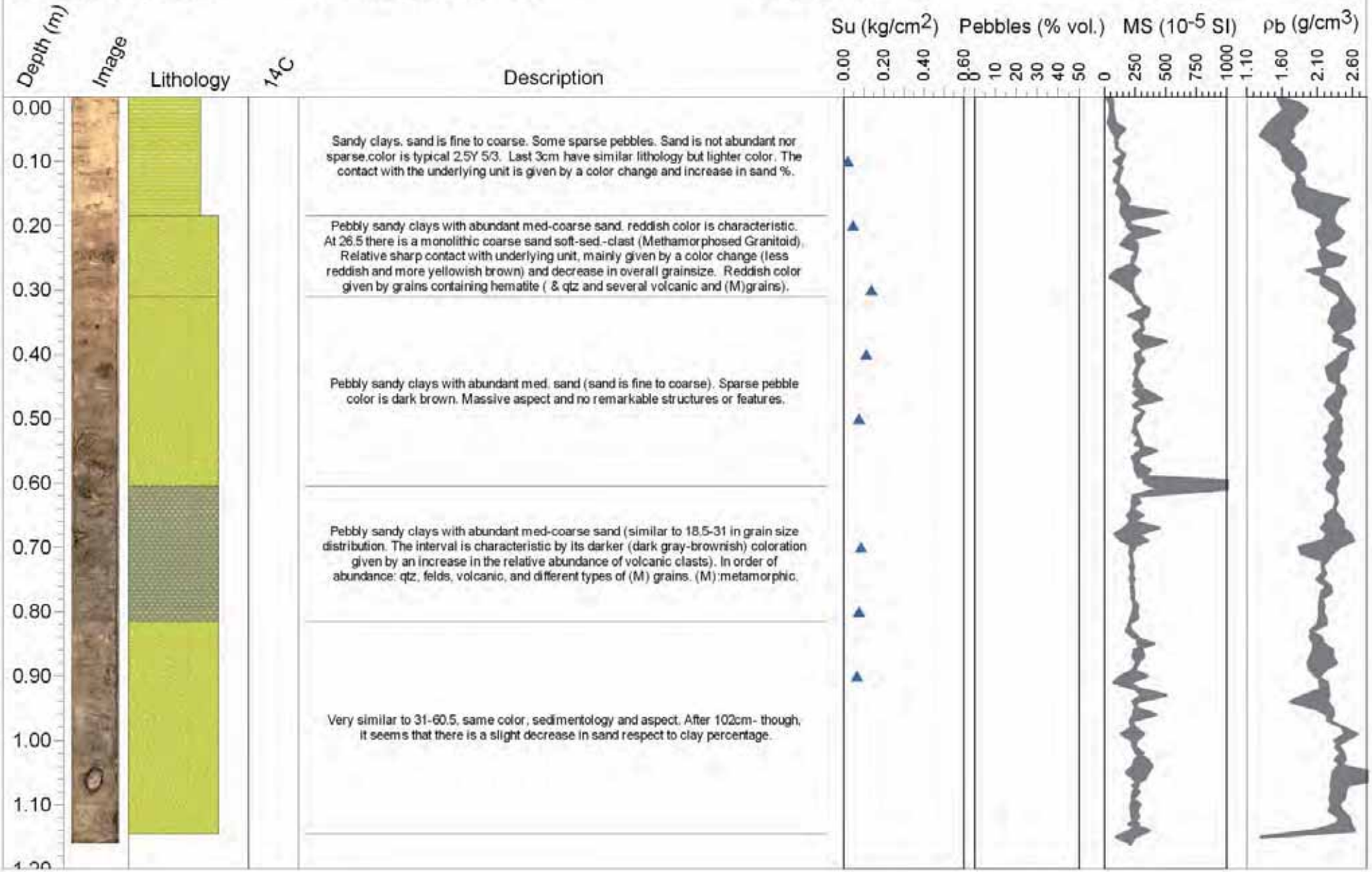

CORE: **KC23** LAT/LON: 72°53.54'S, 106°55.46'W DEPTH (mbsl): 660

KC length (cm): 36 Archive length (cm): 36 CC length (cm): 21

OSO0910

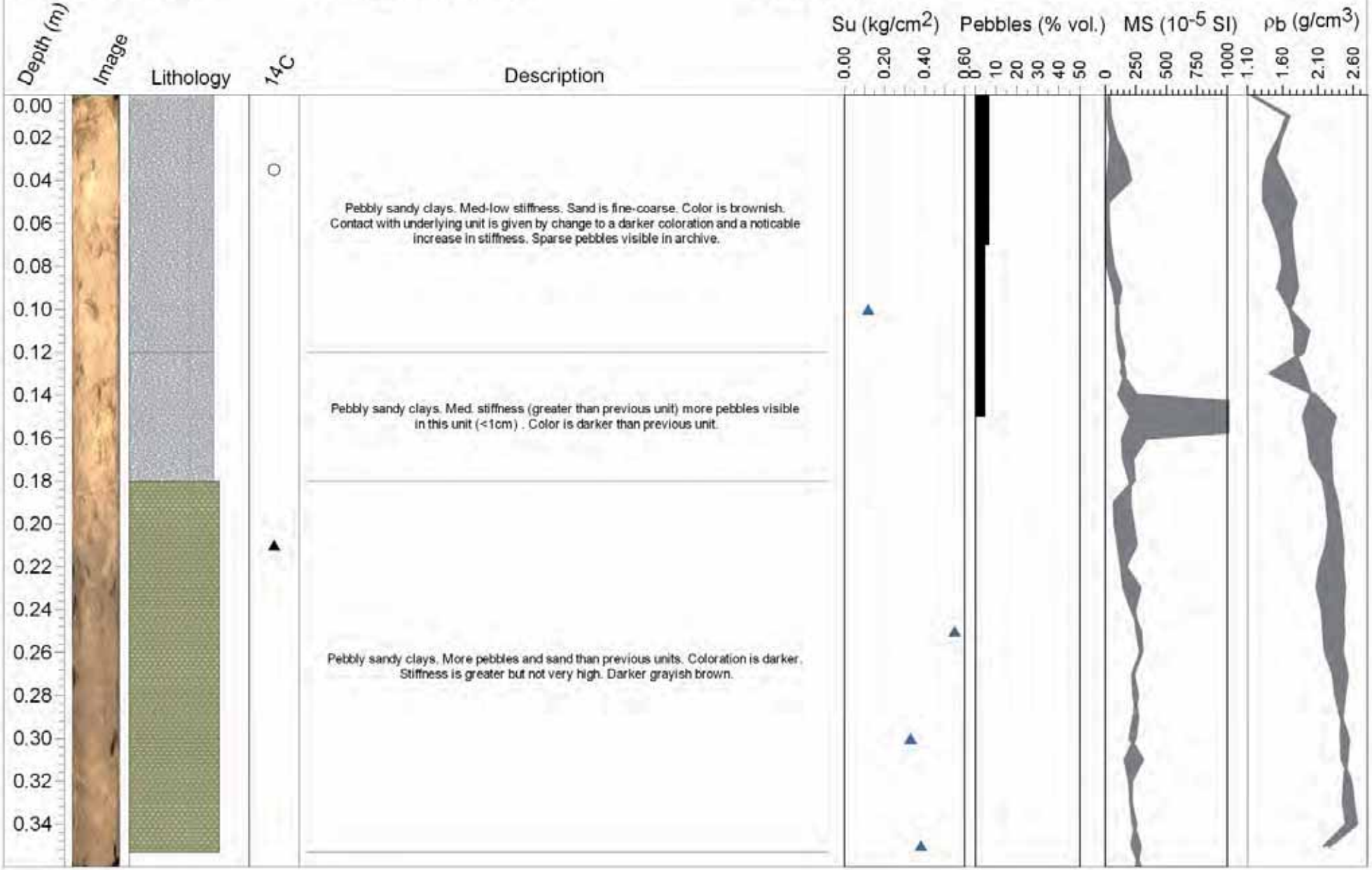

CORE: **KC24** LAT/LON: 73°14.39'S, 106°45.41'W DEPTH (mbsl): 807

KC length (cm): 160 Archive length (cm): 160 CC length (cm): 24

OSO0910

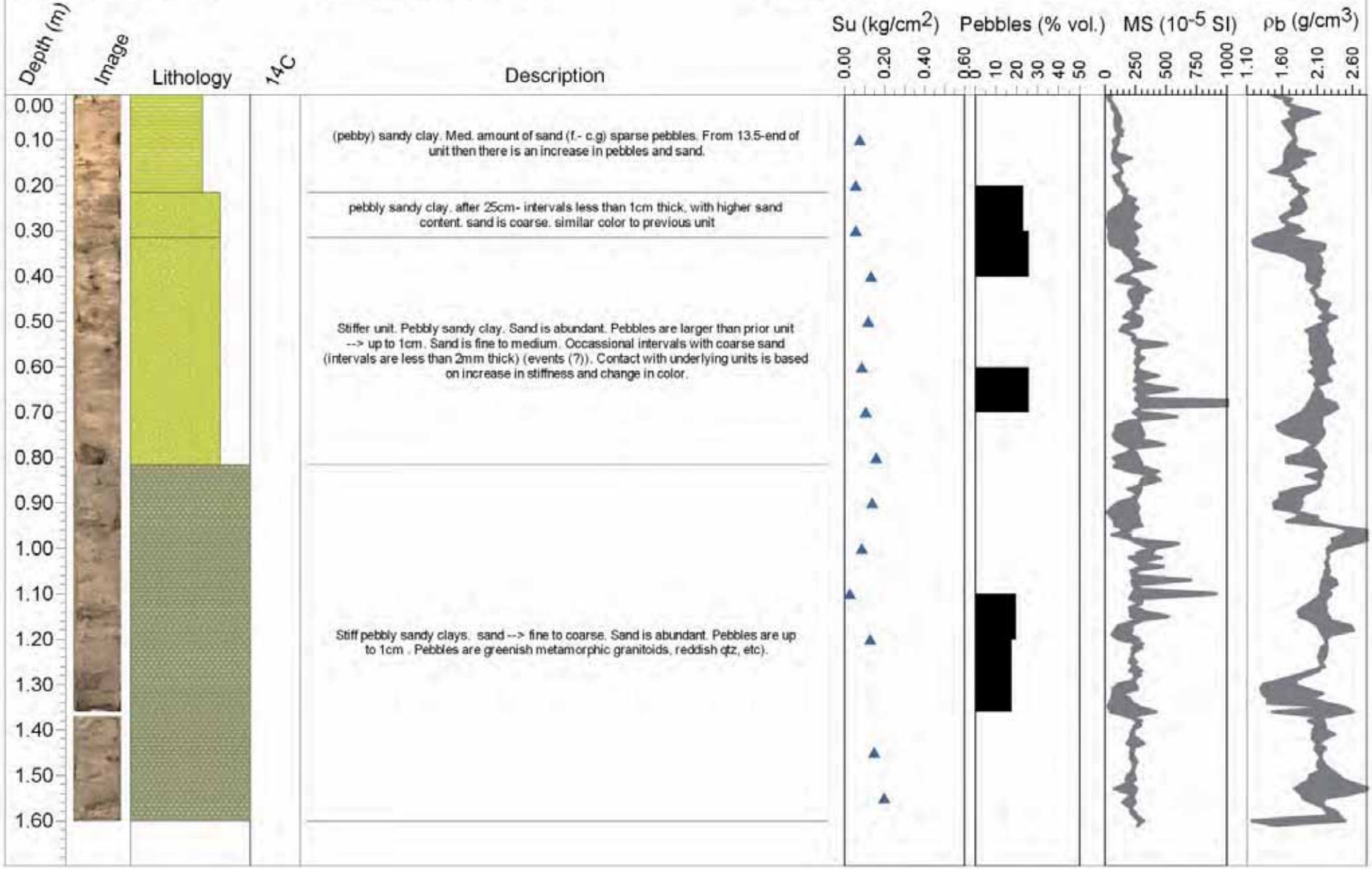

CORE: **KC25** LAT/LON: 73°15.42'S, 107°6.34'W DEPTH (mbsl): 838

KC length (cm): 77 Archive length (cm): 77 CC length (cm): 18

OSO0910

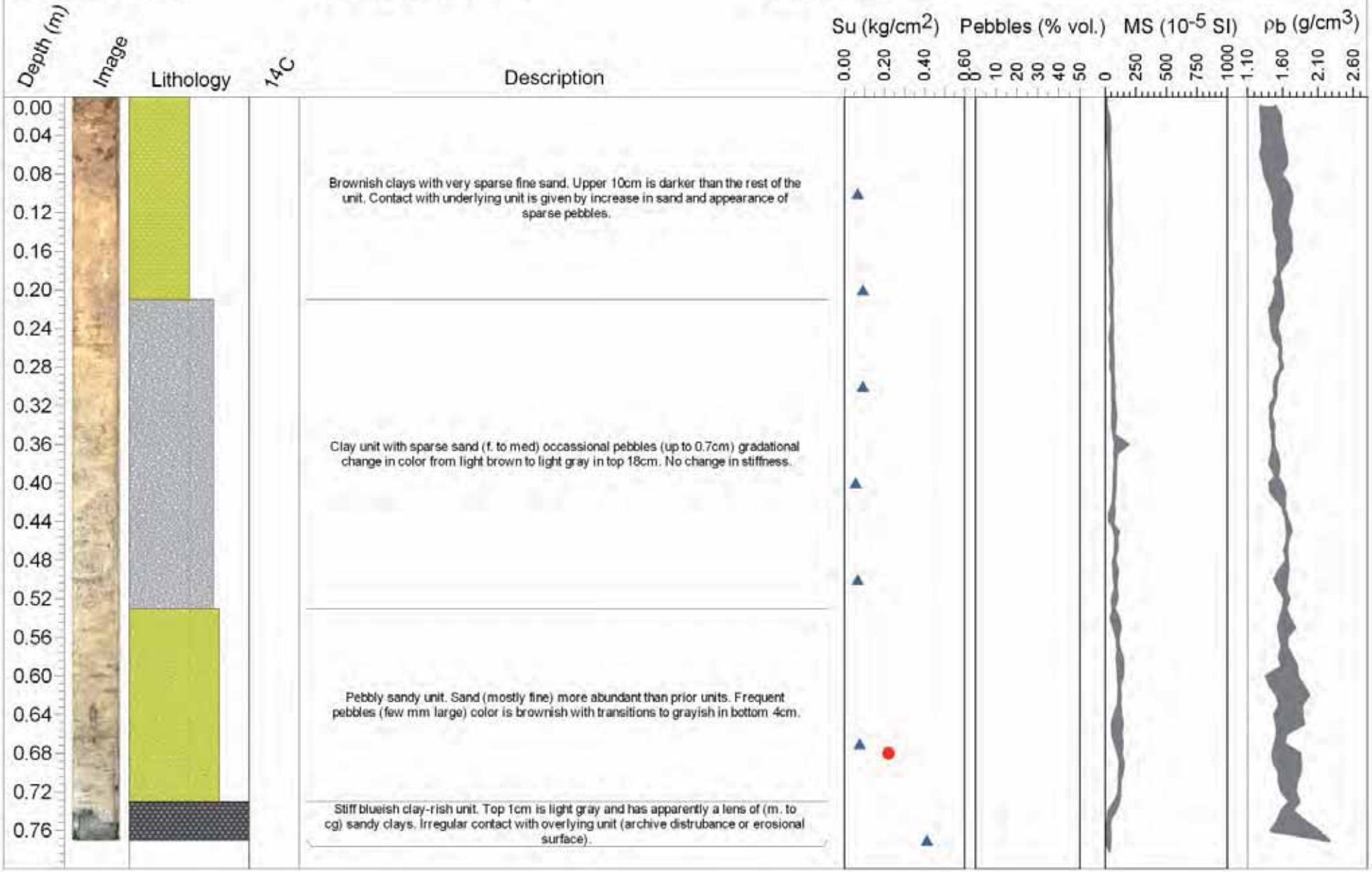

CORE: **KC26** LAT/LON: 73°15.42'S, 107°6.34'W DEPTH (mbsl): 838

KC length (cm): 106 Archive length (cm): 106 CC length (cm): 0

OSO0910

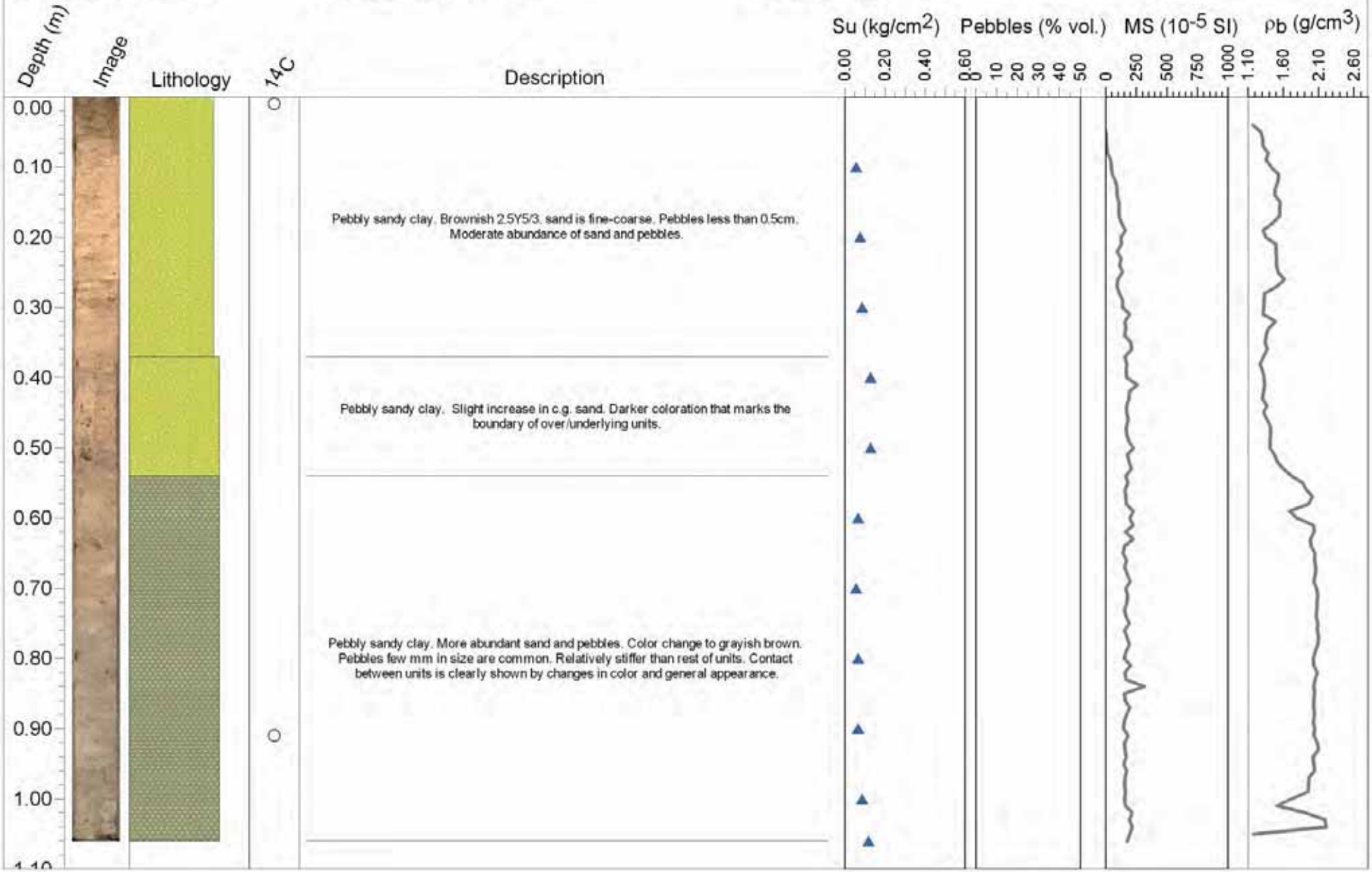

CORE: **KC27** LAT/LON: 72°52.97'S, 107°15.29'W DEPTH (mbsl): 666

KC length (cm): 52 Archive length (cm): 52 CC length (cm): 25

OSO0910

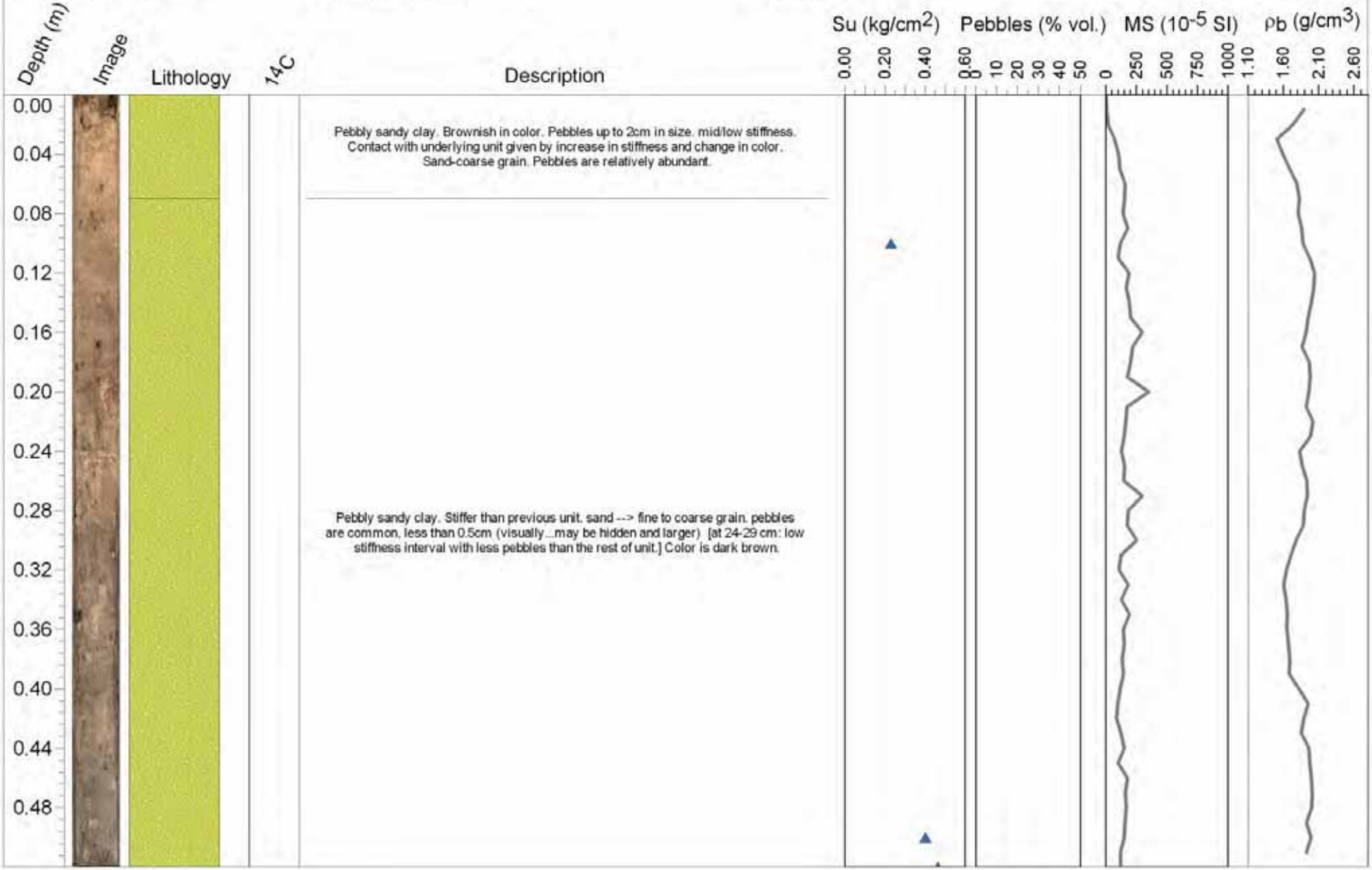

Appendix II

Core: KC04

Depth (mbsl): 729

Lat./Lon.: 72°41.8277'S, 107°6.6311'W

Kasten Core length (cm): 204 **Archive half length (cm):** 208

Cc (cm): 12.8

OSO0910

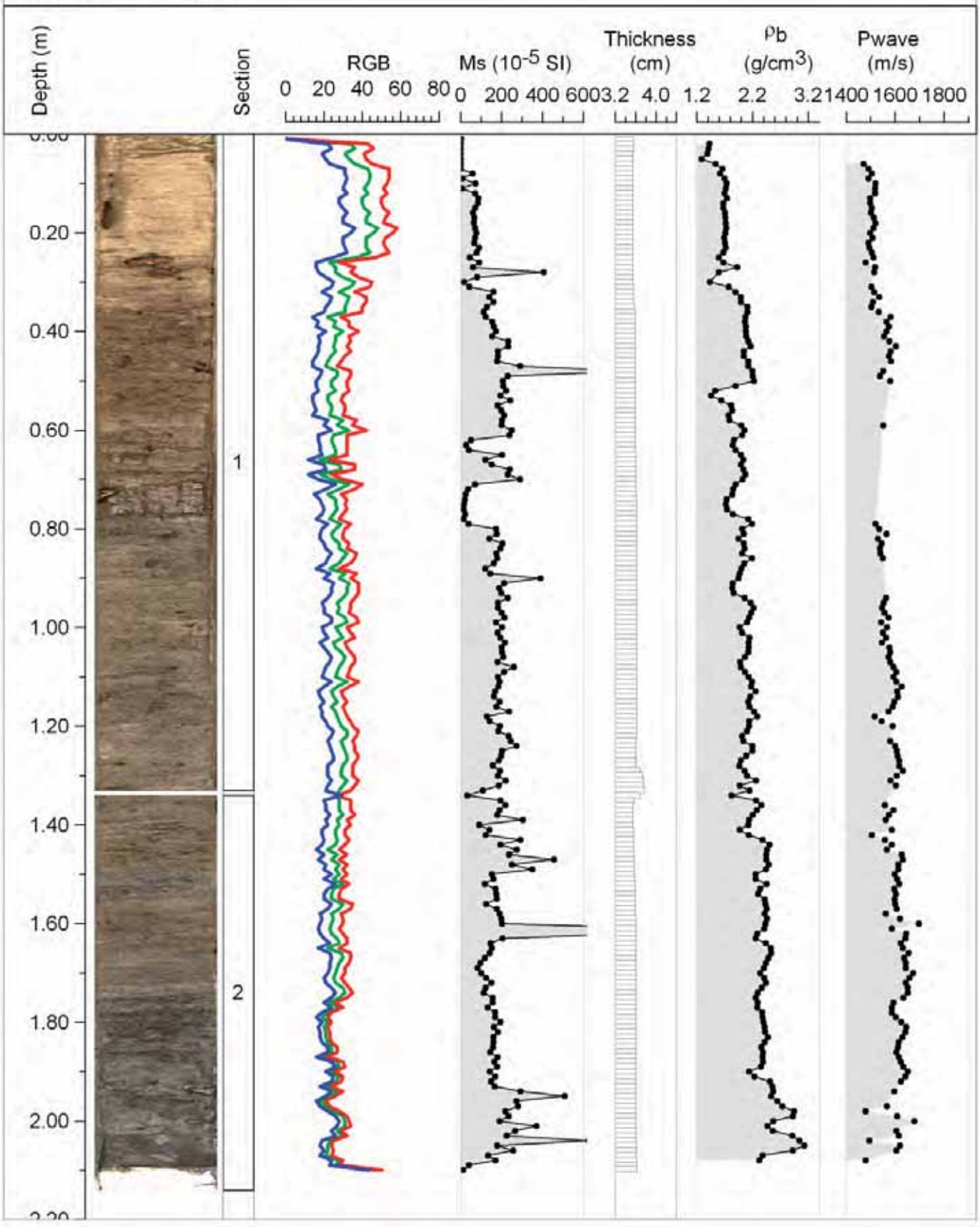

Core: KC05

Depth (mbsl): 729

Lat./Lon.: 72°41.8277'S, 107°6.6311'W

Kasten Core length (cm): 249 **Archive half length (cm):** 245

Cc (cm): 28

OSO0910

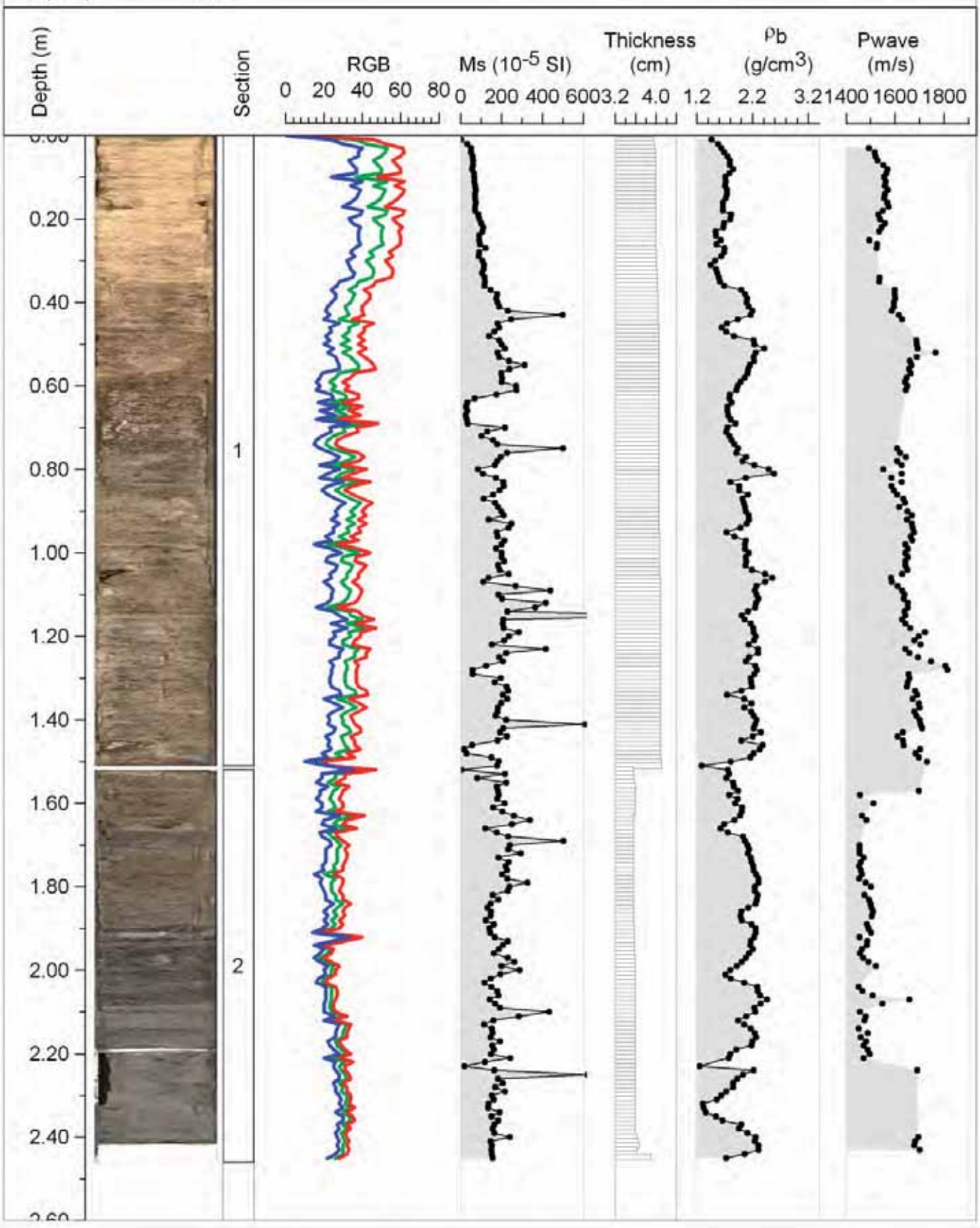

Core: KC06-A

Depth (mbsl): 614

Lat./Lon.: 72°7.95'S, 106°54.60'W

Kasten Core length (cm): 104 **Archive half length (cm):** 103

Cc (cm): 22

OSO0910

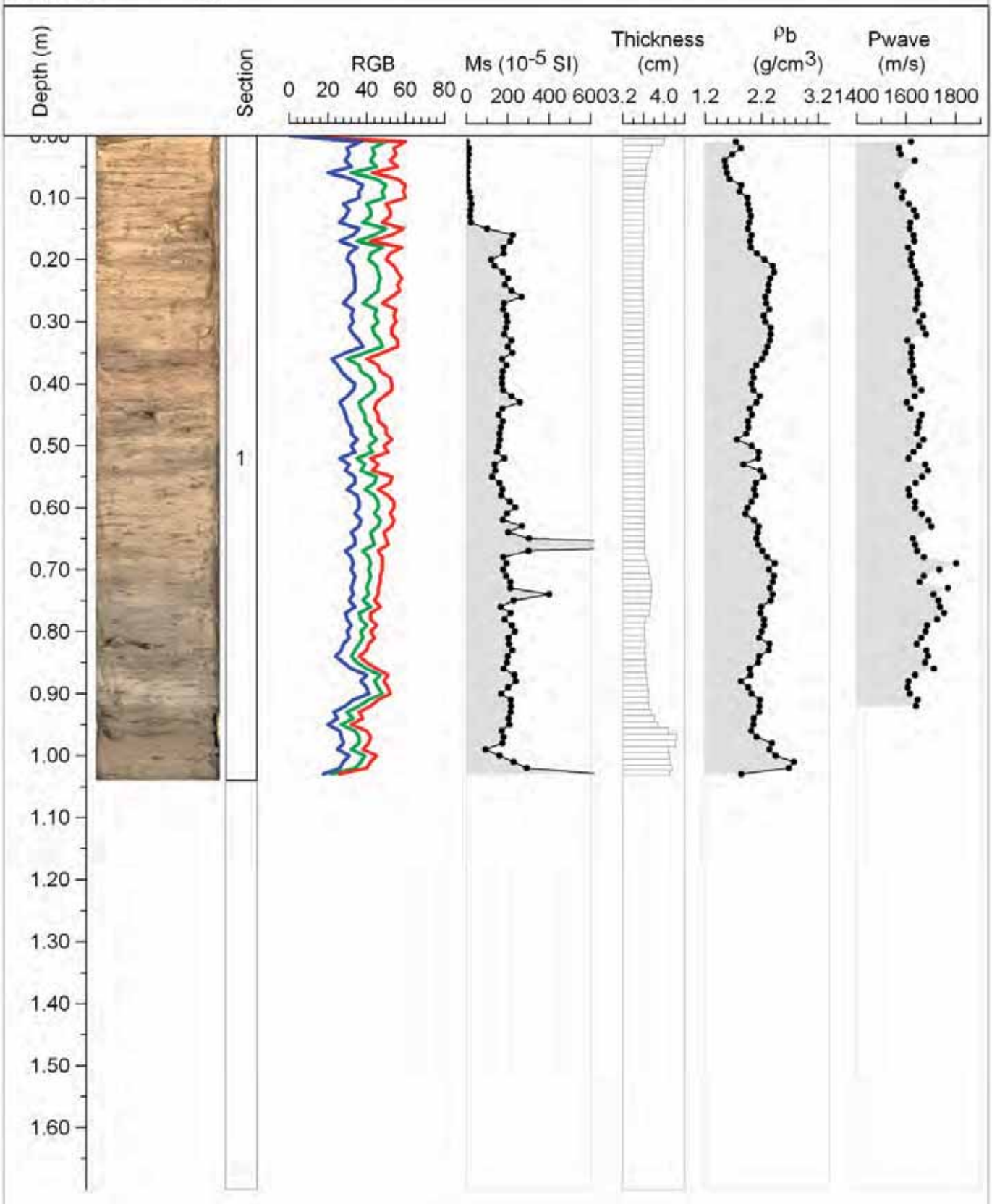

Core: KC06-B

Depth (mbsl): 614

Lat./Lon.: 72°7.95'S, 106°54.60'W

Kasten Core length (cm): 104 **Archive half length (cm):** 103

Cc (cm): 22

OSO0910

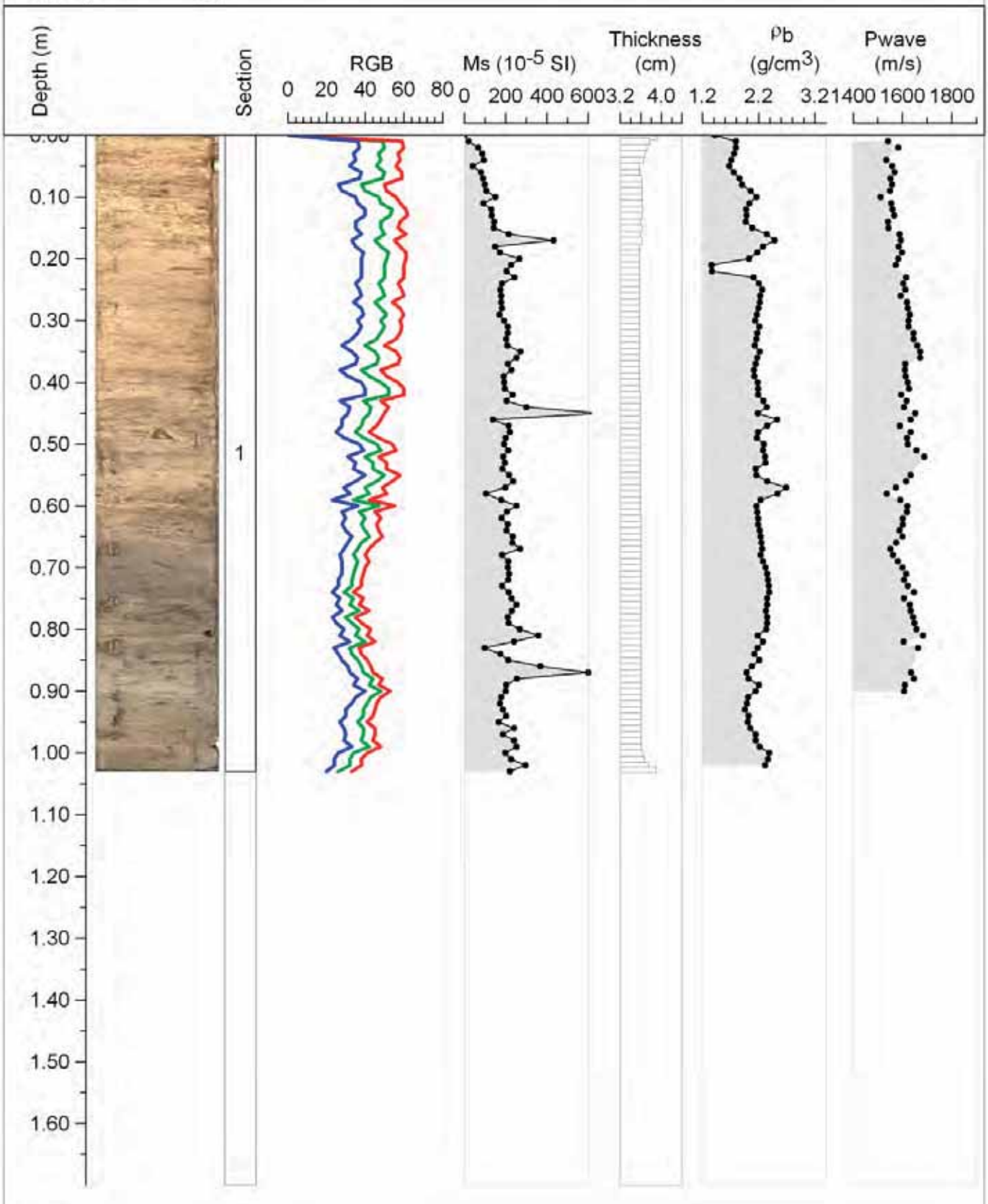

Core: KC07

Depth (mbsl): 707

Lat./Lon.: 72°20.3635'S, 106°52.9350'W

Kasten Core length (cm): 63 **Archive half length (cm):** 50

Cc (cm): 13

OSO0910

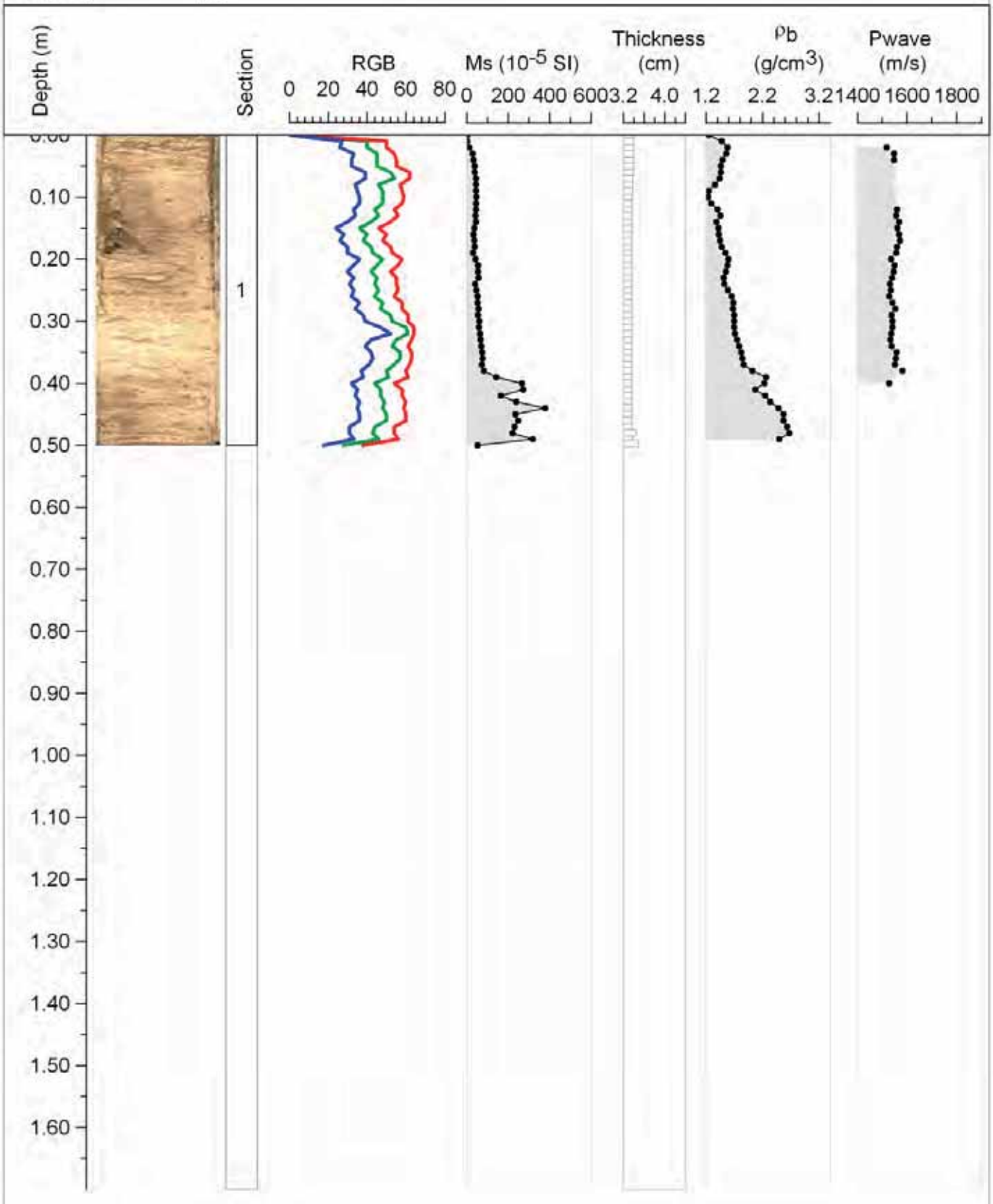

Core: KC08

Depth (mbsl): 711

Lat./Lon.: 72°20.8110'S, 106°52.6320'W

Kasten Core length (cm): 60 **Archive half length (cm):** 40

Cc (cm): 20

OSO0910

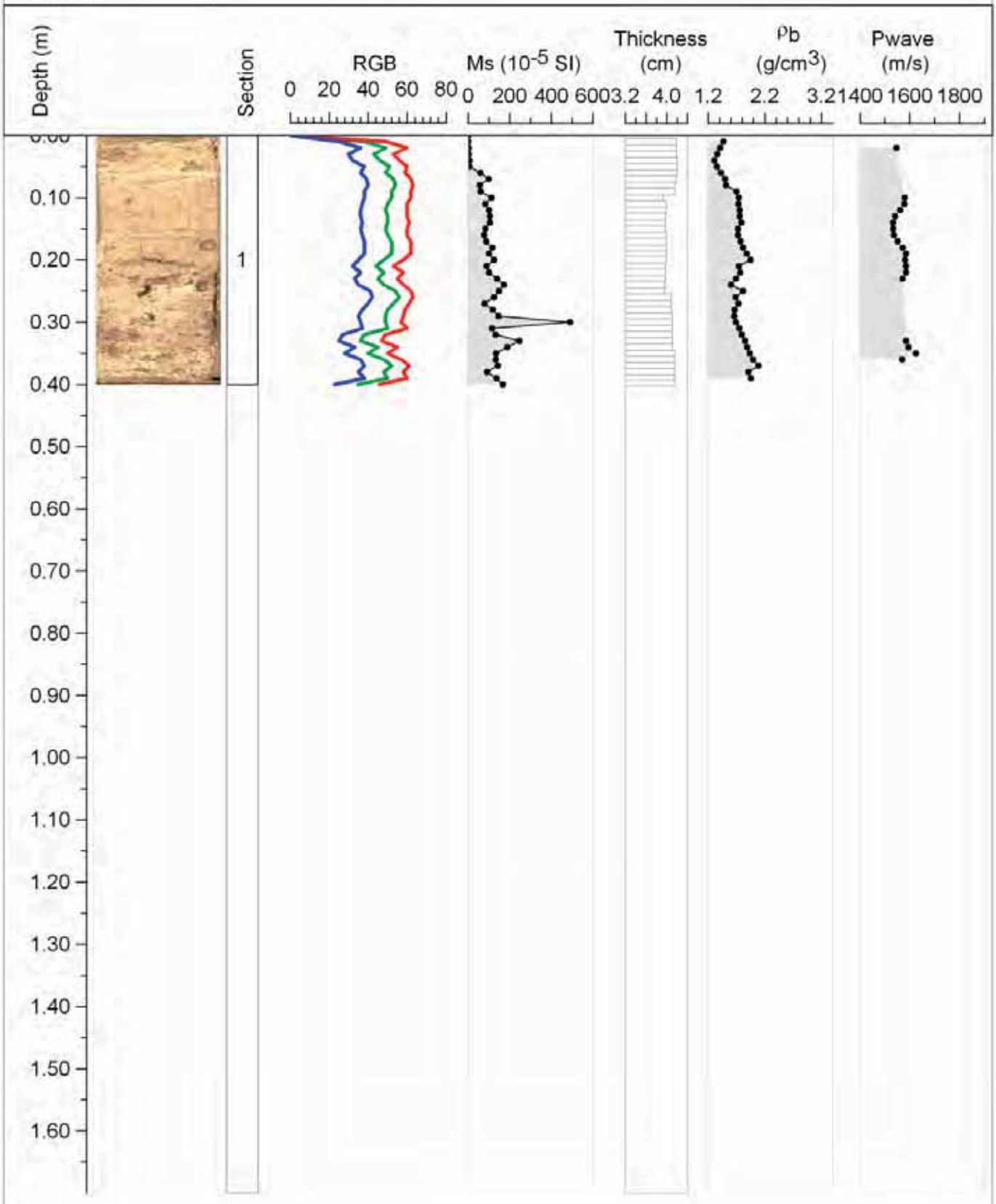

Core: KC09-A

Depth (mbsl): 548

Lat./Lon.: 72°29.2000'S, 106°38.3400'W

Kasten Core length (cm): 45 **Archive half length (cm):** 45

Cc (cm): 24

OSO0910

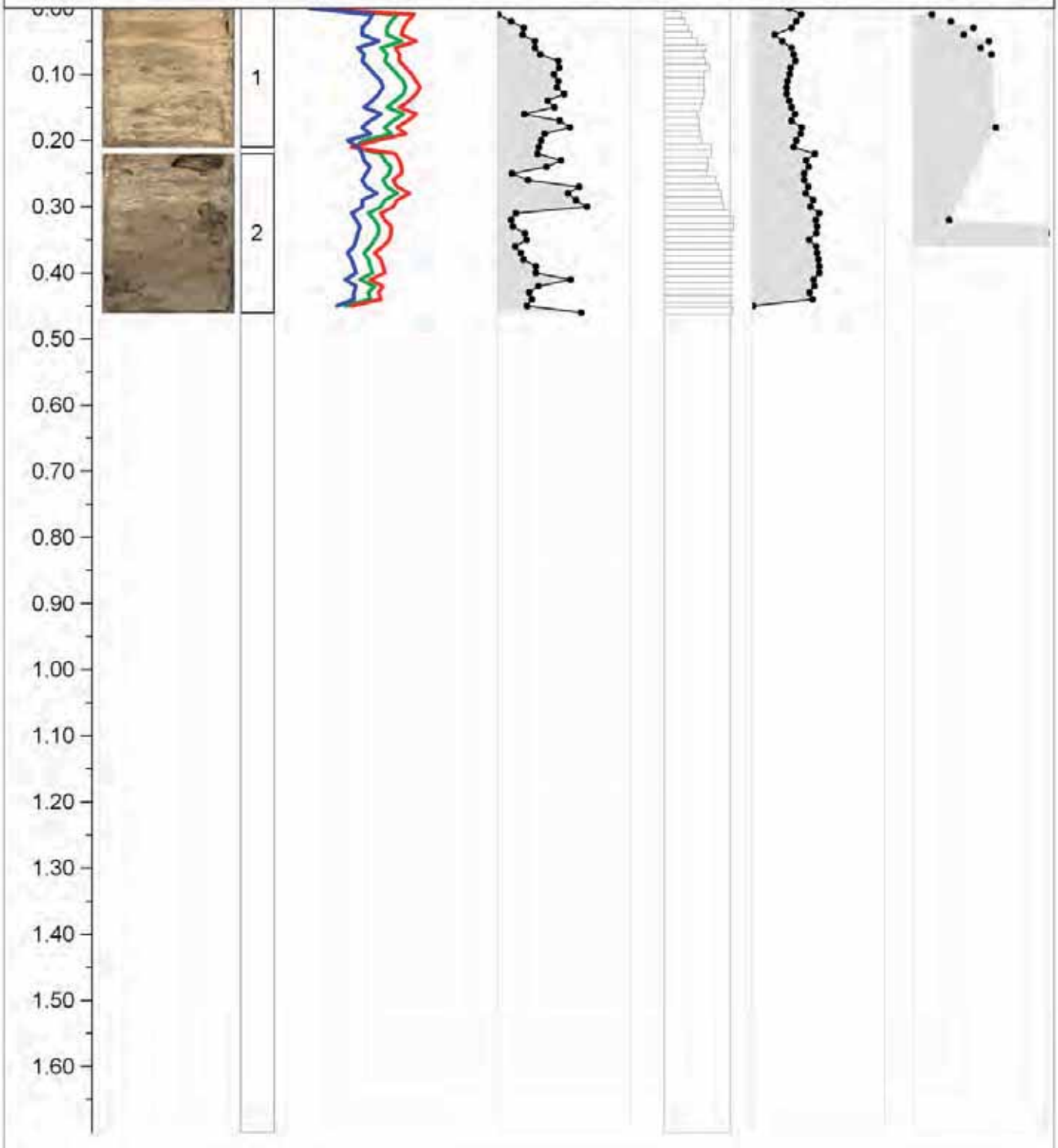

Core: KC09-B

Depth (mbsl): 548

Lat./Lon.: 72°29.2000'S, 106°38.3400'W

Kasten Core length (cm): 45 **Archive half length (cm):** 45

Cc (cm): 24

OSO0910

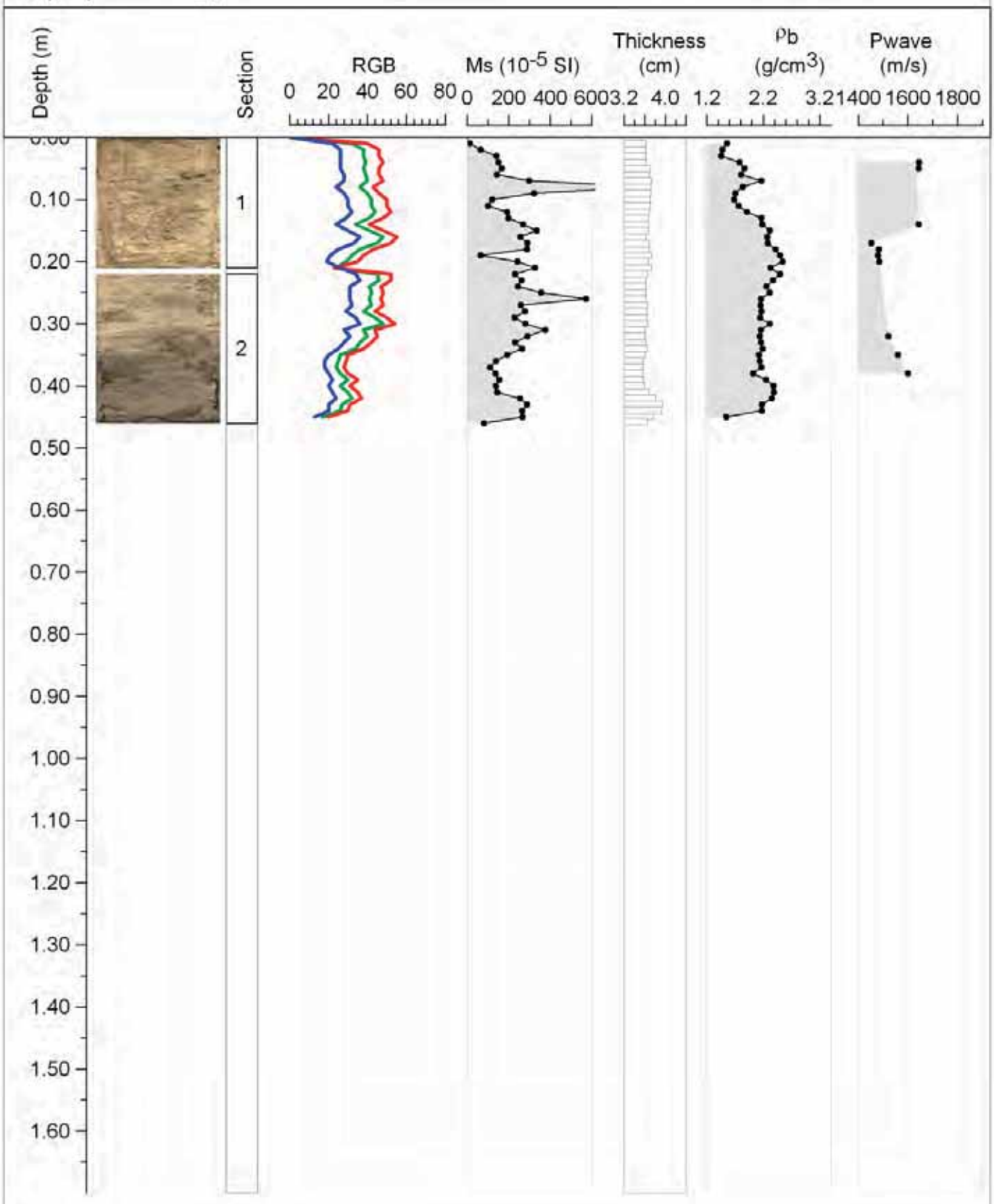

Core: KC10-A

Depth (mbsl): 687

Lat./Lon.: 72°29.5404'S, 106°46.4141'W

Kasten Core length (cm): 88 **Archive half length (cm):** 72

Cc (cm): 13

OSO0910

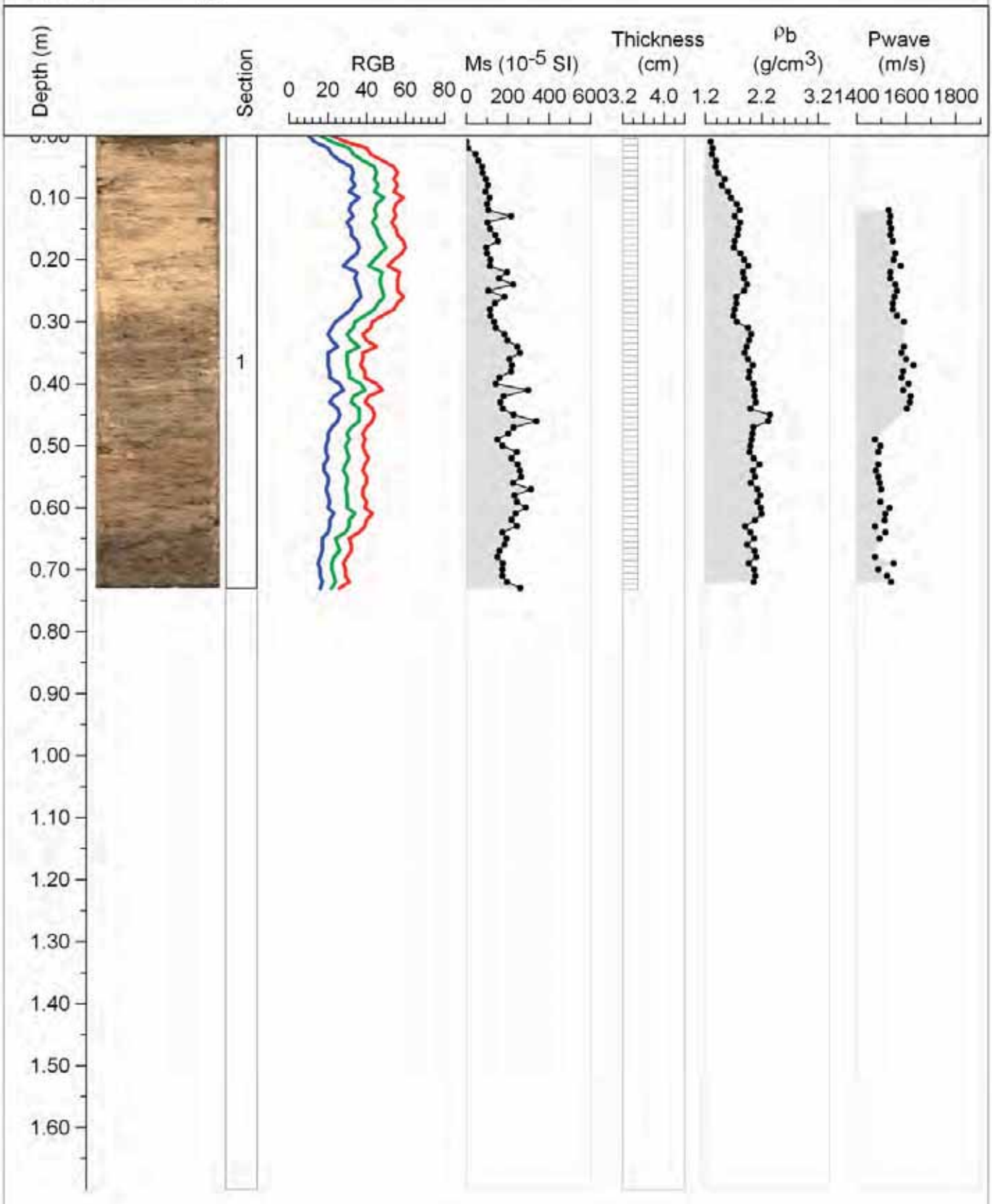

Core: KC10-B

Depth (mbsl): 687

Lat./Lon.: 72°29.5404'S, 106°46.4141'W

Kasten Core length (cm): 88 **Archive half length (cm):** 88

Cc (cm): 13

OSO0910

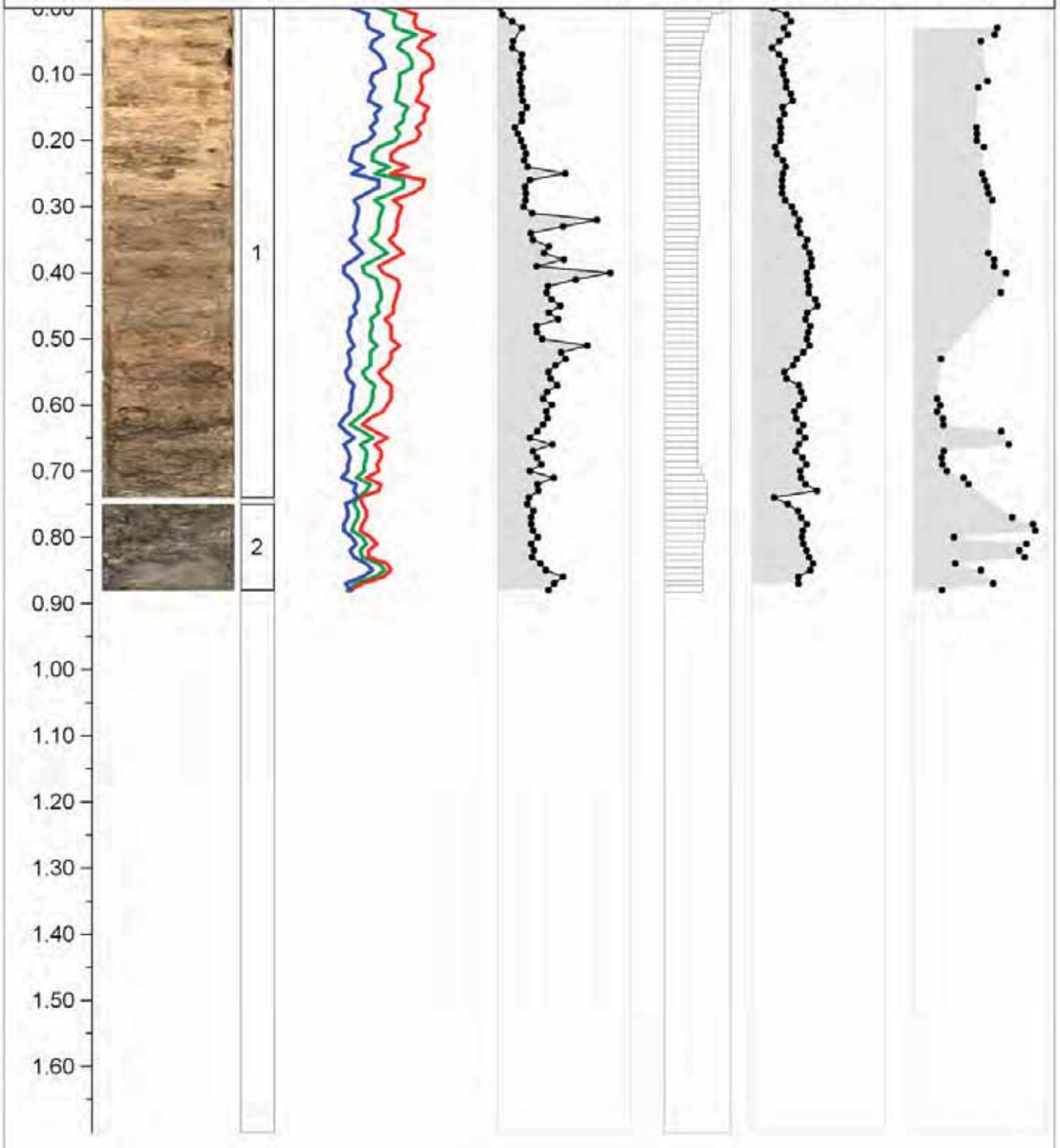

Core: KC11-A

Depth (mbsl): 733

Lat./Lon.: 72°34.57'S, 107°09.11'W

Kasten Core length (cm): 150 **Archive half length (cm):** 145

Cc (cm): 16

OSO0910

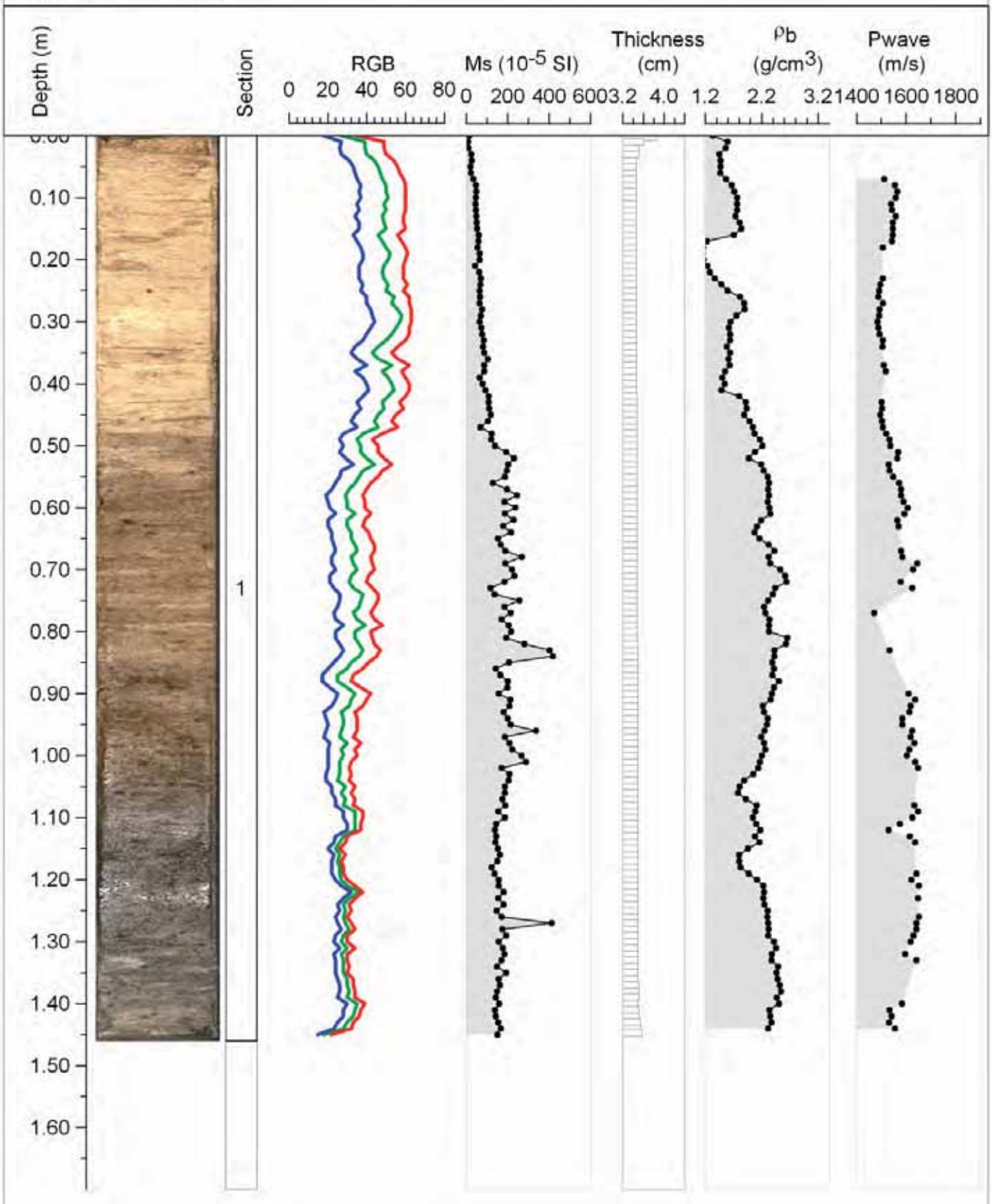

Core: KC11-B

Depth (mbsl): 733

Lat./Lon.: 72°34.57'S, 107°09.11'W

Kasten Core length (cm): 150 **Archive half length (cm):** 146

Cc (cm): 16

OSO0910

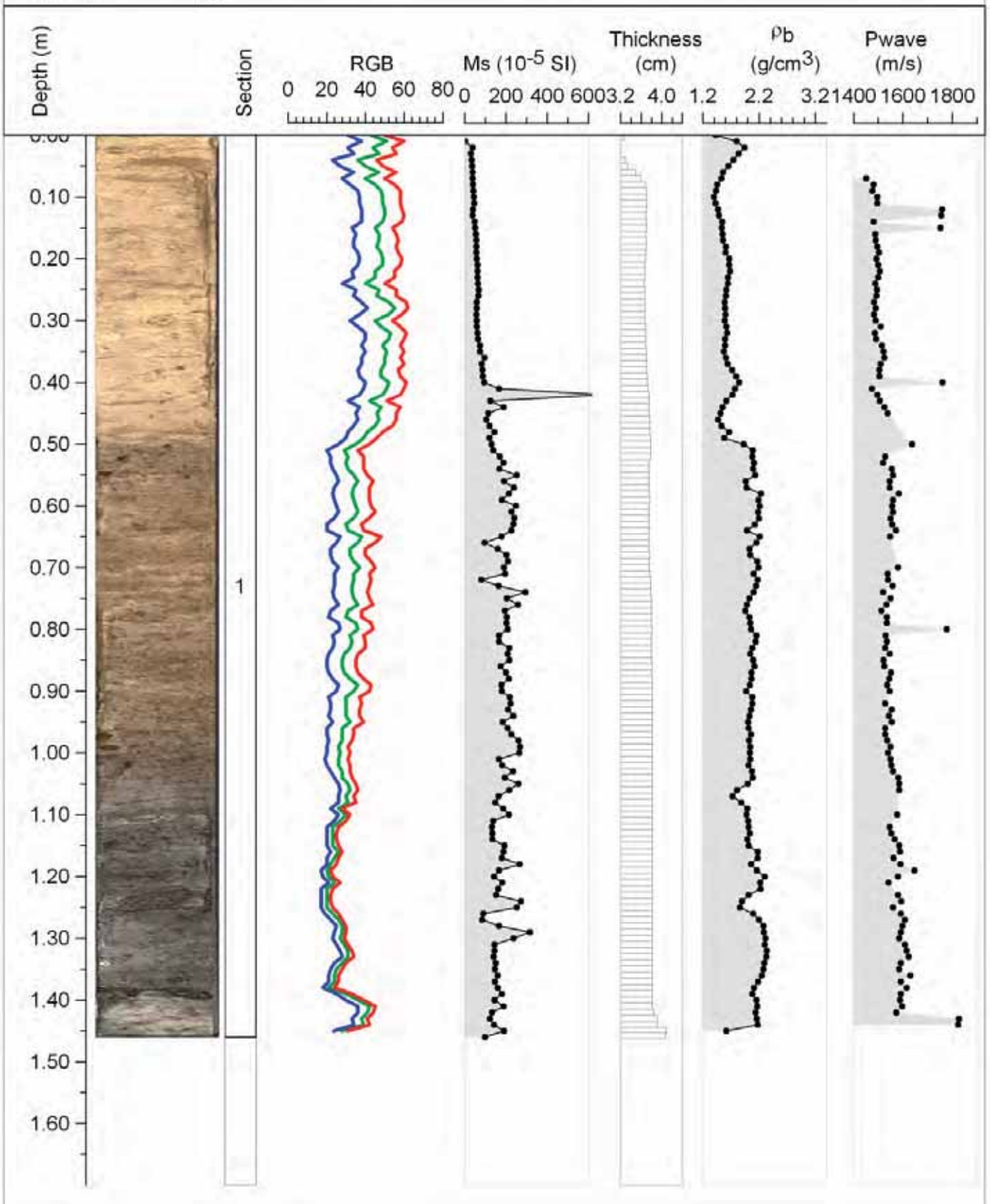

Core: KC14-A

Depth (mbsl): 639

Lat./Lon.: 72°39.02'S, 107°30.78'W

Kasten Core length (cm): 72 **Archive half length (cm):** 71

Cc (cm): 16

OSO0910

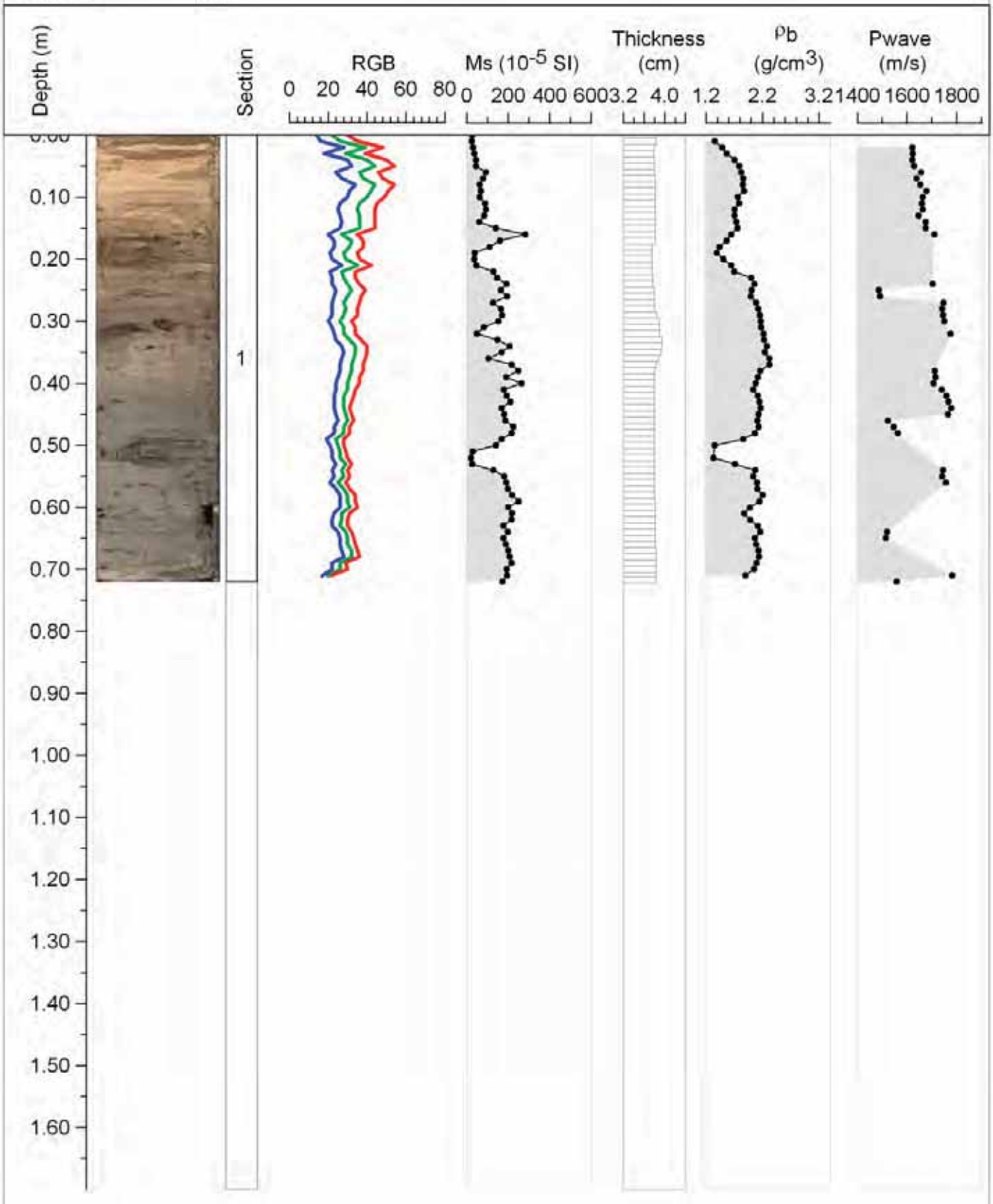

Core: KC14-B

Depth (mbsl): 639

Lat./Lon.: 72°39.02'S, 107°30.78'W

Kasten Core length (cm): 72 **Archive half length (cm):** 63

Cc (cm): 16

OSO0910

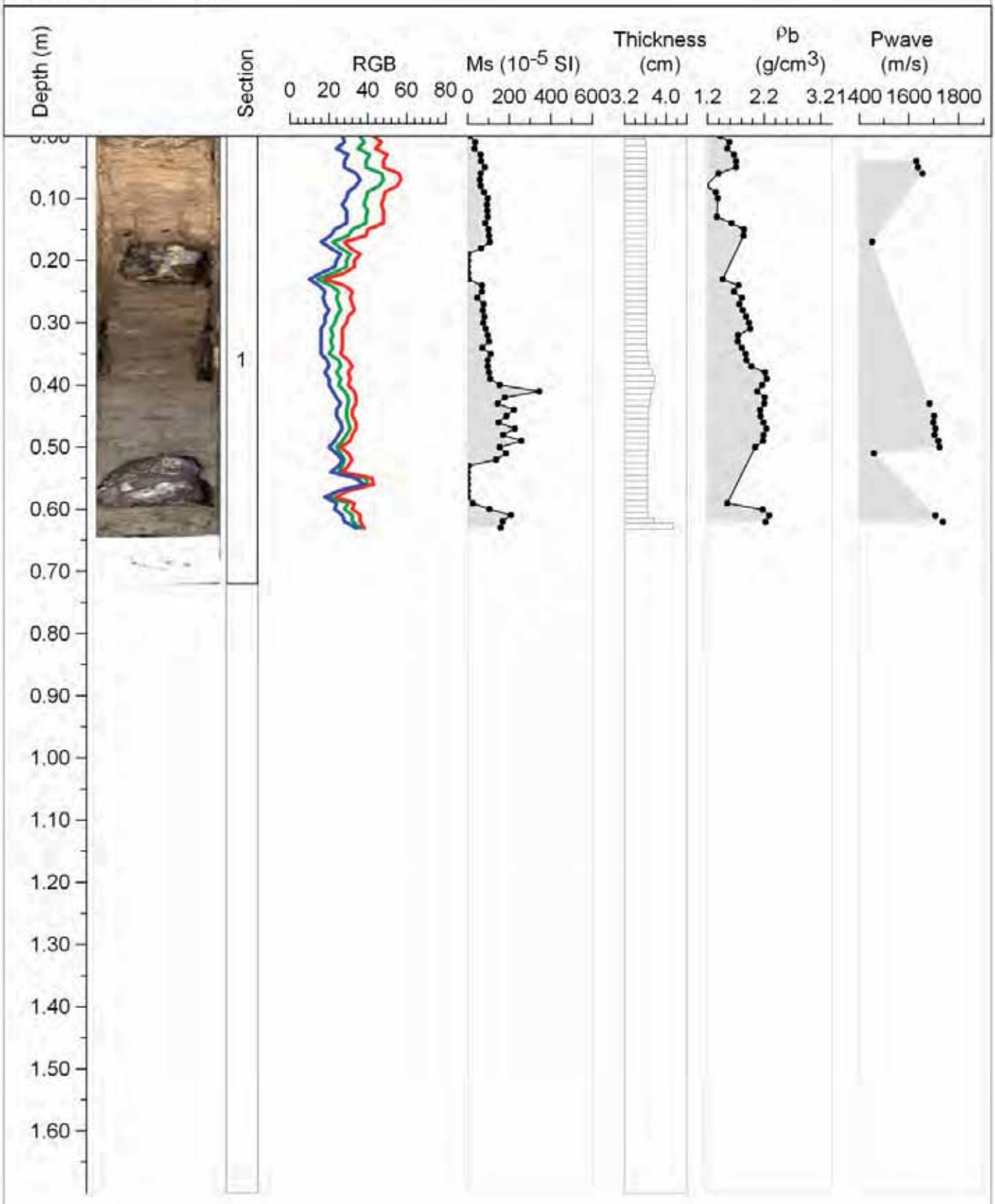

Core: KC15-A
Depth (mbsl): 1257
Lat./Lon.: 73°21.62'S, 101°50.17'W
Kasten Core length (cm): 130 **Archive half length (cm):** 131
Cc (cm): 14

OSO0910

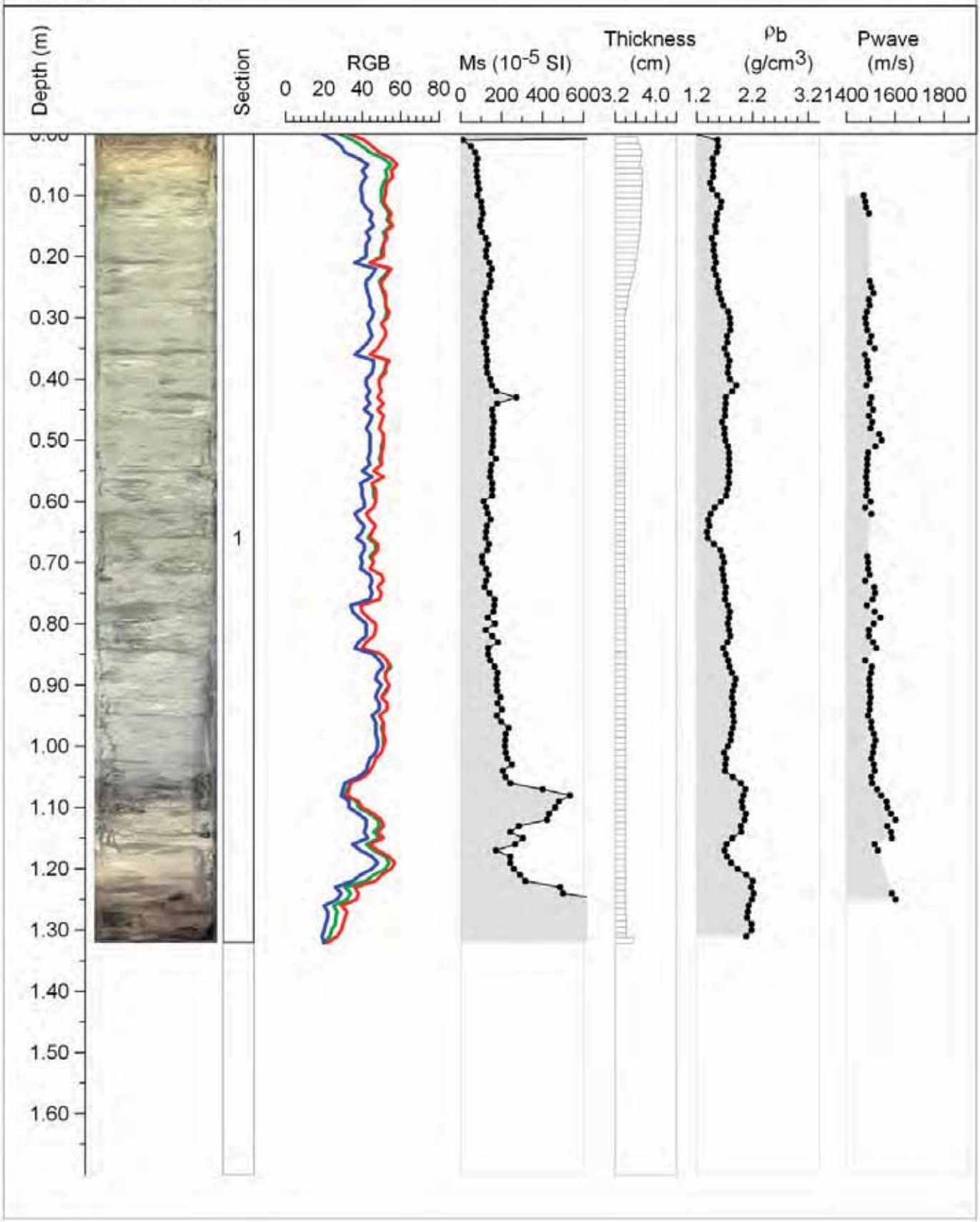

Core: KC15-B

Depth (mbsl): 1257

Lat./Lon.: 73°21.62'S, 101°50.17'W

Kasten Core length (cm): 130 **Archive half length (cm):** 119

Cc (cm): 14

OSO0910

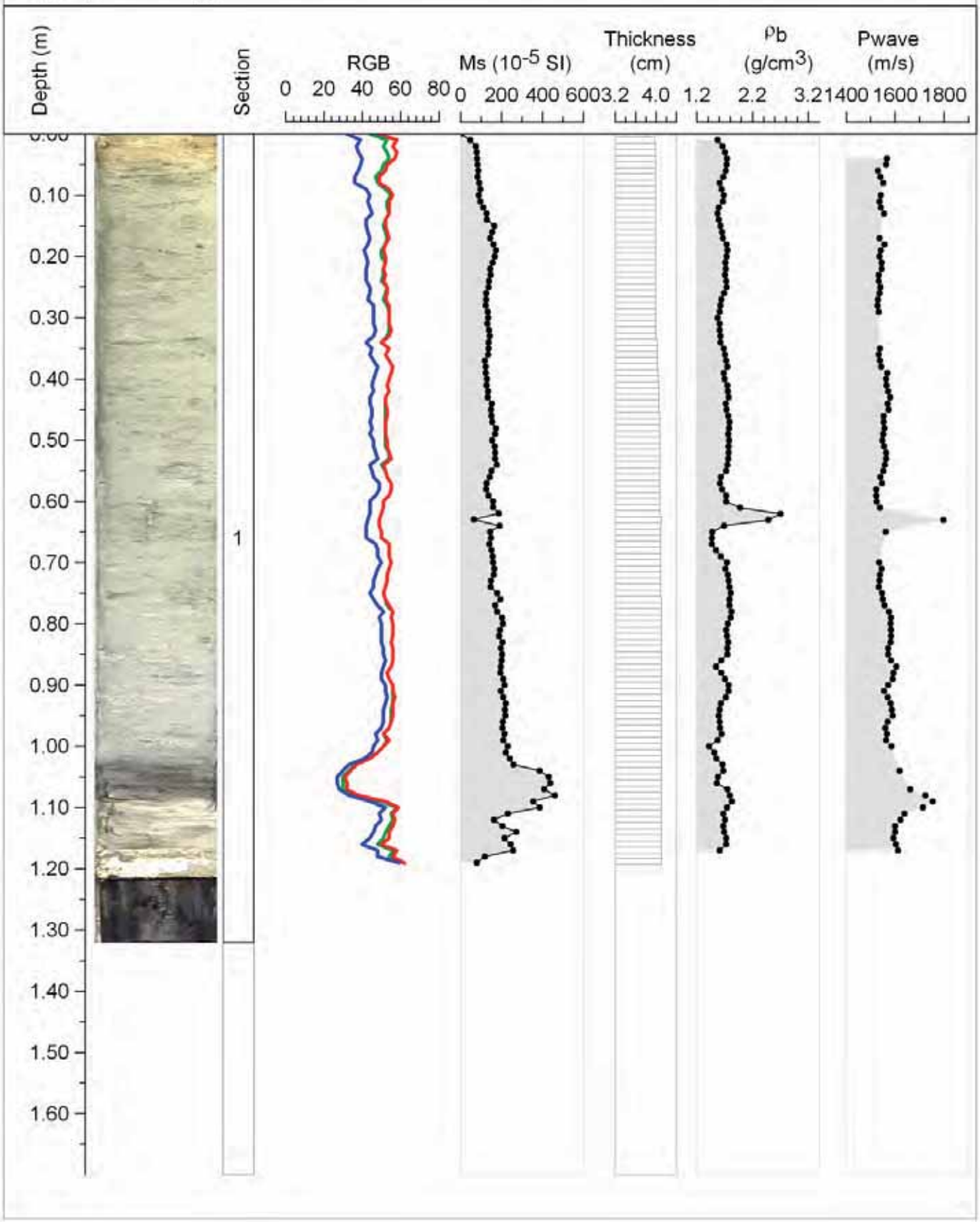

Core: KC16-A

Depth (mbsl): 706

Lat./Lon.: 73°27.24'S, 102°4.75'W

Kasten Core length (cm): 38 **Archive half length (cm):** 39

Cc (cm): 12

OSO0910

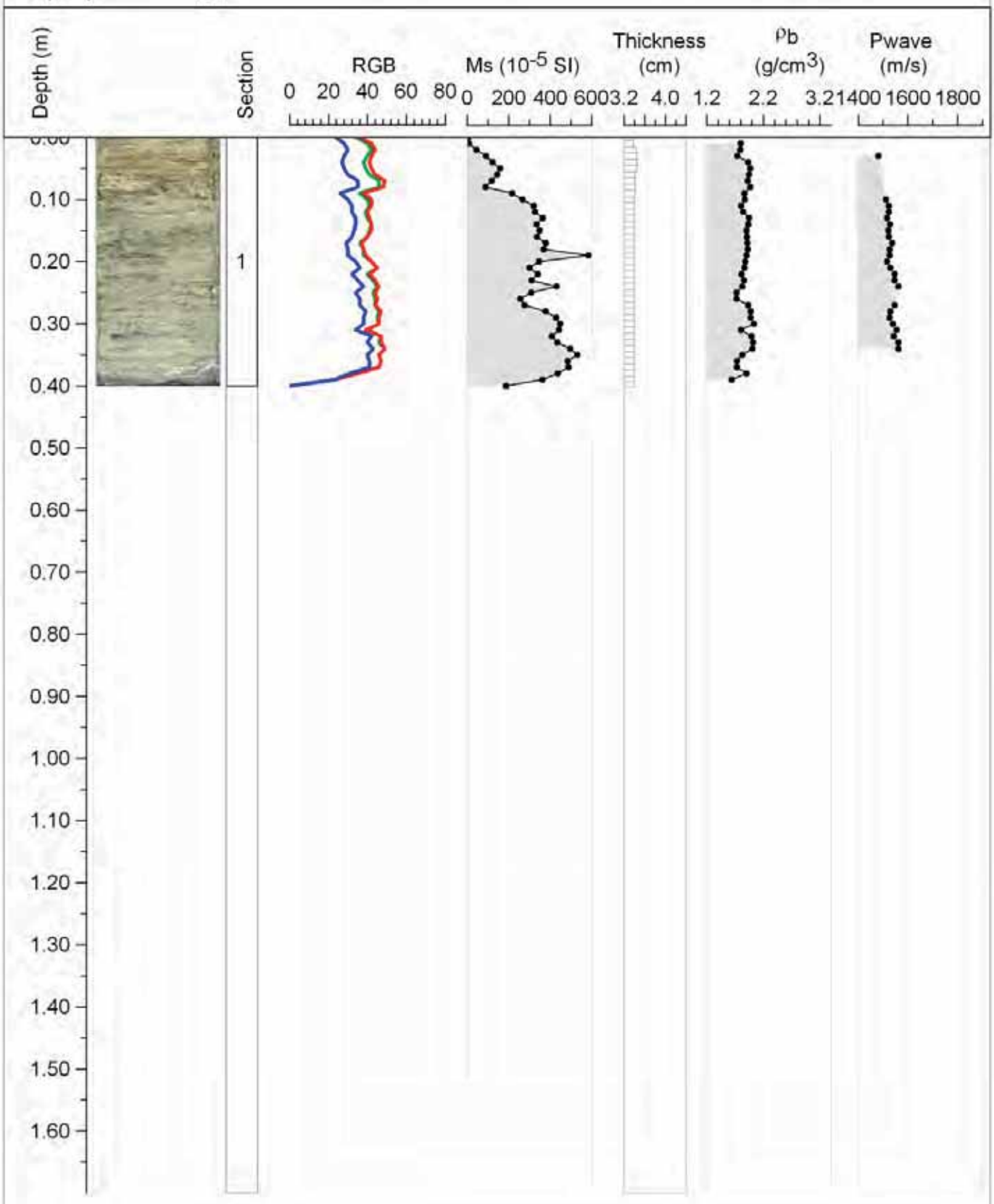

Core: KC16-B

Depth (mbsl): 706

Lat./Lon.: 73°27.24'S, 102°4.75'W

Kasten Core length (cm): 38 **Archive half length (cm):** 39

Cc (cm): 12

OSO0910

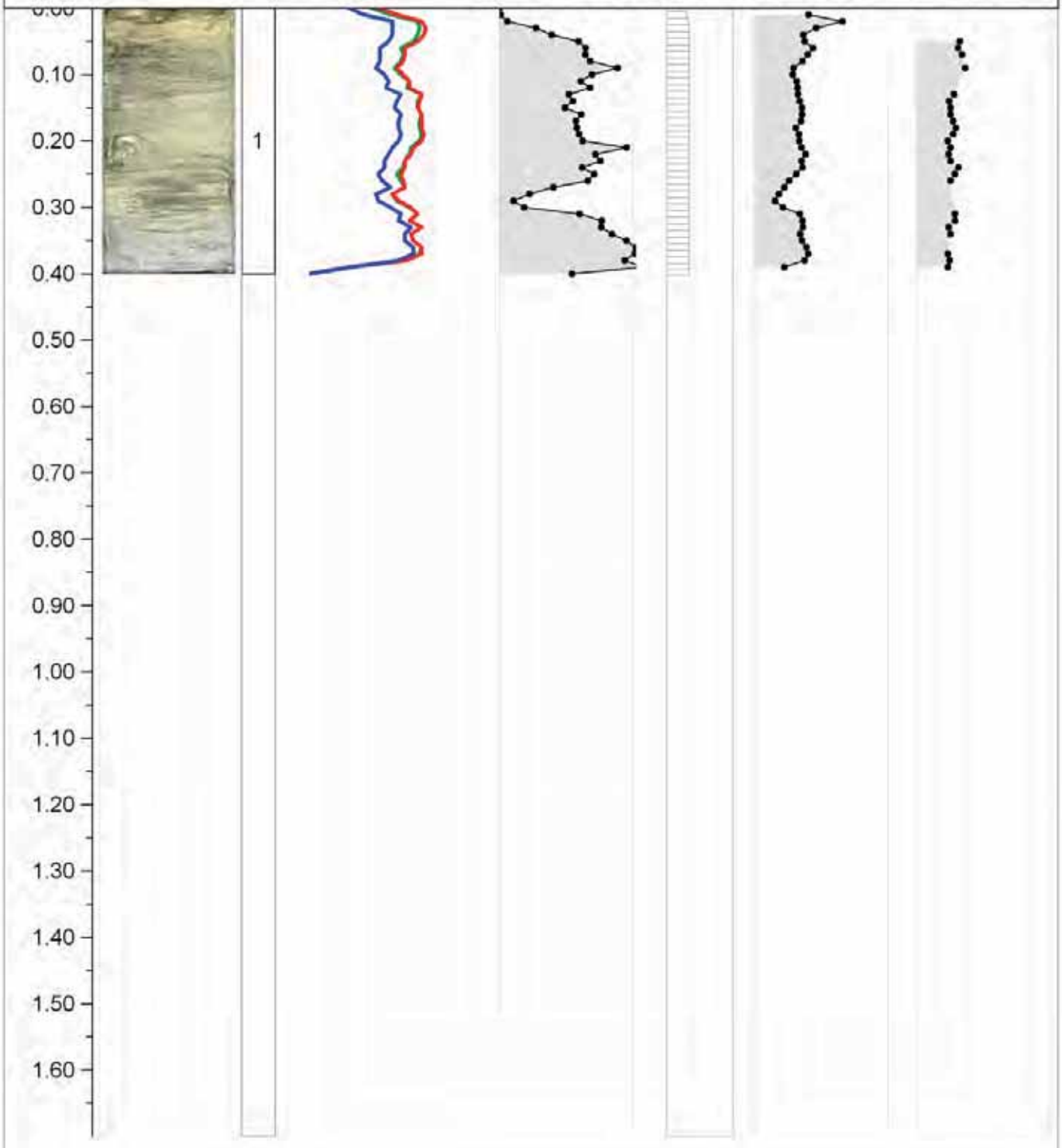

Core: KC17-A

Depth (mbsl): 855

Lat./Lon.: 73°25.18'S, 102°49.60'W

Kasten Core length (cm): 147 **Archive half length (cm):** 147

Cc (cm): 21

OSO0910

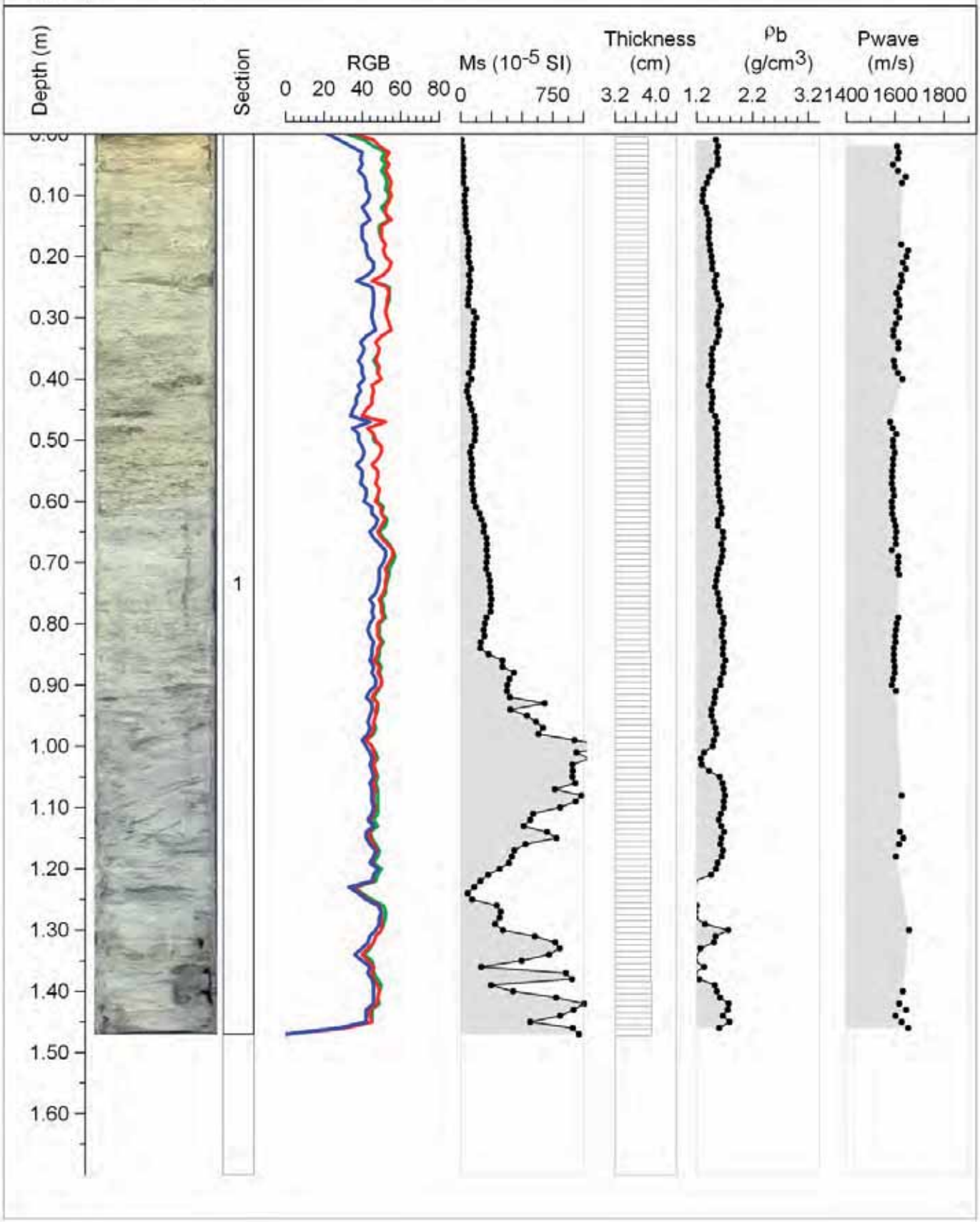

Core: KC17-B

Depth (mbsl): 855

Lat./Lon.: 73°25.18'S, 102°49.60'W

Kasten Core length (cm): 147 **Archive half length (cm):** 149

Cc (cm): 21

OSO0910

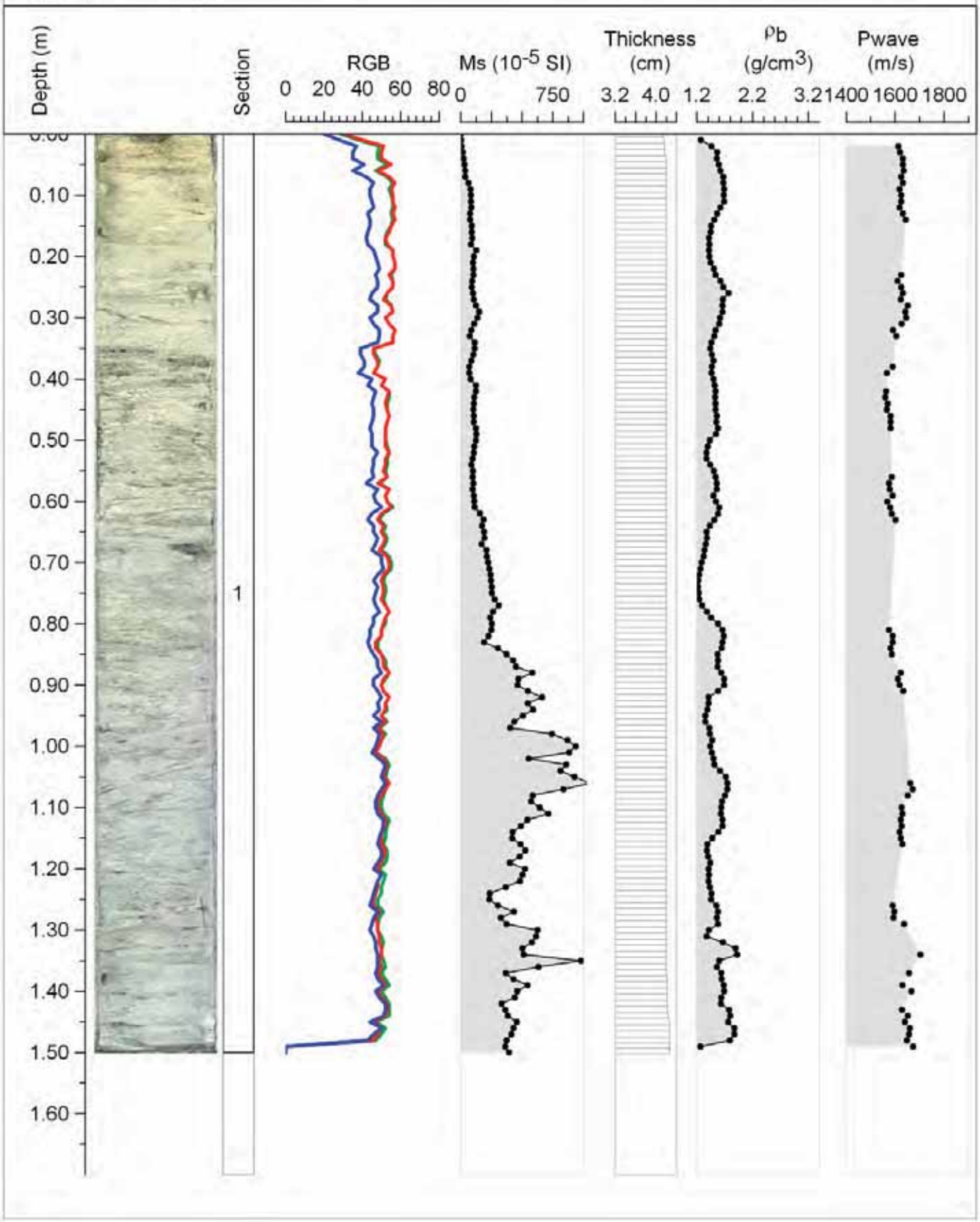

Core: KC18-A

Depth (mbsl): 894

Lat./Lon.: 73°23.01'S, 106°52.26'W

Kasten Core length (cm): 148.5 **Archive half length (cm):** 148

Cc (cm): 29.5

OSO0910

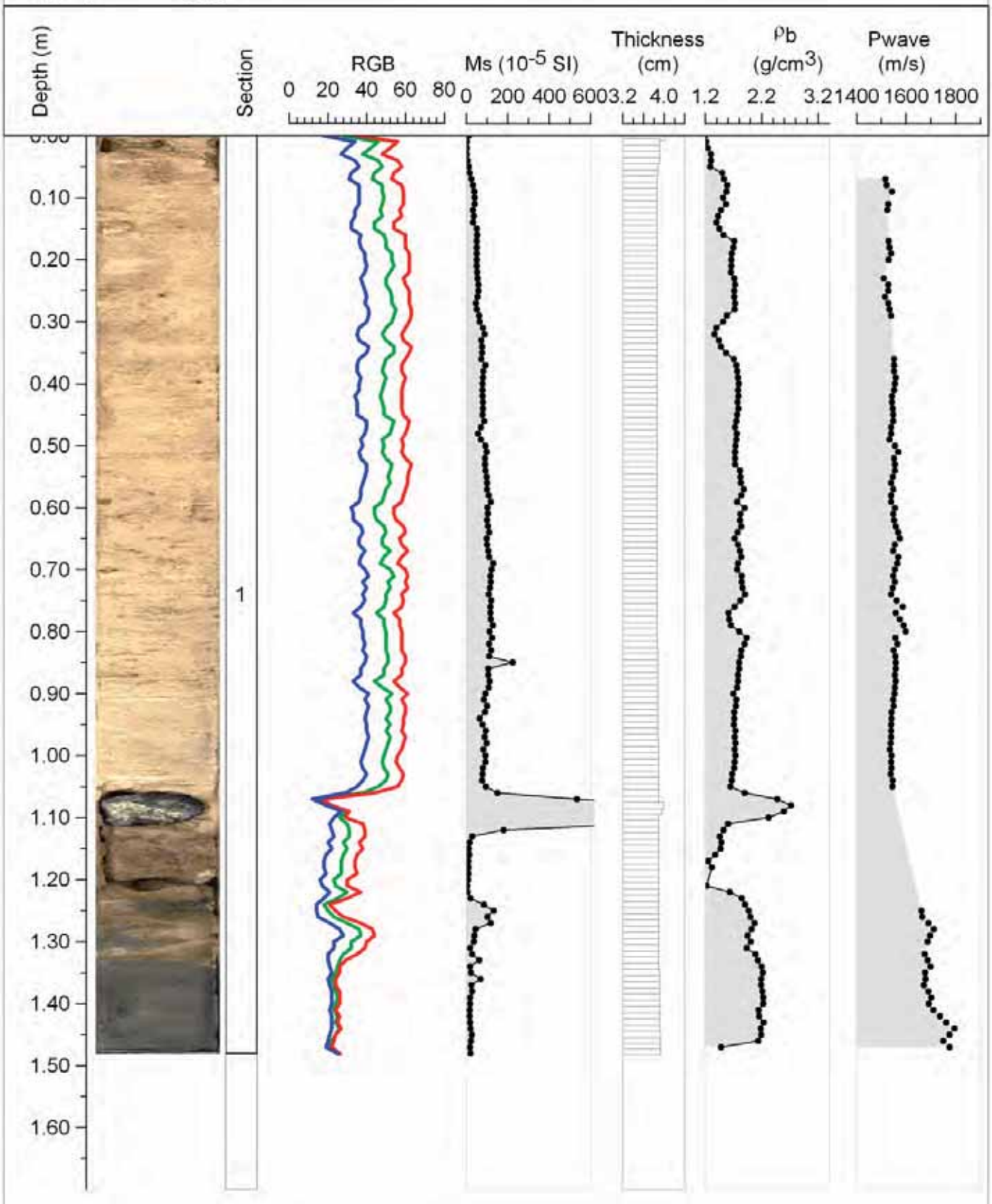

Core: KC18-B

Depth (mbsl): 894

Lat./Lon.: 73°23.01'S, 106°52.26'W

Kasten Core length (cm): 148.5 **Archive half length (cm):** 148

Cc (cm): 29.5

OSO0910

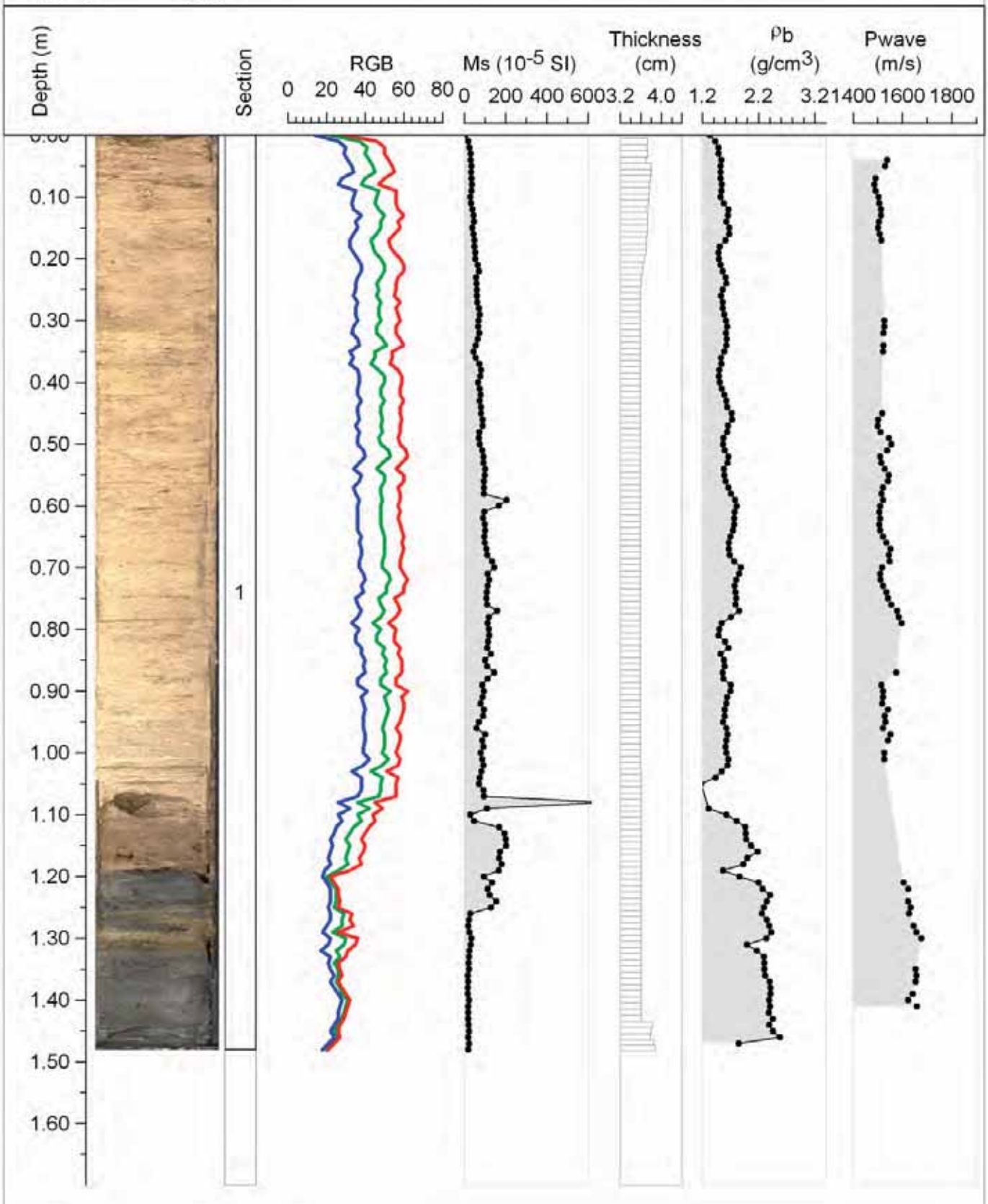

Core: KC19-A

Depth (mbsl): 782

Lat./Lon.: 73°7.71'S, 106°58.13'W

Kasten Core length (cm): 139 **Archive half length (cm):** 139

Cc (cm): 17

OSO0910

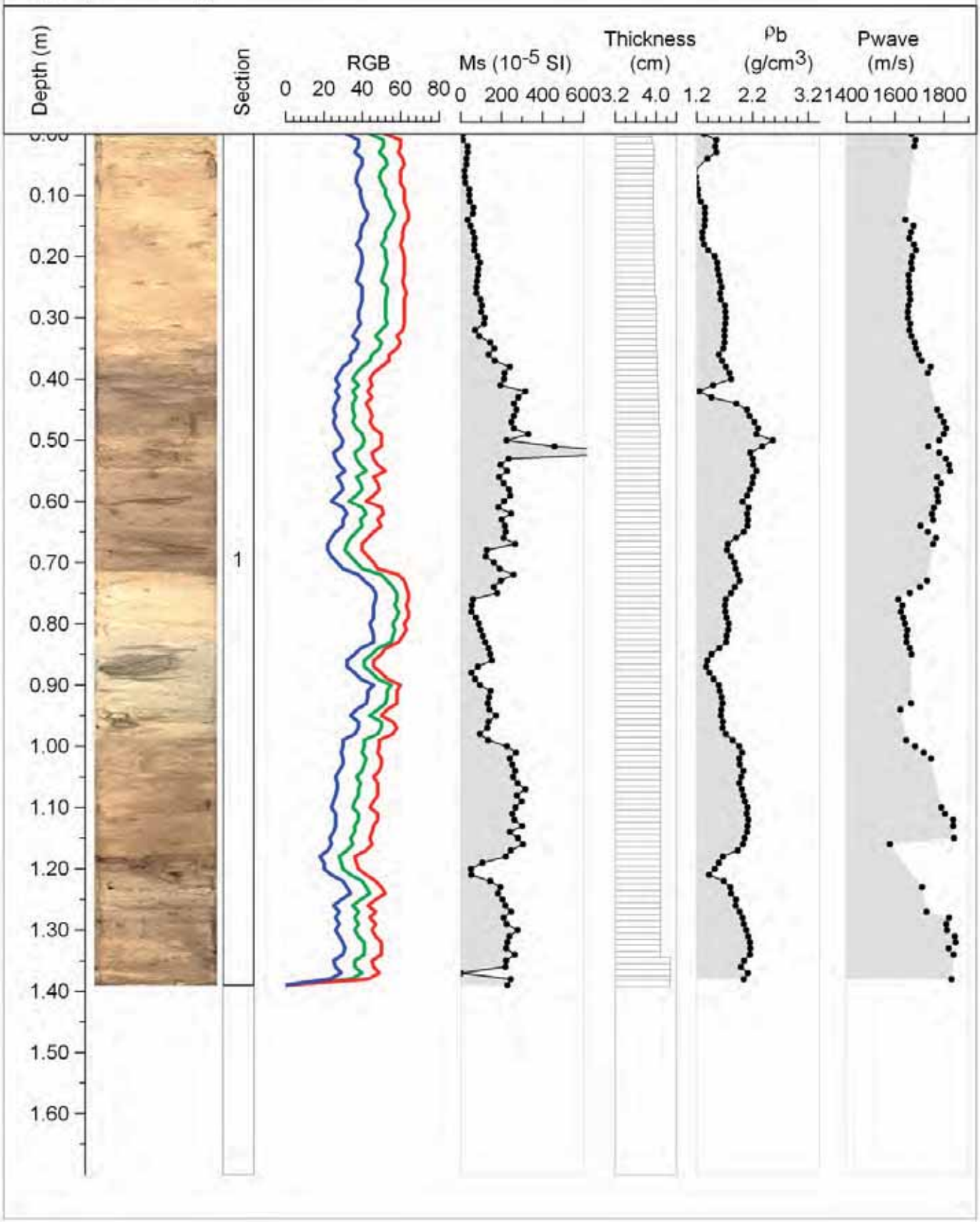

Core: KC19-B

Depth (mbsl): 782

Lat./Lon.: 73°7.71'S, 106°58.13'W

Kasten Core length (cm): 139 **Archive half length (cm):** 139

Cc (cm): 17

OSO0910

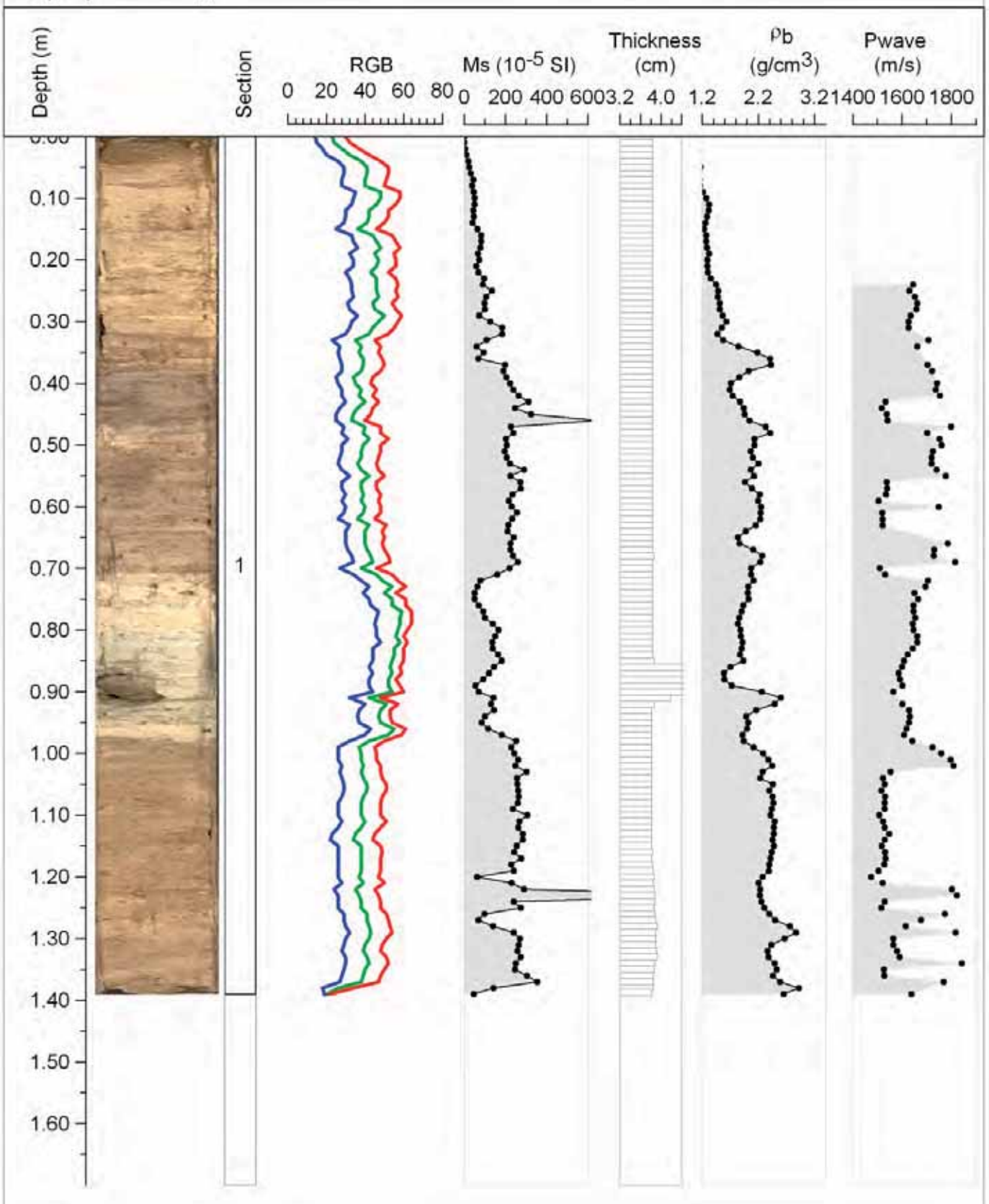

Core: KC22-A

Depth (mbsl): 724

Lat./Lon.: 72°49.12'S, 106°57.80'W

Kasten Core length (cm): 115 **Archive half length (cm):** 115

Cc (cm): 18

OSO0910

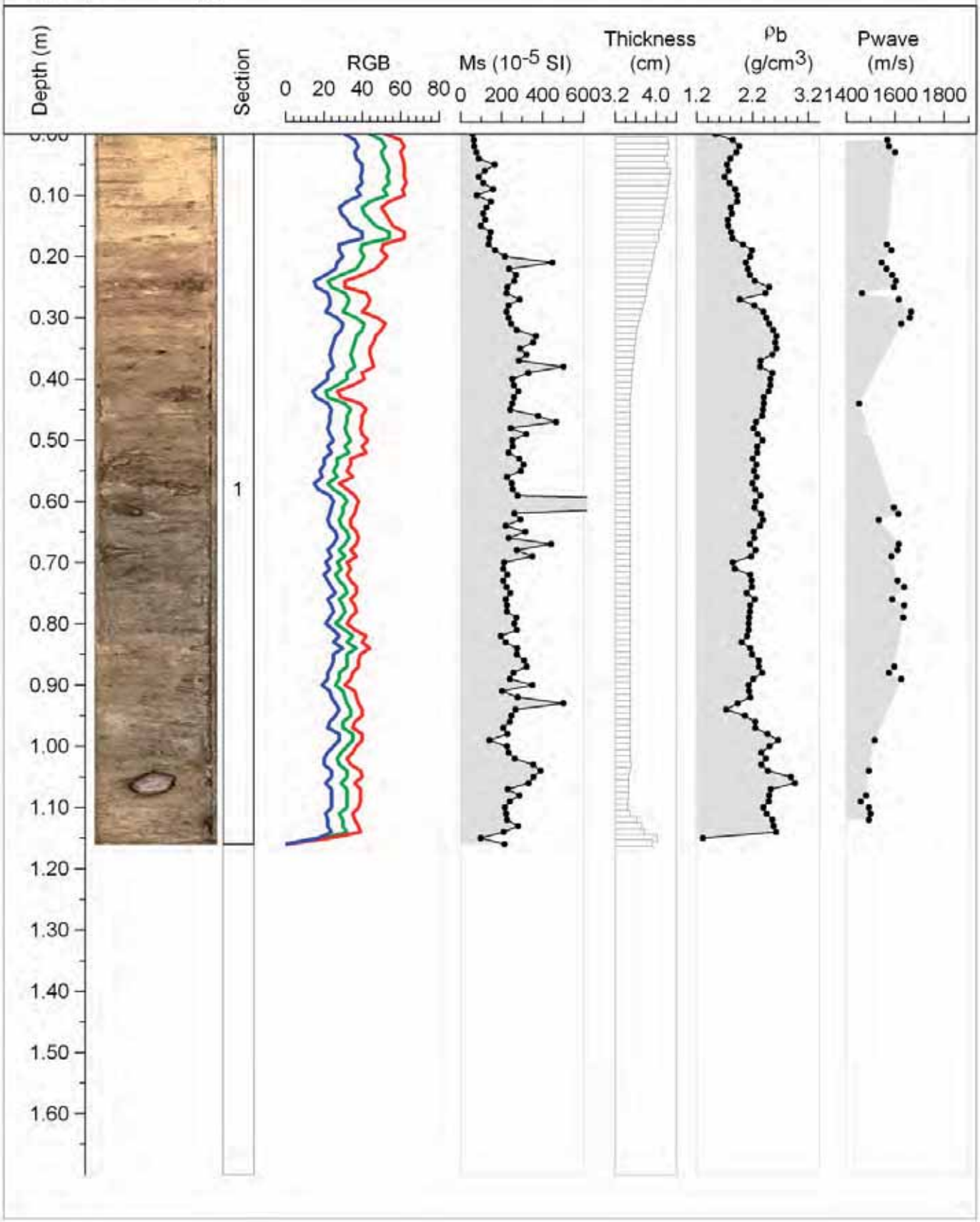

Core: KC22-B

Depth (mbsl): 724

Lat./Lon.: 72°49.12'S, 106°57.80'W

Kasten Core length (cm): 115 **Archive half length (cm):** 115

Cc (cm): 18

OSO0910

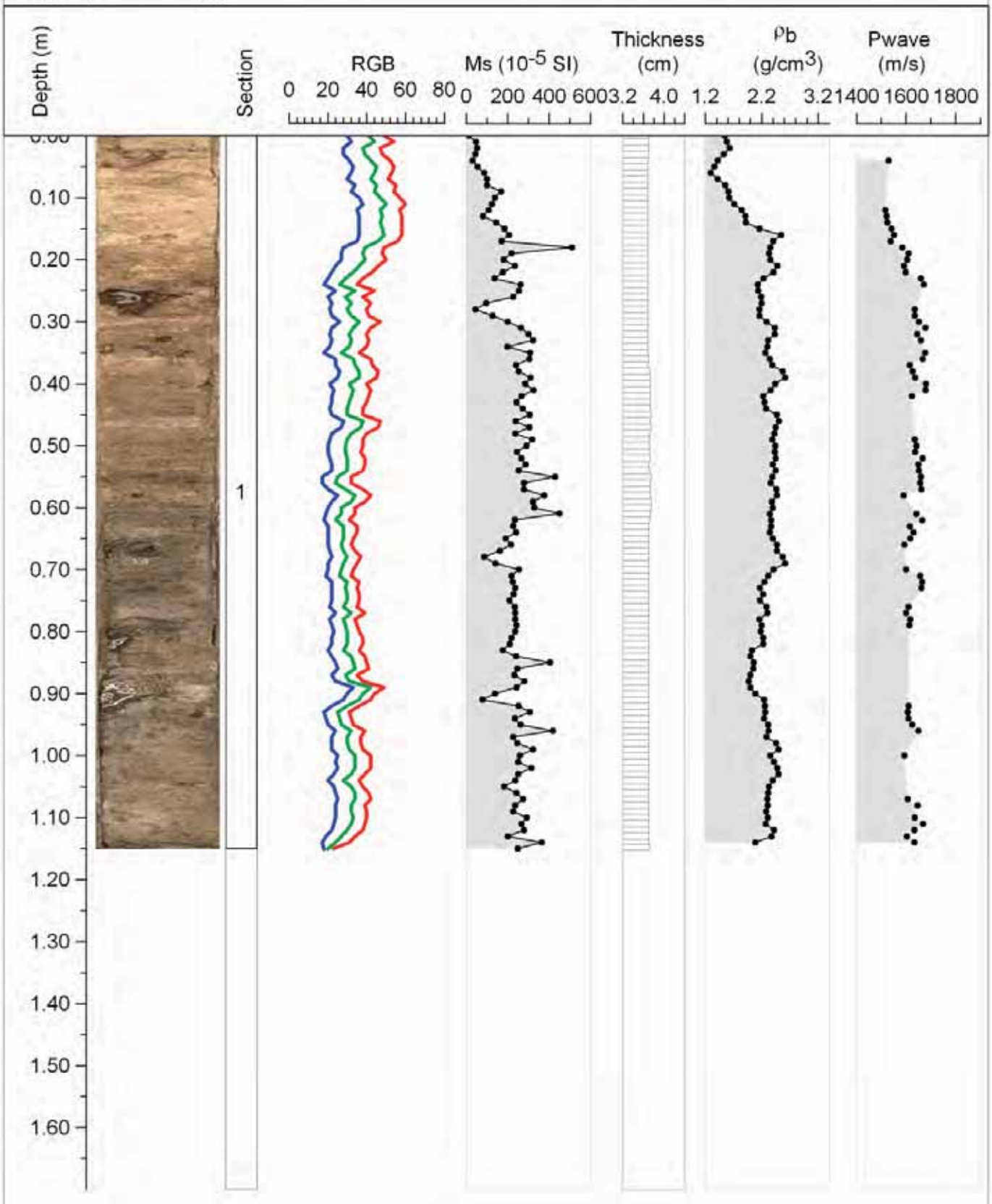

Core: KC23-A

Depth (mbsl): 660

Lat./Lon.: 72°53.54'S, 106°55.46'W

Kasten Core length (cm): 36 **Archive half length (cm):** 36

Cc (cm): 21

OSO0910

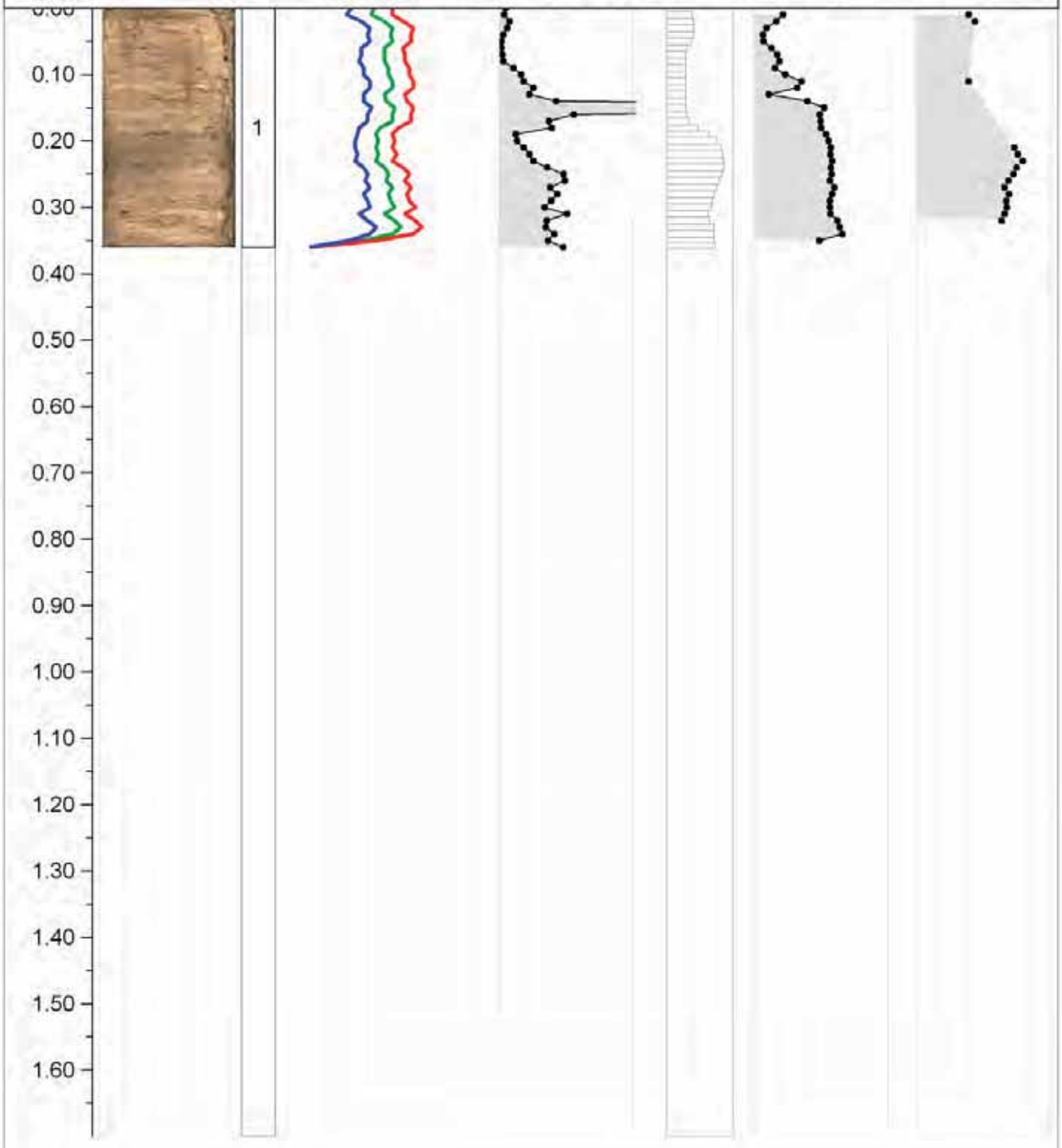

Core: KC23-B

Depth (mbsl): 660

Lat./Lon.: 72°53.54'S, 106°55.46'W

Kasten Core length (cm): 36 **Archive half length (cm):** 36

Cc (cm): 21

OSO0910

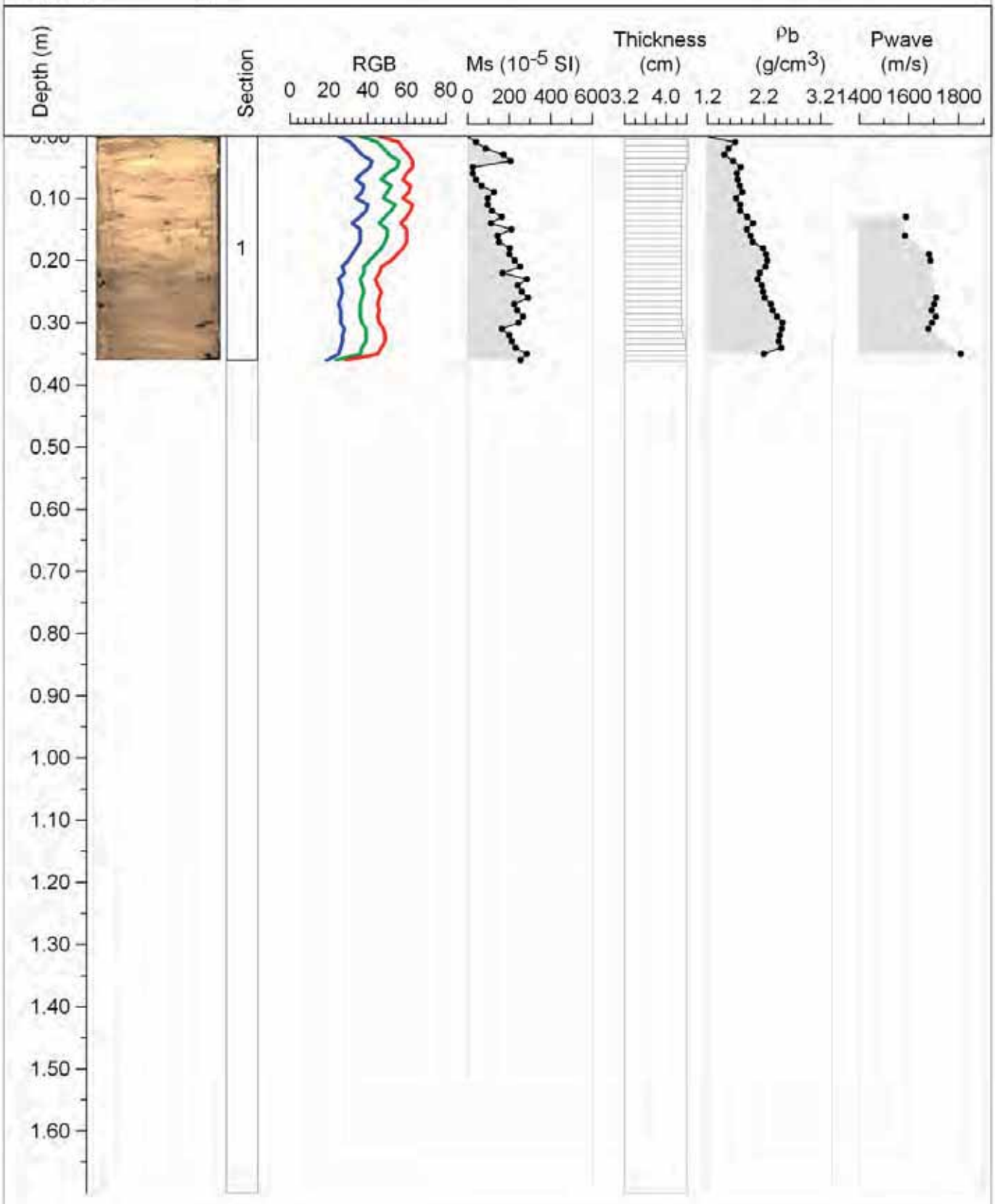

Core: KC24-A

Depth (mbsl): 807

Lat./Lon.: 73°14.39'S, 106°45.41'W

Kasten Core length (cm): 160 **Archive half length (cm):** 161

Cc (cm): 24

OSO0910

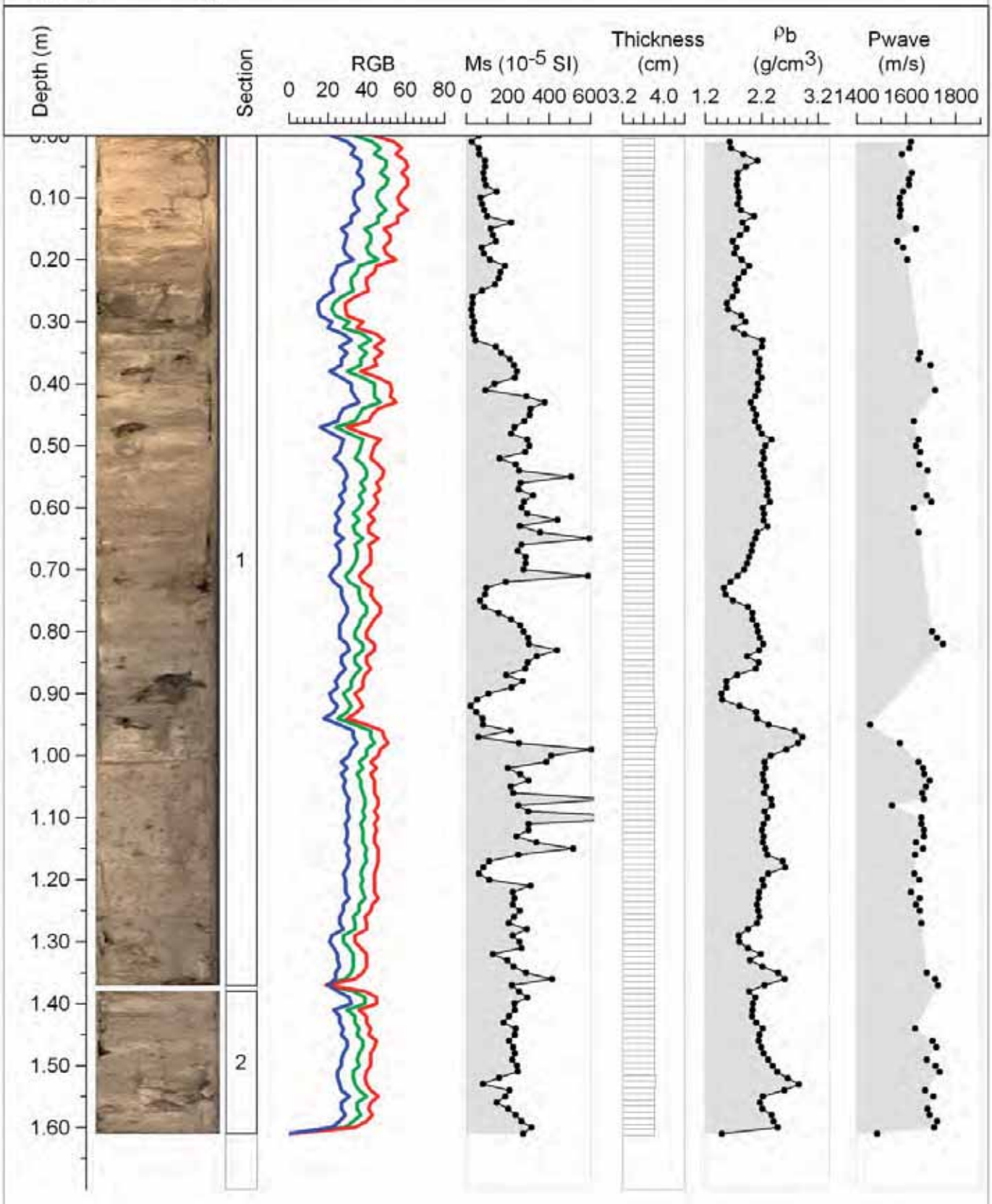

Core: KC24-B

Depth (mbsl): 807

Lat./Lon.: 73°14.39'S, 106°45.41'W

Kasten Core length (cm): 160 **Archive half length (cm):** 160

Cc (cm): 24

OSO0910

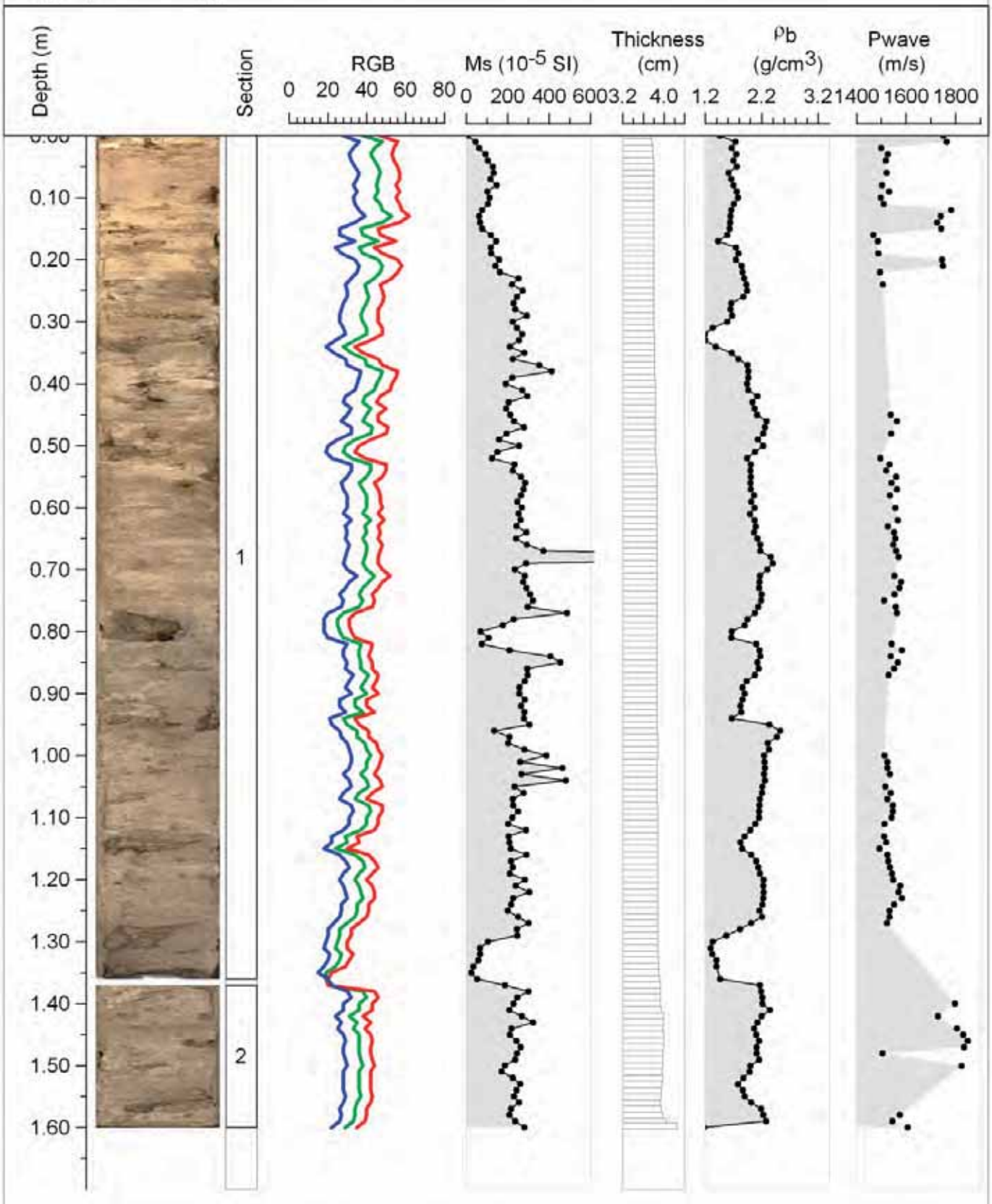

Core: KC25-A

Depth (mbsl): 838

Lat./Lon.: 73°15.42'S, 107°6.34'W

Kasten Core length (cm): 77 **Archive half length (cm):** 77

Cc (cm): 18

OSO0910

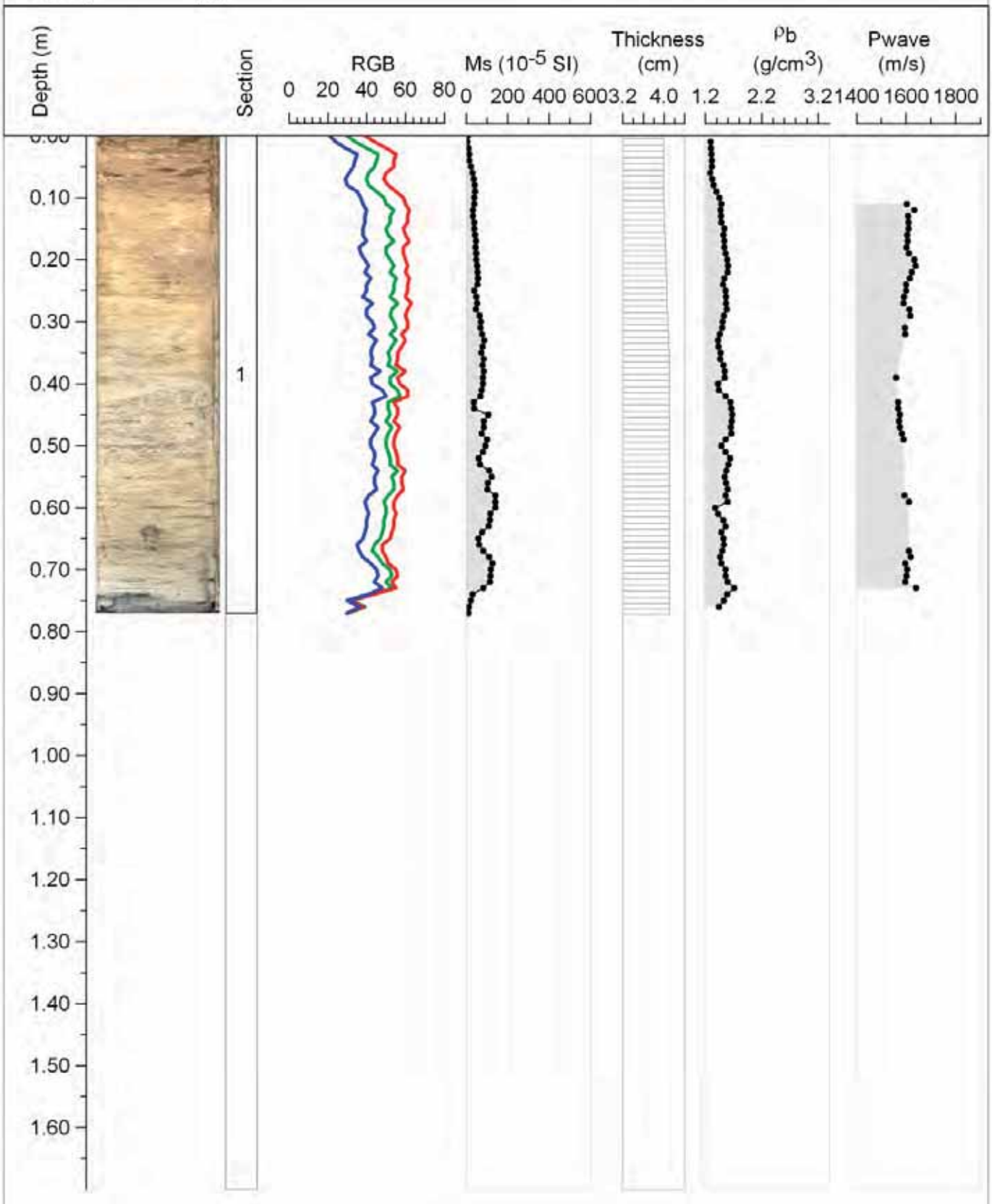

Core: KC25-B

Depth (mbsl): 838

Lat./Lon.: 73°15.42'S, 107°6.34'W

Kasten Core length (cm): 77 **Archive half length (cm):** 77

Cc (cm): 18

OSO0910

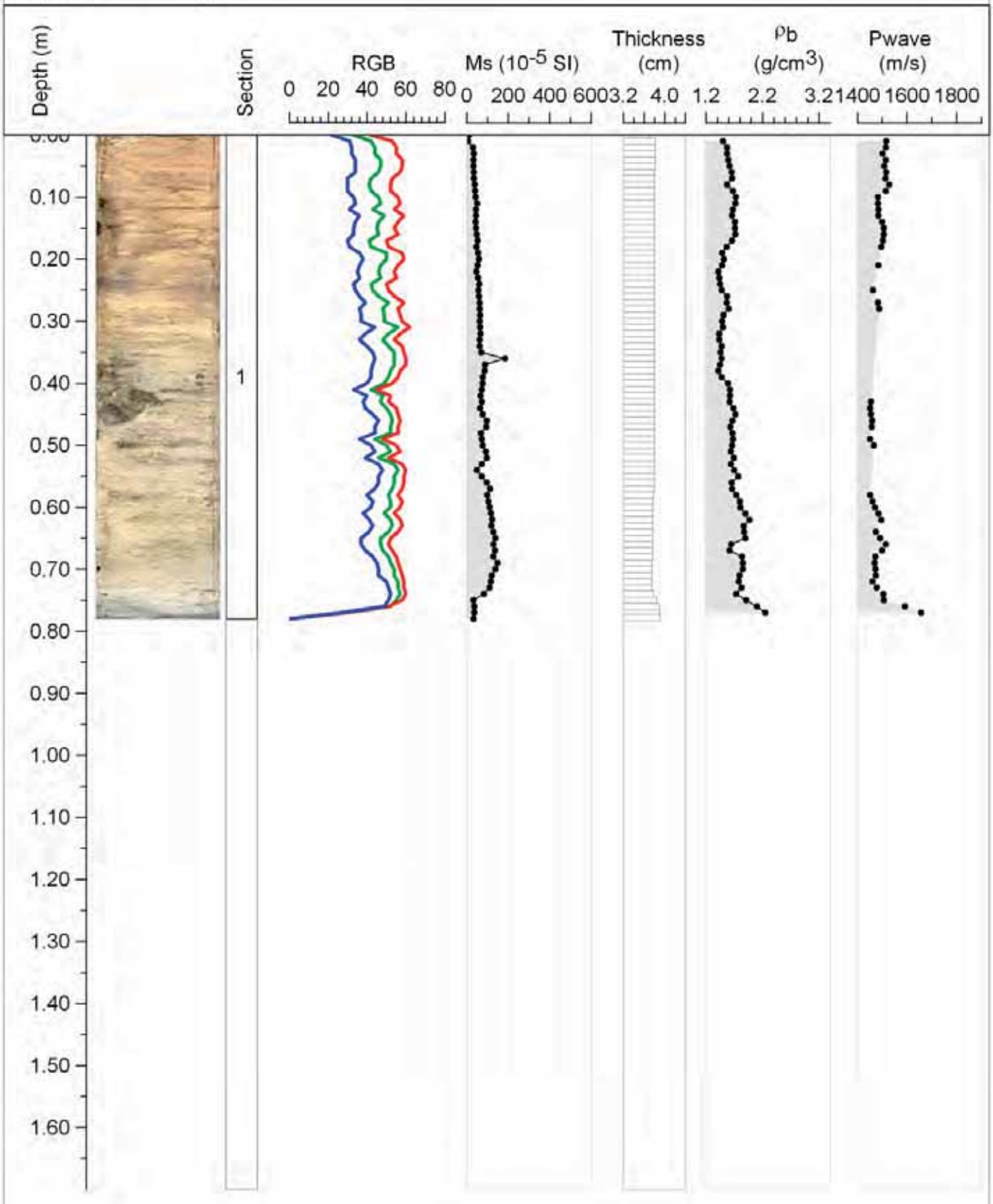

Core: KC26

Depth (mbsl): 838

Lat./Lon.: 73°15.42'S, 107°6.34'W

Kasten Core length (cm): 106 **Archive half length (cm):** 106

Cc (cm): 18

OSO0910

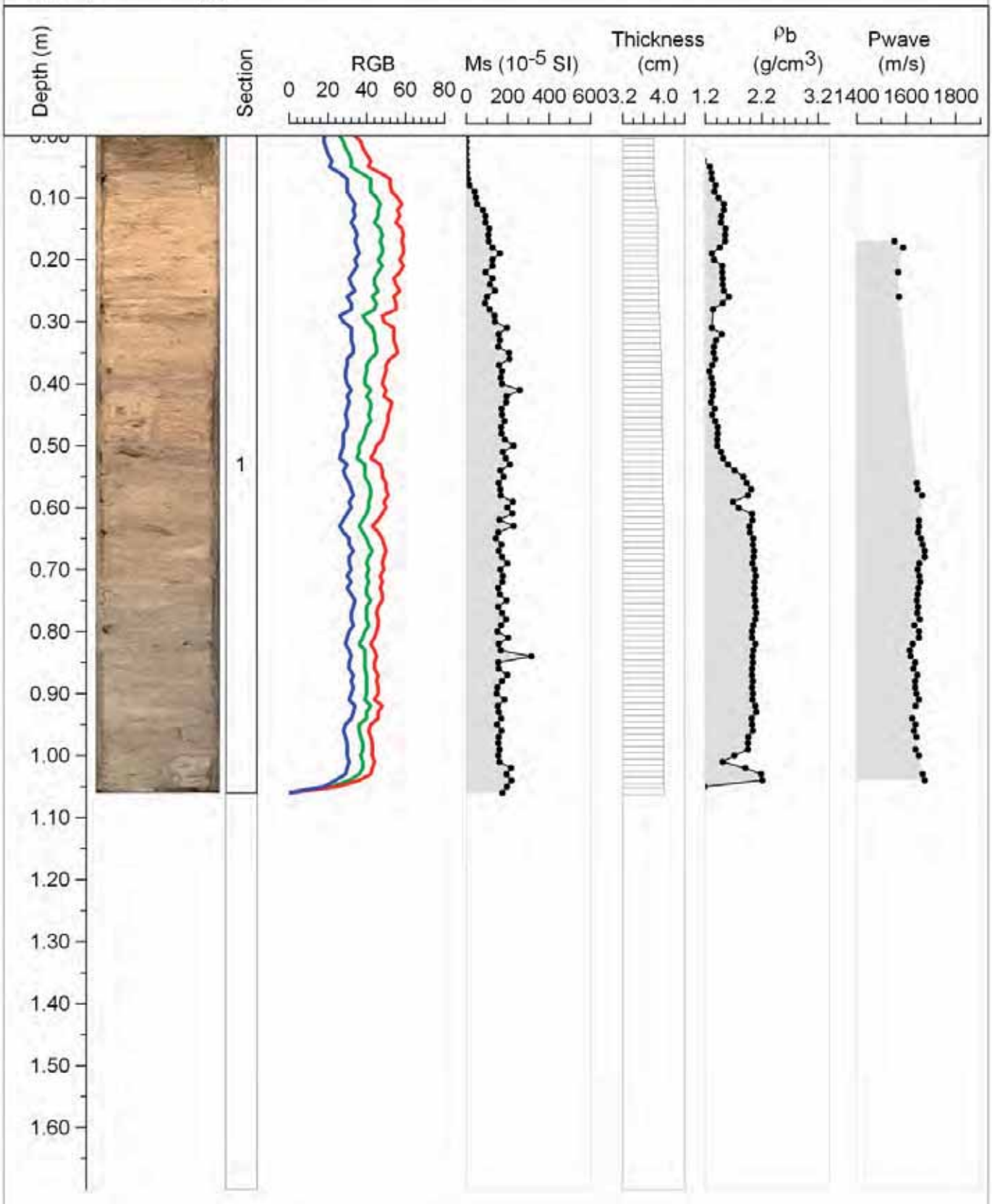

Core: KC27

Depth (mbsl): 666

Lat./Lon.: 72°52.97'S, 107°15.29'W

Kasten Core length (cm): 52 **Archive half length (cm):** 52

Cc (cm): 25

OSO0910

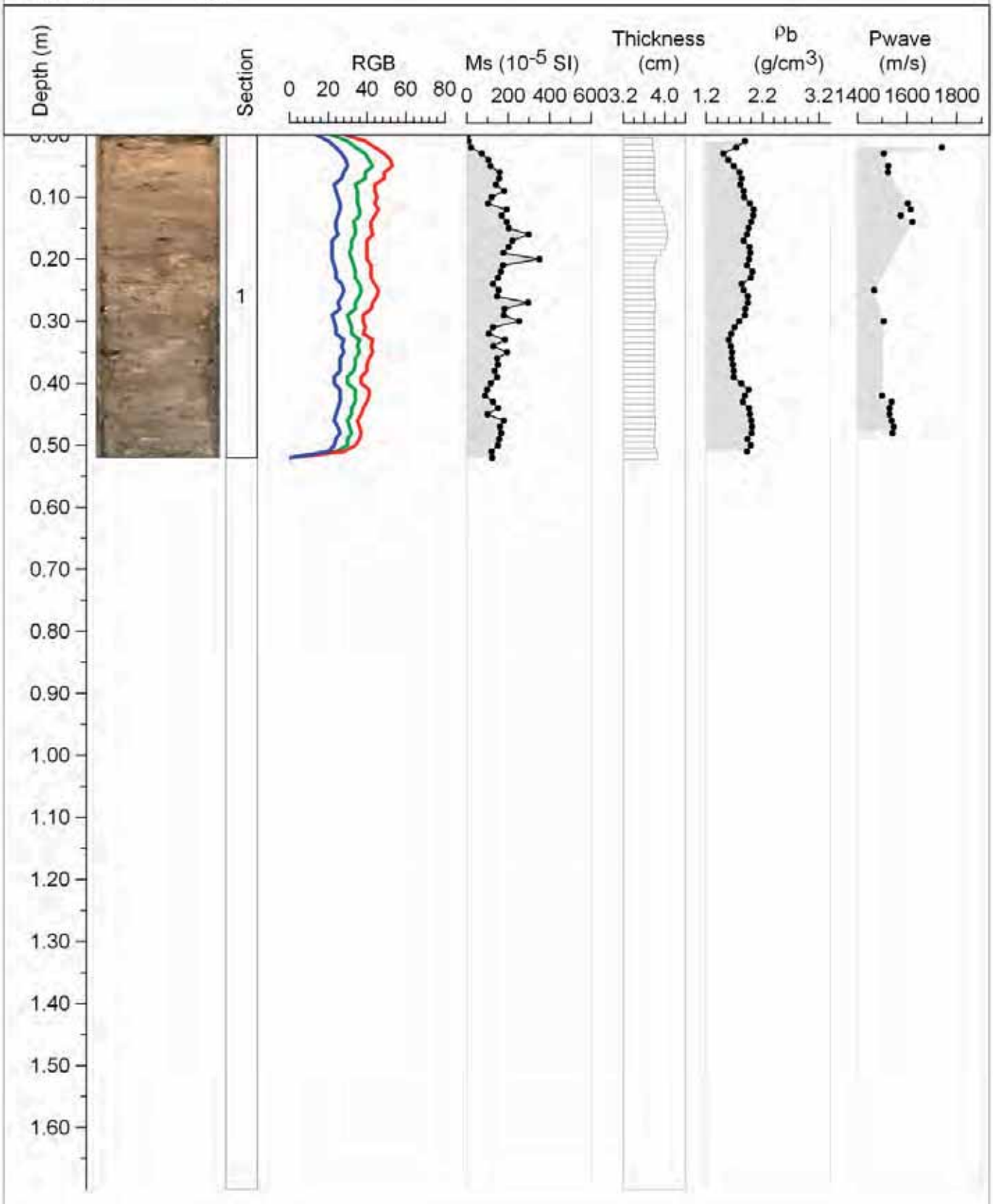

Appendix III

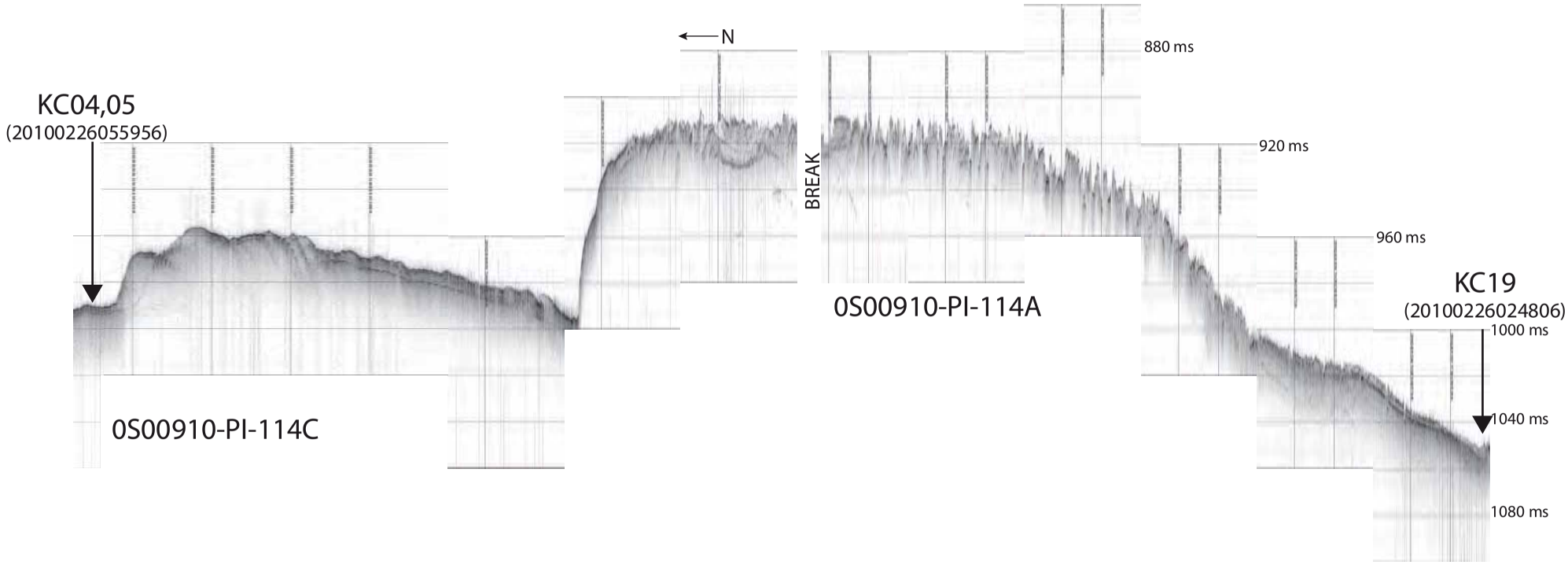
KC04,05
(20100226055956)
N
880 ms
920 ms
960 ms
BREAK
0S00910-PI-114A
KC19
(20100226024806)
1000 ms
1040 ms
1080 ms
0S00910-PI-114C

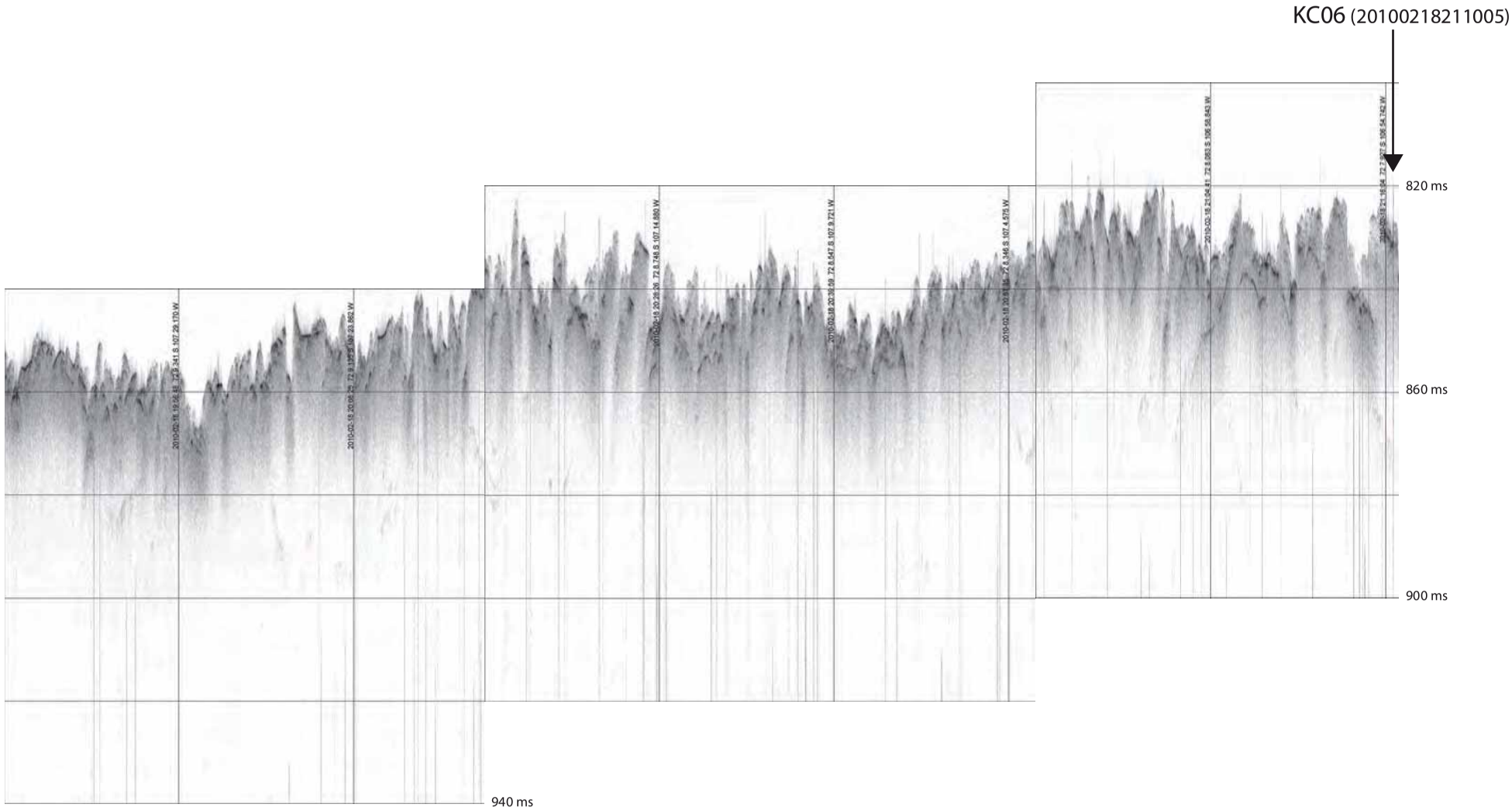

OSO0910-PI-17A

Line 15-A

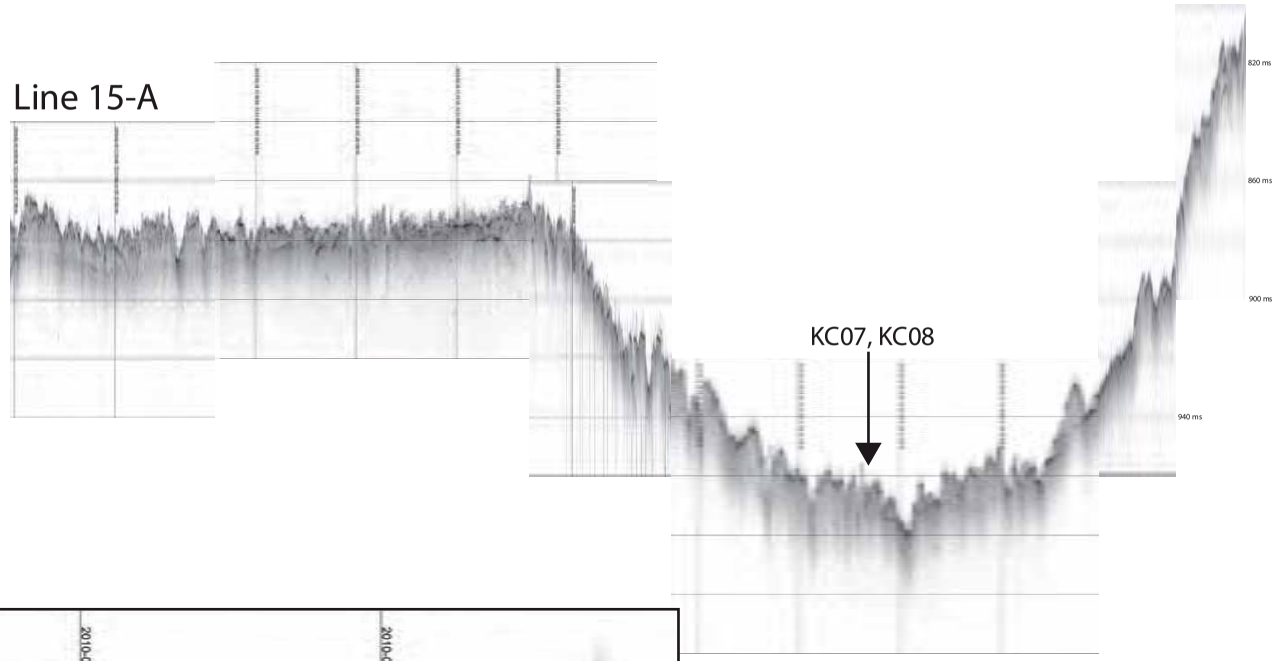

KC07, KC08 (20100218161214)

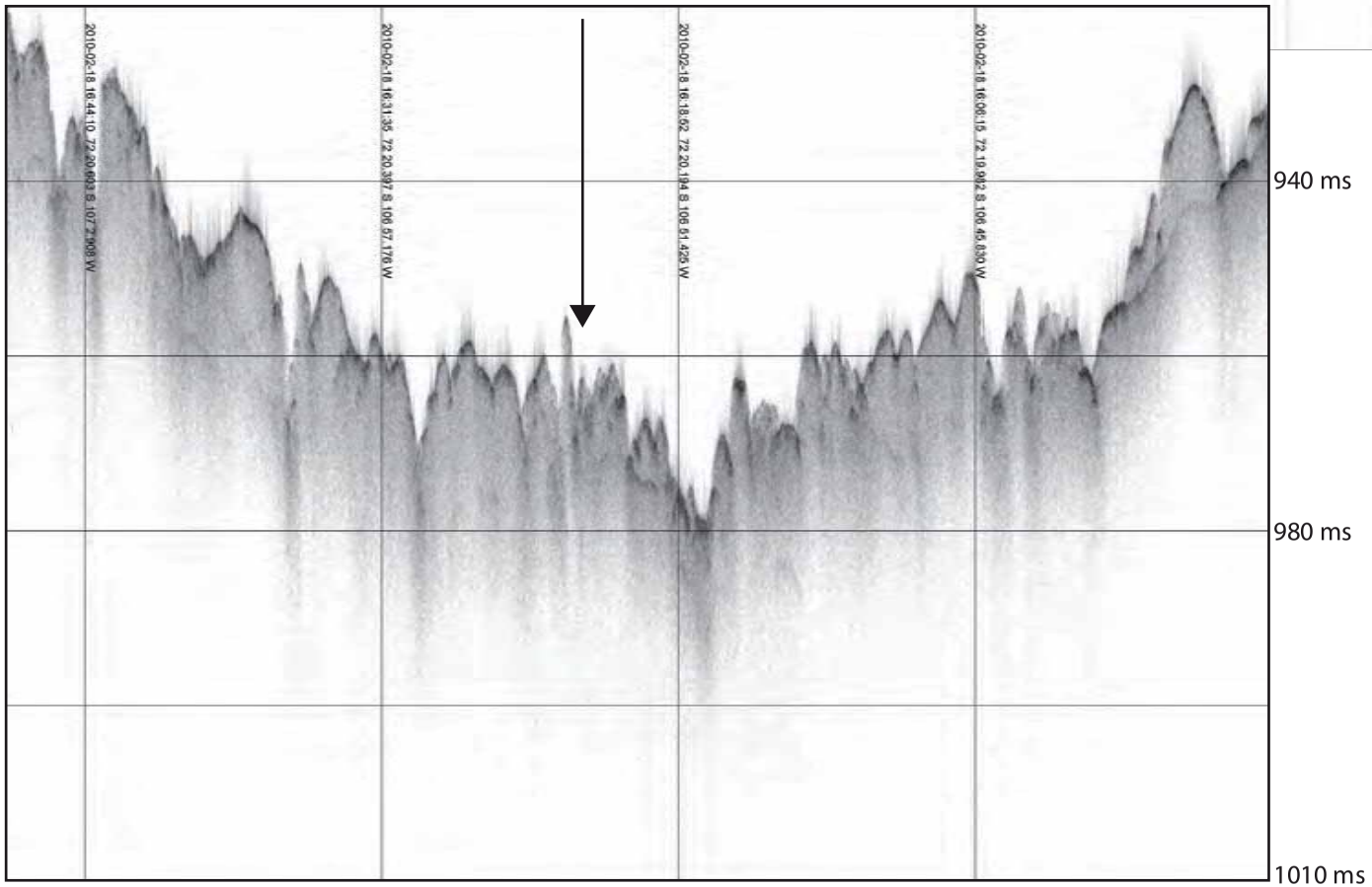

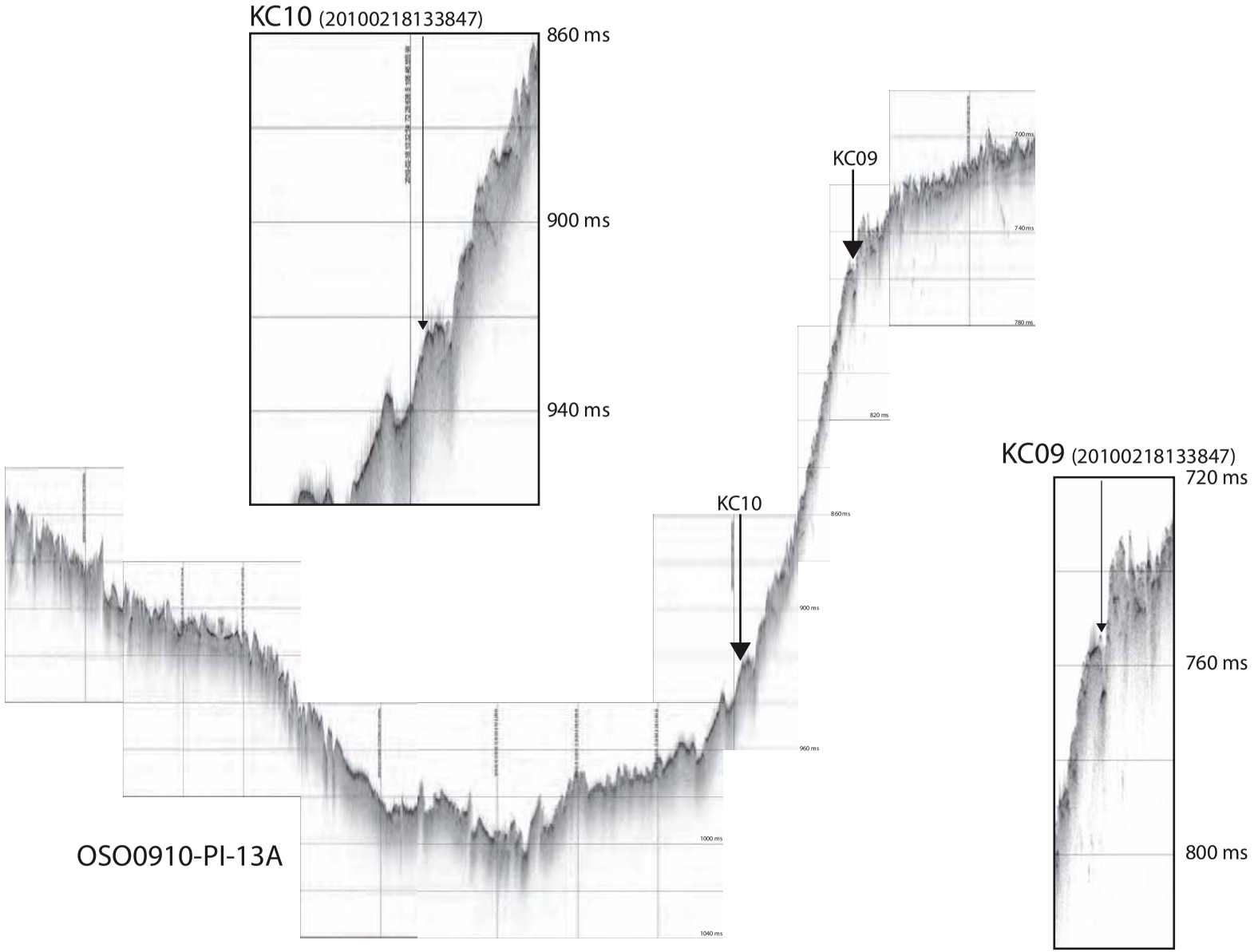
KC10 (20100218133847)
860 ms
900 ms
940 ms
KC09
700 ms
740 ms
780 ms
820 ms
KC10
860 ms
900 ms
960 ms
1000 ms
1040 ms
OSO0910-PI-13A
KC09 (20100218133847)
720 ms
760 ms
800 ms

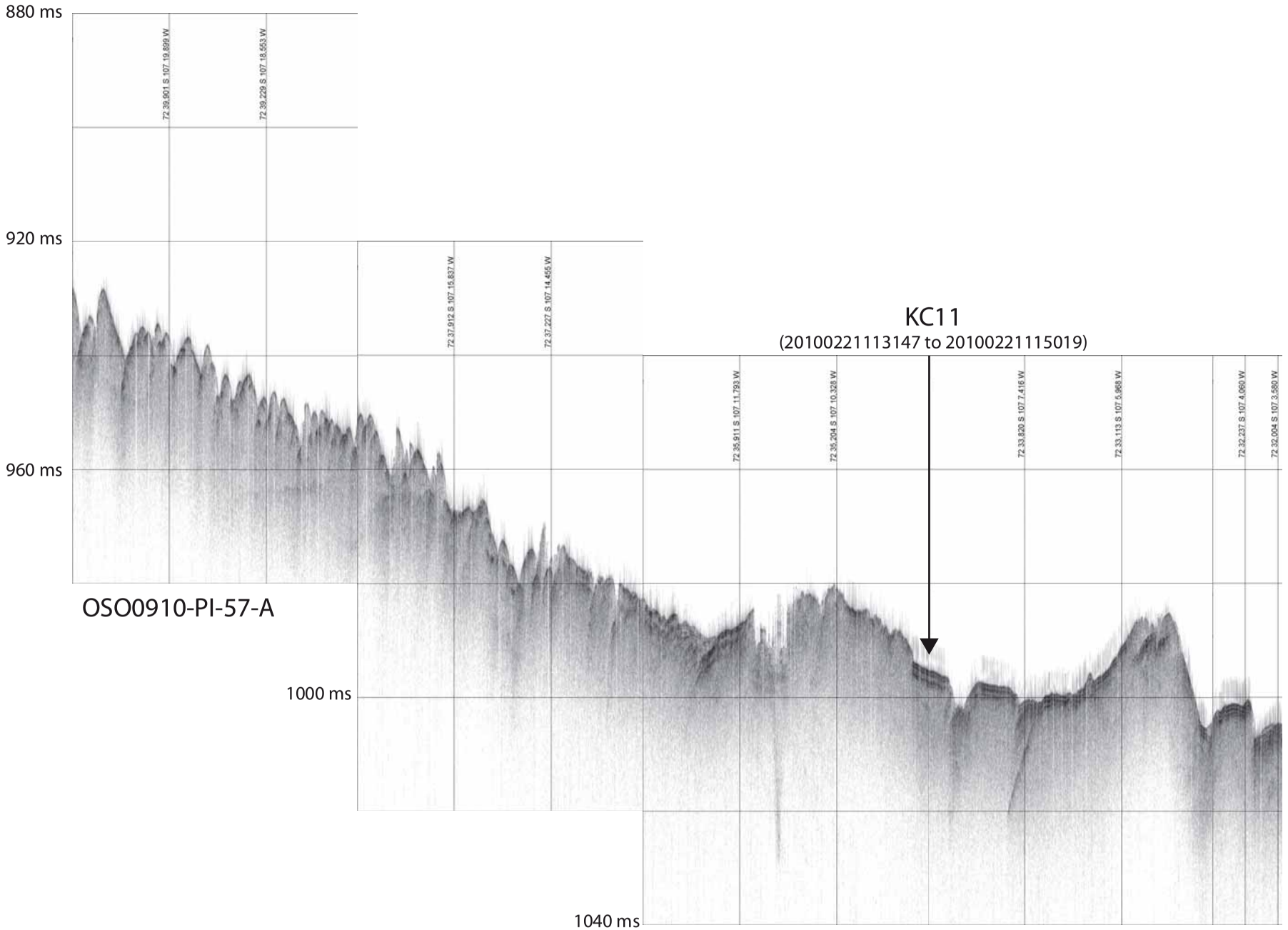
880 ms
920 ms
960 ms
1000 ms
1040 ms
72 39.901 S 107 19.899 W
72 39.229 S 107 18.553 W
72 37.912 S 107 15.837 W
72 37.227 S 107 14.455 W
72 35.911 S 107 11.793 W
72 35.204 S 107 10.328 W
72 33.820 S 107 7.416 W
72 33.113 S 107 5.968 W
72 32.237 S 107 4.060 W
72 32.004 S 107 3.580 W
KC11
(20100221113147 to 20100221115019)
OSO0910-PI-57-A

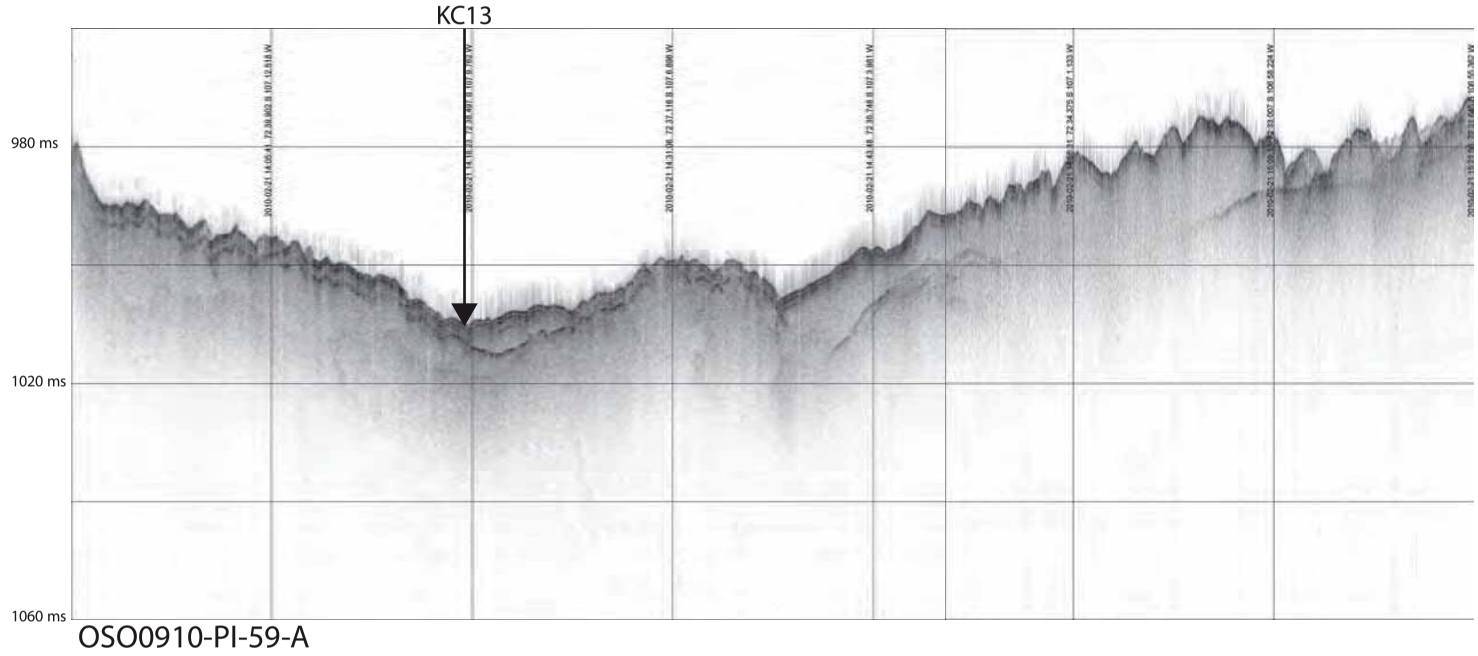

OSO0910-PI-59-A

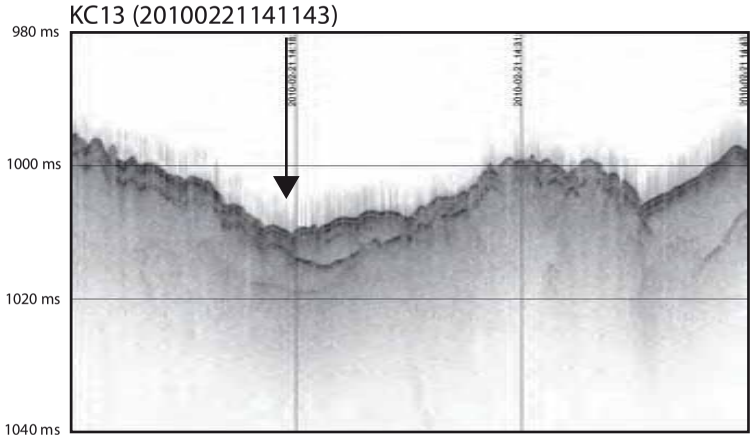

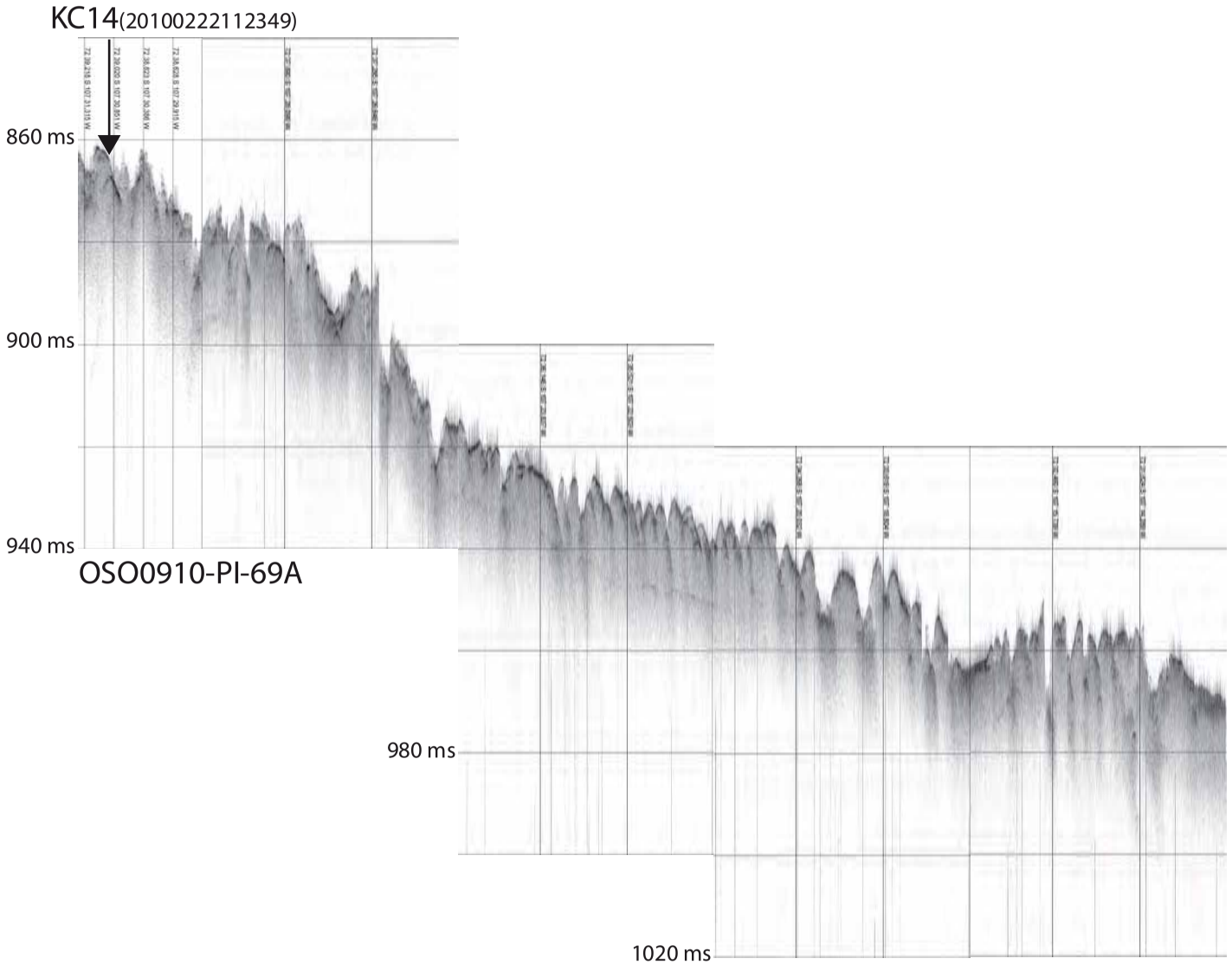
KC14(20100222112349)
860 ms
900 ms
940 ms
OSO0910-PI-69A
980 ms
1020 ms

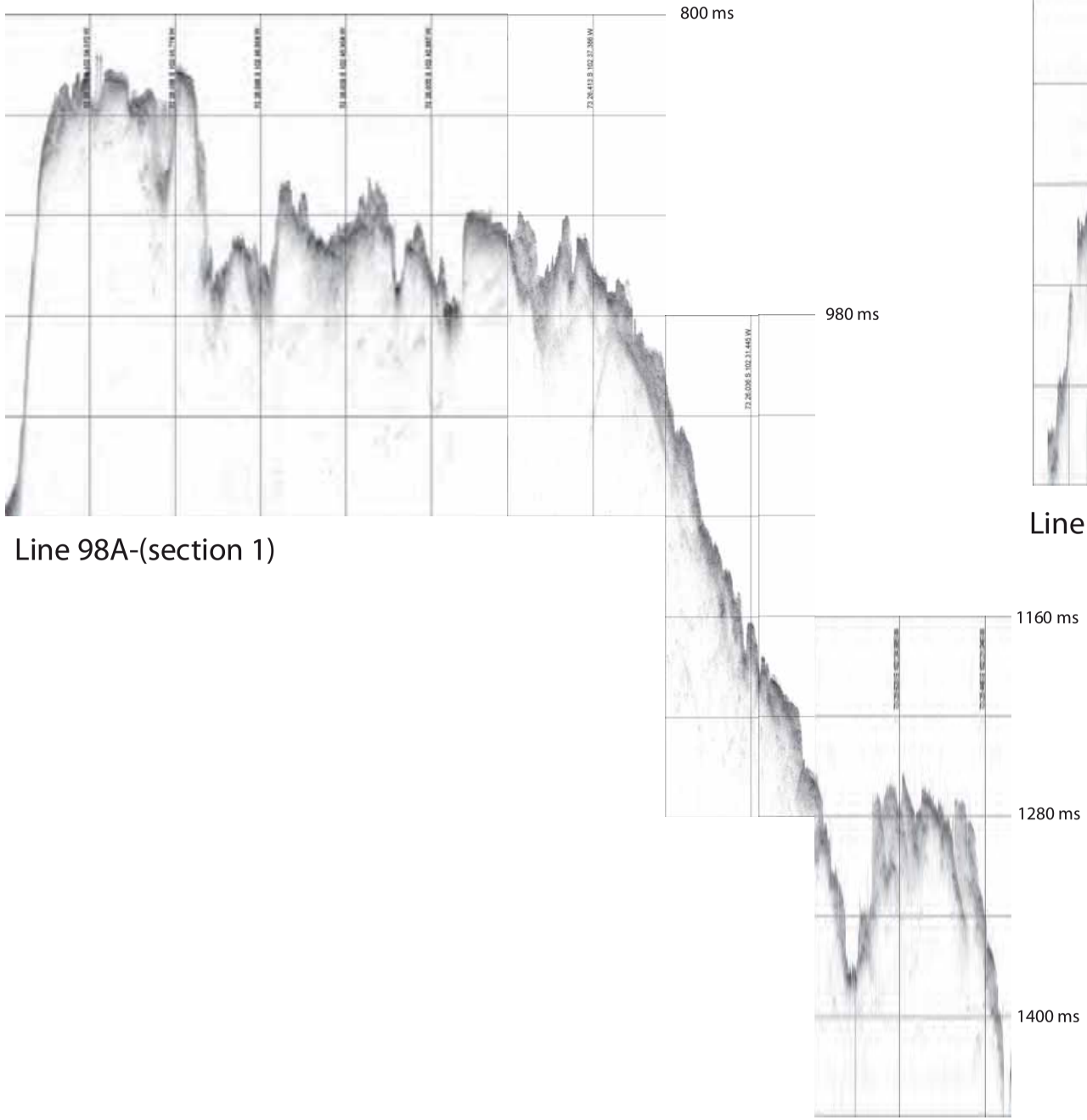

Line 98A-(section 1)

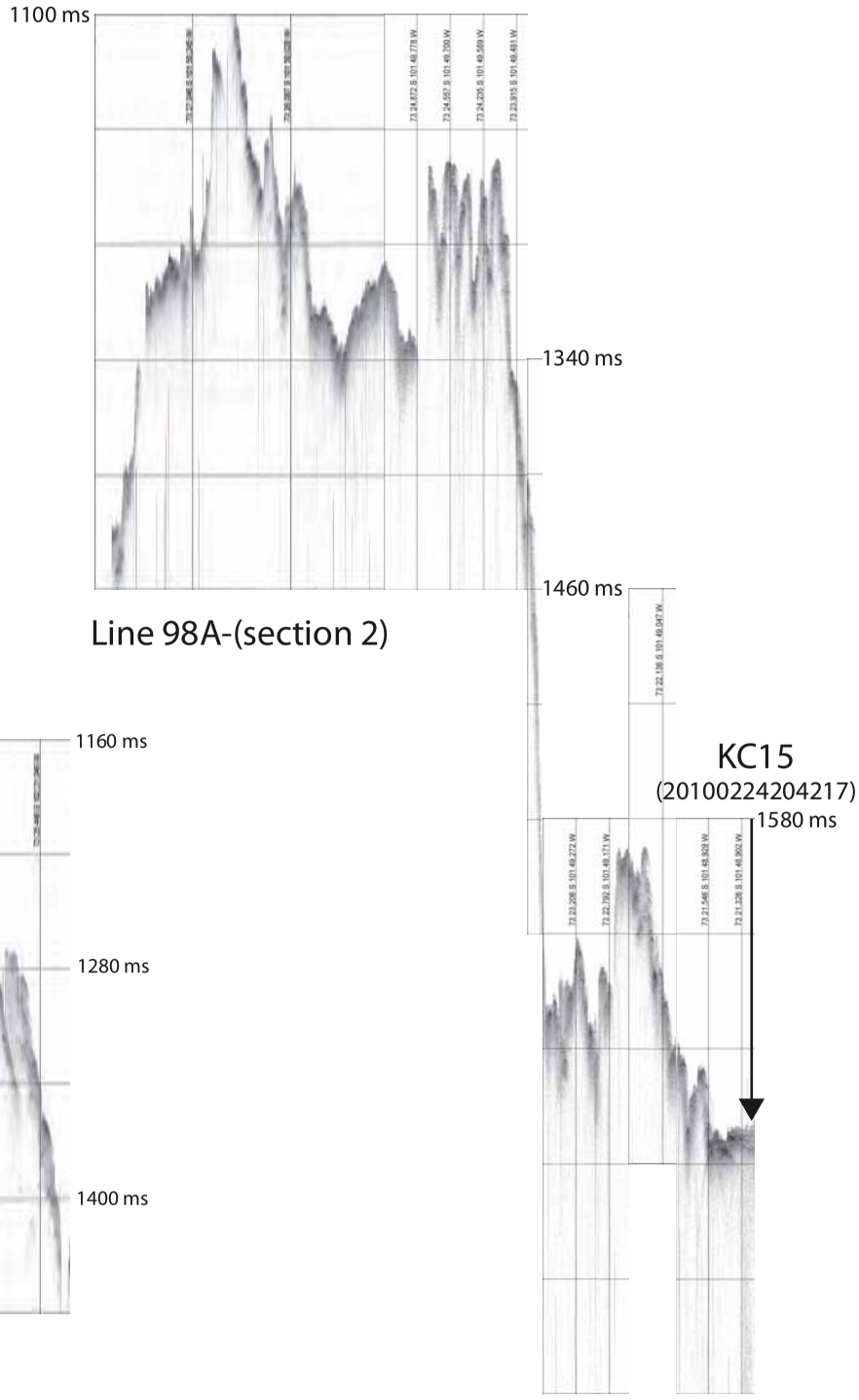

Line 98A-(section 2)

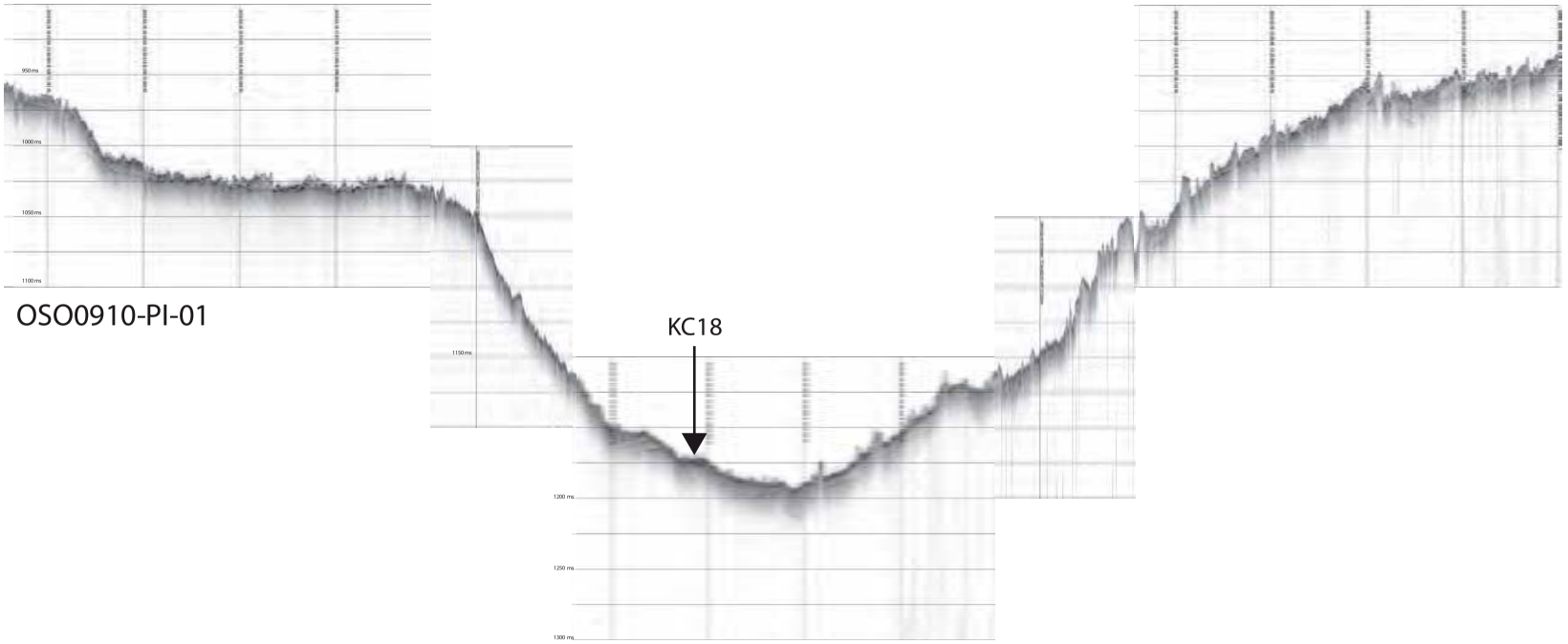

KC18 (20100216165105)

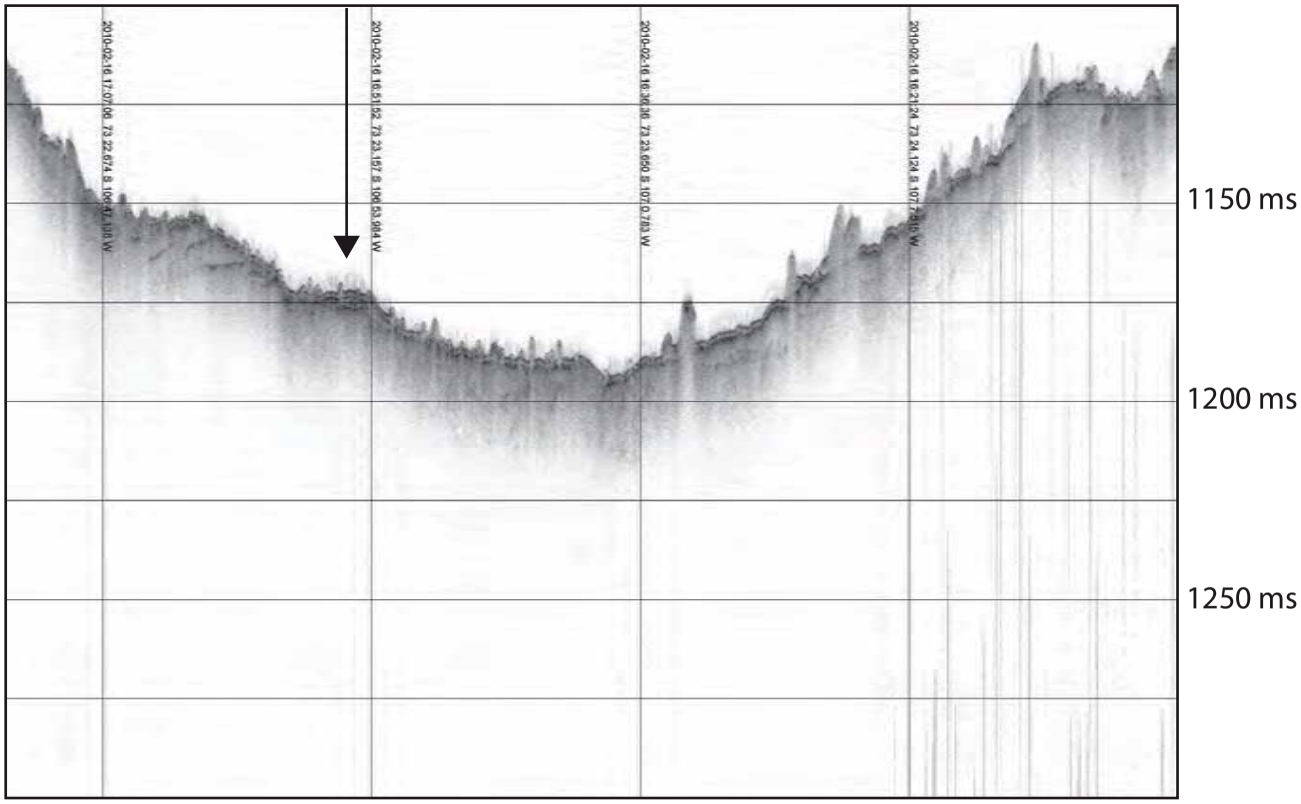

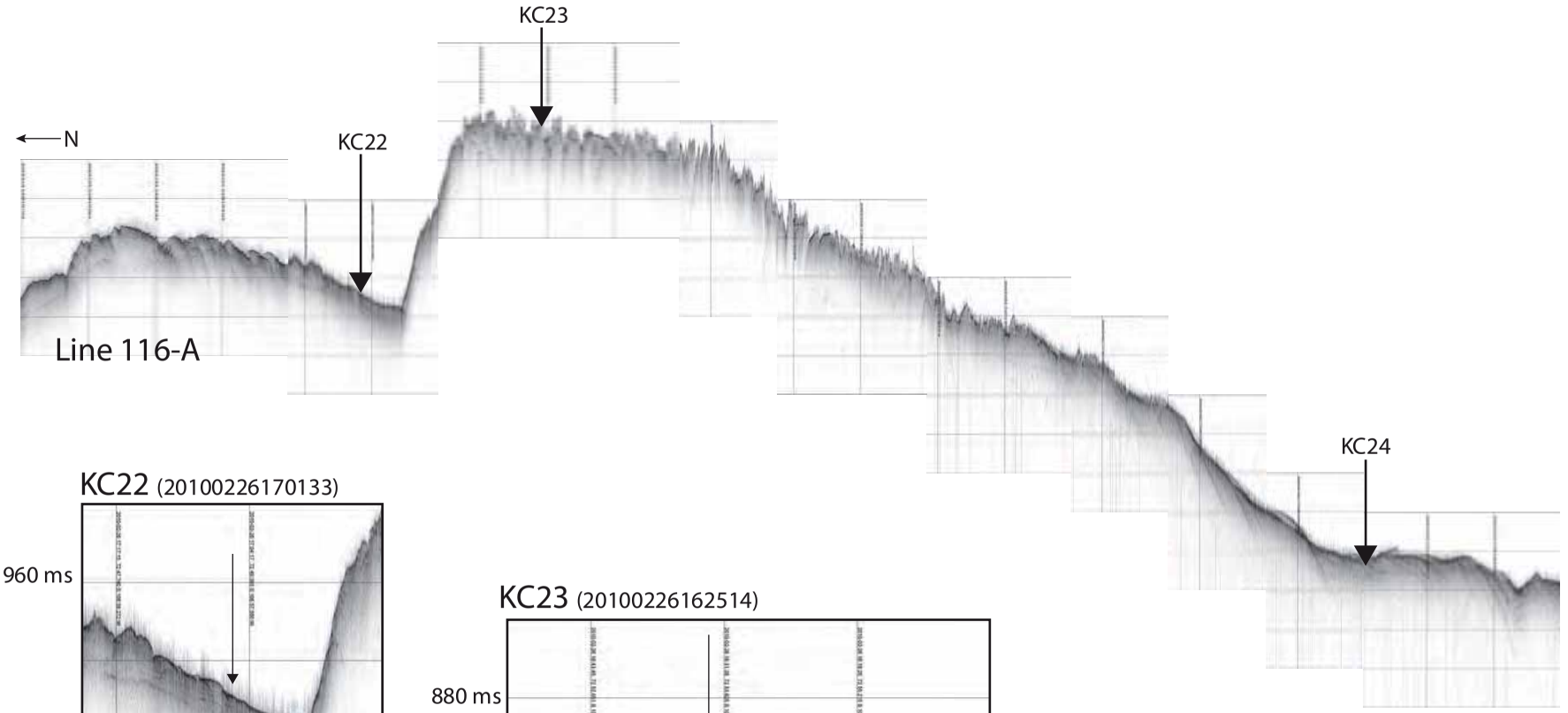

KC22 (20100226170133)

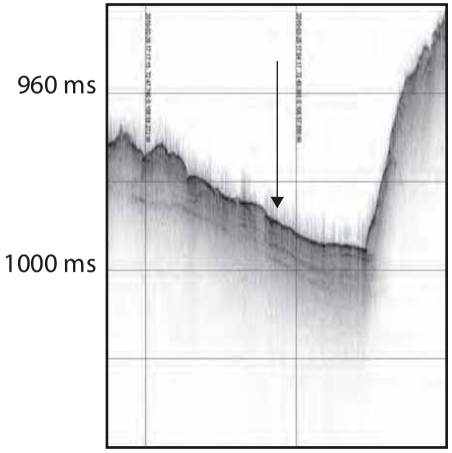

KC23 (20100226162514)

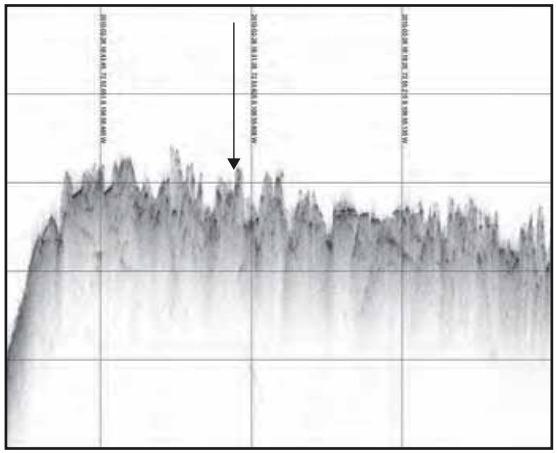

KC24 (20100226135025)

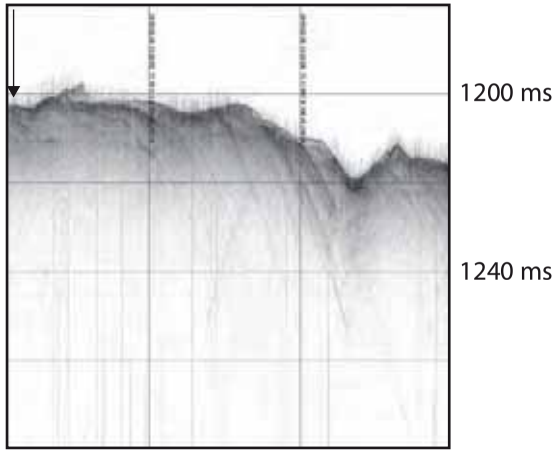

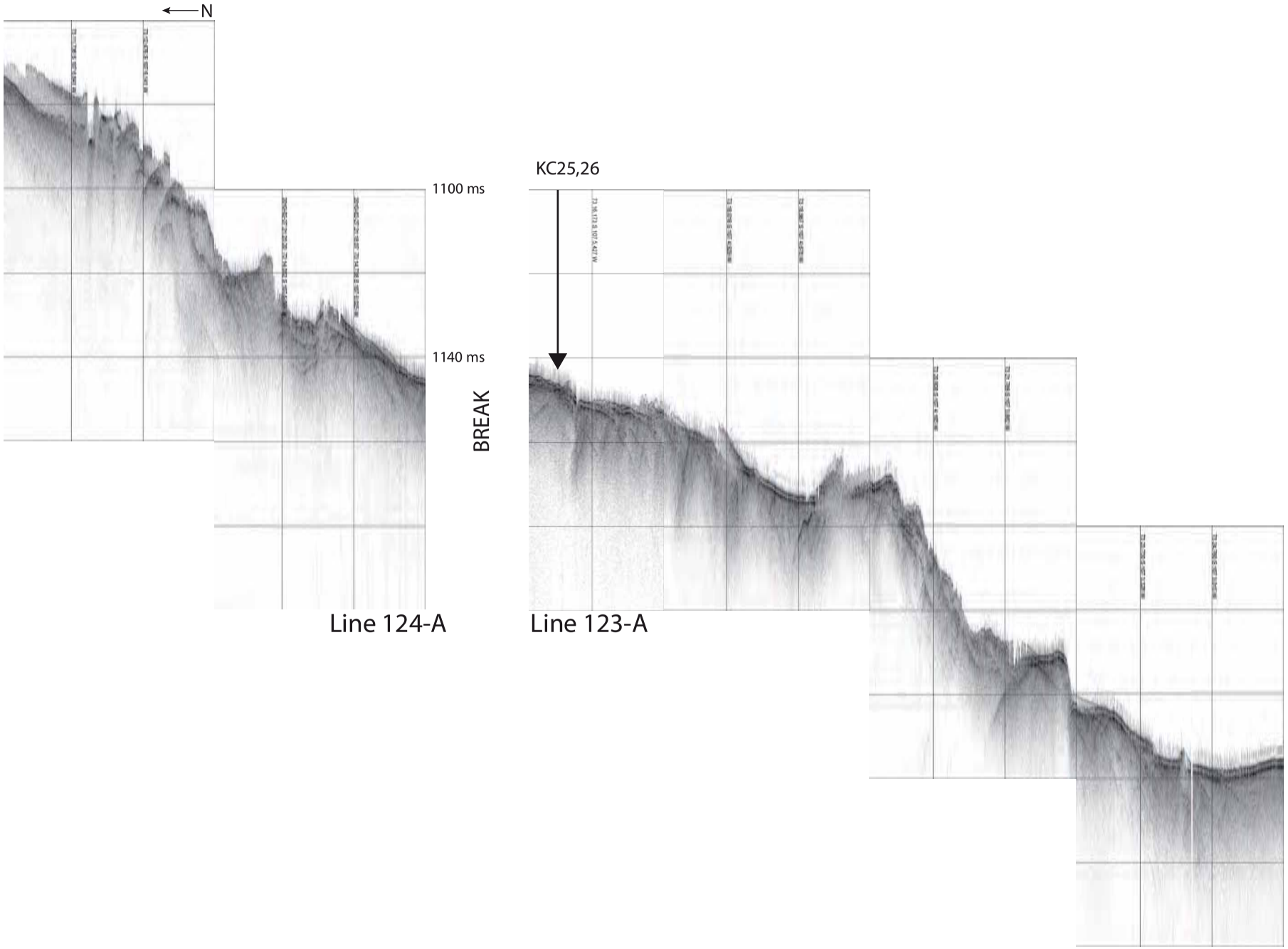
N
1100 ms
1140 ms
BREAK
KC25,26
Line 124-A
Line 123-A

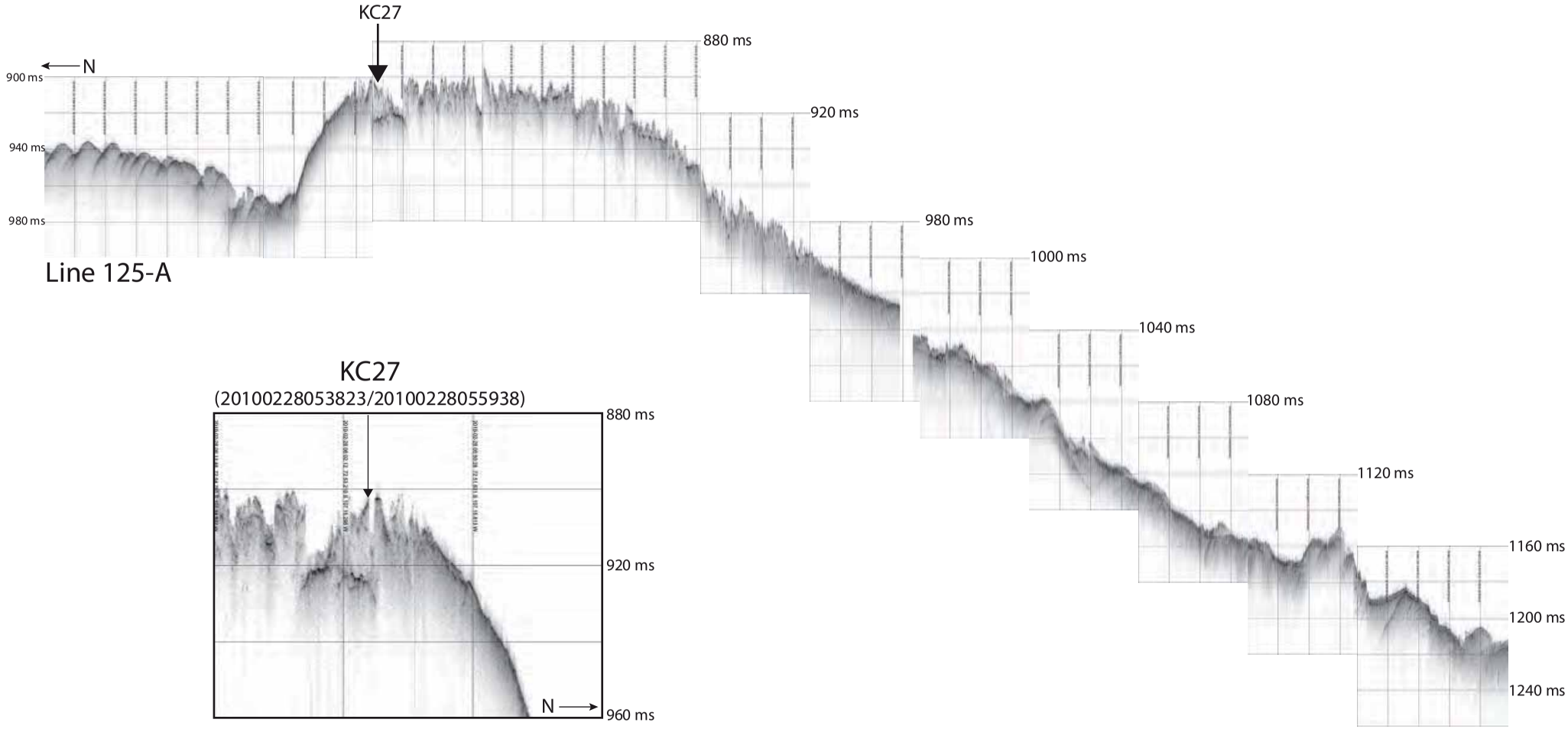

KC27

(20100228053823/20100228055938)

Appendix IV

Sample Number	Sample ID	Core ID	Water Depth(m)	Latitude	Longitude	Sample Top (cm)	Sample Bottom (cm)	Core Length (cm)	Description
01	OSO0910_KC-08_30_01	OSO0910_KC-08	711	-72.3469	-106.8439	30	30	40	Shell Fragment; may have moved during coring since a bit soupy at the top
02	OSO0910-KC-05_195-200_02	OSO0910_KC-05	729	-72.6971	-107.1105	195	200	245	Shell Frag? not a very certain sample
03	OSO0910_KC-06_70-80_03	OSO0910_KC-06	614	-72.1325	-106.91	70	80	102.8	shell fragment- good sample
04	OSO0910_KC-06_80-85_04	OSO0910_KC-06	614	-72.1325	-106.91	80	85	102.8	shell fragment- good sample
05	OSO0910_KC-06_90-92_05	OSO0910_KC-06	614	-72.1325	-106.91	90	92	102.8	281 N. pachyderma forams
06	OSO0910_KC-09_0-10_06	OSO0910_KC-09	548	-72.292	-106.3834	0	10	45	bryzoan- in bag
07	OSO0910_KC-09_10-20_07	OSO0910_KC-09	548	-72.292	-106.3834	10	20	45	brittle star fragment- potentially modern
08	OSO0910_KC-09_21-34_08	OSO0910_KC-09	548	-72.292	-106.3834	21	34	45	urchin spine?
09	OSO0910_KC-10_37_09	OSO0910_KC-10	687	-72.2954	-106.4641	37	37	88	shell fragment
10	OSO0910_KC-10_49_10	OSO0910_KC-10	687	-72.2954	-106.4641	49	49	88	tiny shell fragment
11	OSO0910_KC-11_54_11	OSO0910_KC-11	733	-72.3457	-107.911	54	54	150	Best shell sample of the day
12	OSO0910_KC-10_10-20_12	OSO0910_KC-10	687	-72.2954	-106.4641	10	20	88	brachiopod
13	OSO0910_KC-09_0-10_13	OSO0910_KC-09	548	-72.292	-106.3834	0	10	45	brachiopod
14	OSO0910_KC-11_67-14	OSO0910_KC-11	733	-72.3457	-107.911	67	67	150	sedimentary clast- not radiocarbon
15	OSO0910_KC-13_120-130_15	OSO0910_KC-13	742	-72.6407	-107.1687	120	130	226	rocks- double check but not likely a sample
16	OSO0910_KC-13_150-160_16	OSO0910_KC-13	742	-72.6407	-107.1687	150	160	226	shell frags
17	OSO0910_KC-13_170-180_17	OSO0910_KC-13	742	-72.6407	-107.1687	170	180	226	2 (?) shells , bivalves
18	OSO0910_KC-09_30-32_18	OSO0910_KC-09	548	-72.292	-106.3834	30	32	45	250 forams- N. pachyderma
19	OSO0910_KC-10_30-32_19	OSO0910_KC-10	687	-72.2954	-106.4641	30	32	88	330 forama- N. pachyderma
20	OSO0910_KC-15_110_20	OSO0910_KC-15	1257	-73.3603	-101.8362	110	110	130	in bottom sandy unit, shell frags (questionable sample)
21	OSO0910_KC-15_cc_21	OSO0910_KC-15	1257	-73.3603	-101.8362	cc	130	130	3 frags of shell
22	OSO0910_KC-16_0-10_22	OSO0910_KC-16	706	-73.454	-102.0792	0	10	38	articulated bivalves (3) WM 'still alive?'
23	OSO0910_KC-16_cc_23	OSO0910_KC-16	706	-73.454	-102.0792	cc	38	38	bivalve WM' 90% chance still living" suspect sample , yellow life jelly seen
24	OSO0910KC-18_131.5-148.5_24	OCO0910_KC-18	894	-73.3835	-106.871	131.5	148.5	148.5	Till Pellets: Not Radiocarbon. Subglacial pollen potential. Outcrop sample
25	OSO0910_KC-23_0-7_25	OSO0910_KC-23	660	-72.8923	-106.9243	0	7	36	two different types of shell fragments
26	OSO0910_KC-27_0-10_26	OSO0910_KC-27	666	-72.8828	-107.2548	0	10	52	brachiopod and an agglutianted foram
27	OSO0910_KC-15_110-112_27	OSO0910_KC-15	1257	-73.3603	-101.8362	110	112	130	110 N. pachyderma- from below clay unit in Ferrero Bay, dates clay
28	OSO0910_KC-19_90-92_28	OSO0910_KC-19	782	-73.1285	-106.9688	90	92	139	150 N. pachyderma
29	OSO0910_KC-23_20-22_29	OSO0910_KC-23	660	-72.8923	-106.9243	20	22	36	110 N. pachyderma-- important sample, dates wedge, no more sample left
30	OSO0910_KC-26_0-2_30	OSO0910_KC-26	689	-72.8645	-107.2223	0	2	106	Shell fragment- dyed with Rose Bengal dye- dyes life
31	OSO0910_KC-26_90-92_31	OSO0910_KC-26	689	-72.8645	-107.2223	90	92	106	shell fragment- small , white

Appendix V

XBT/XCTD locations

Date	Probe	Latitude	Longitude	Depth m

XBT/XCTD locations

Date	Probe	Latitude	Longitude	Depth m
2/5/10	T-7	-77.7539	166.2408	168
2/8/10	T-5	-77.0770	167.5406	320
2/8/10	Deep Blue	-77.0424	168.8466	None
2/8/10	Deep Blue	-77.1284	173.8462	498
2/8/10	Deep Blue	-77.1560	175.4130	626
2/9/10	Deep Blue	-77.2419	179.0279	724
2/9/10	Deep Blue	-77.2745	-179.4930	651
2/9/10	Deep Blue	-77.3050	-177.4304	611
2/9/10	Deep Blue	-77.3359	-175.3890	549
2/9/10	Deep Blue	-77.3457	-173.9940	528
2/9/10	Deep Blue	-77.3541	-173.0863	509
2/9/10	Deep Blue	-77.3350	-171.7880	456
2/9/10	Deep Blue	-77.4092	-170.2621	542
2/9/10	Deep Blue	-77.4647	-166.4530	423
2/10/10	Deep Blue	-77.4929	-164.4911	493
2/10/10	Deep Blue	-77.4090	-162.4914	661
2/10/10	Deep Blue	-77.3974	-162.2987	646
2/10/10	Deep Blue	-77.3849	-162.0991	630
2/10/10	XCTD-1	-77.3283	-161.1269	629
2/10/10	T-5	-77.3283	-161.1269	648

Date	Probe	Latitude	Longitude	Depth m
2/10/10	Deep Blue	-77.3283	-161.1269	621
2/10/10	Deep Blue	-77.3283	-161.1269	581
2/10/10	Deep Blue	-77.1756	-161.4797	579
2/10/10	Deep Blue	-77.1402	-161.6013	570
2/10/10	Deep Blue	-77.1042	-161.7184	557
2/10/10	Deep Blue	-77.0665	-161.8350	540
2/10/10	Deep Blue	-77.0291	-161.9563	530
2/10/10	Deep Blue	-76.9911	-162.0866	528
2/10/10	Deep Blue	-76.9532	-162.2181	531
2/10/10	Deep Blue	-76.9508	-162.2254	531
2/10/10	Deep Blue	-76.9161	-162.4236	545
2/10/10	XCTD-1	-76.9167	-162.4783	550
2/10/10	Deep Blue	-76.9165	-162.5615	564
2/10/10	Deep Blue	-76.9165	-162.7342	577
2/10/10	XCTD-1	-76.9165	-162.9355	591
2/10/10	Deep Blue	-76.9161	-163.0445	579
2/10/10	XCTD-1	-76.9161	-163.1367	584
2/10/10	XCTD-1	-76.9243	-163.2718	596
2/11/10	T-7	-76.7014	-158.4054	308

2/11/10	Deep Blue	-76.6335	-157.0372	390
2/11/10	Deep Blue	-76.6335	-156.3859	742
2/11/10	T-5	-76.6458	-156.0754	617
2/11/10	Deep Blue	-76.5627	-154.8404	552
2/11/10	Deep Blue	-76.5532	-154.8325	587
2/11/10	T-5	-76.4771	-154.5950	539
2/11/10	Deep Blue	-76.2382	-153.8791	466
2/11/10	Deep Blue	-76.2313	-153.8513	595
2/11/10	Deep Blue	-76.1904	-153.6431	1926
2/11/10	T-5	-76.1220	-153.4518	2898
2/11/10	T-5	-75.6393	-151.8657	3417

Date	Probe	Latitude	Longitude	Depth m
2/12/10	T-5	-74.9523	-151.1089	3770
2/12/10	T-5	-73.8507	-150.6956	4097
2/12/10	T-5	-73.8466	-150.6897	4097
2/12/10	T-5	-73.8137	-150.6774	4111
2/13/10	T-5	-72.8510	-142.4203	4096
2/13/10	T-5	-72.8492	-142.3993	4096
2/15/10	T-5	-71.9717	-119.9747	1932
2/15/10	T-5	-71.9820	-119.9474	1905
2/15/10	T-5	-71.9849	-119.9446	1893
2/15/10	T-5	-71.9866	-119.9410	1885
2/15/10	T-5	-71.9954	-119.8719	1825
2/15/10	T-5	-72.0245	-119.6784	1627
2/15/10	T-5	-72.0826	-119.3965	1296
2/15/10	T-5	-72.1228	-119.2082	1052
2/15/10	T-5	-72.1671	-119.0080	782
2/15/10	T-5	-72.1990	-118.8977	532
2/16/10	T-7	-73.4528	-107.8999	669
2/16/10	T-5	-73.1271	-106.2034	631
2/16/10	T-5	-73.1365	-106.5095	658
2/16/10	T-5	-73.1571	-106.7914	766
2/16/10	T-5	-73.1795	-107.0957	782
2/16/10	T-5	-73.2014	-107.4019	757
2/17/10	T-5	-73.2197	-107.6945	662
2/17/10	T-7	-73.1858	-107.4070	747
2/17/10	T-7	-72.7834	-106.2390	528
2/18/10	T-7	-72.6572	-107.7164	583
2/18/10	Deep Blue	-72.5355	-107.6921	624
2/18/10	Deep Blue	-72.5201	-107.3832	662
2/18/10	Deep Blue	-72.5051	-107.0472	724
2/18/10	Deep Blue	-72.4933	-106.7619	671

Date	Probe	Latitude	Longitude	Depth m
2/18/10	Deep Blue	-72.4754	-106.4332	505
2/20/10	Deep Blue	-72.4818	-106.5810	963
2/20/10	Deep Blue	-72.3757	-106.9251	705
2/20/10	T-7	-72.3757	-106.9251	705
2/20/10	T-7	-72.4581	-106.9788	728
2/20/10	T-7	-72.4581	-106.9788	728
2/21/10	T-7	-72.4785	-107.1001	720
2/21/10	T-7	-72.4785	-107.1001	720
2/21/10	T-7	-72.6366	-107.2737	695
2/21/10	T-7	-72.6366	-107.2737	695
2/21/10	T-7	-72.6366	-107.2737	695
2/21/10	T-7	-72.3958	-106.6167	609
2/22/10	T-7	-72.5649	-107.2378	711
2/22/10	T-7	-72.5649	-107.2378	711
2/22/10	T-7	-72.5614	-107.2306	616
2/23/10	T-7	-72.6371	-106.9069	709
2/23/10	T-7	-72.6768	-106.8582	611
2/23/10	Deep Blue	-72.9824	-106.5716	618
2/23/10	Deep Blue	-73.0430	-106.3074	609
2/23/10	Deep Blue	-73.0474	-106.2848	611
2/23/10	Deep Blue	-73.1029	-105.9189	577
2/23/10	Deep Blue	-73.1054	-105.8872	570
2/24/10	Deep Blue	-73.2482	-105.6206	447
2/24/10	Deep Blue	-73.2684	-105.1541	398
2/24/10	Deep Blue	-73.3508	-104.5920	524
2/24/10	Deep Blue	-73.3887	-104.0534	627
2/24/10	Deep Blue	-73.3526	-103.5078	850
2/24/10	T-7	-73.4609	-102.7705	564
2/25/10	T-5	-73.4546	-102.0886	760
2/25/10	Deep Blue	-73.4384	-103.0218	752

Date	Probe	Latitude	Longitude	Depth m
2/26/10	T-5	-72.8352	-106.9035	652
2/27/10	T-5	-72.9435	-106.8545	662
2/27/10	T-5	-72.9702	-106.8434	671
2/27/10	T-5	-73.1165	-106.7777	734
2/27/10	T-5	-73.2398	-106.7521	792
2/28/10	Deep Blue	-72.8864	-107.2019	654
2/28/10	Deep Blue	-73.1575	-107.1797	763
3/1/10	Deep Blue	-71.9060	-104.3297	670
3/1/10	Deep Blue	-71.8579	-103.7090	744
3/2/10	Deep Blue	-71.8342	-103.3927	758
3/2/10	Deep Blue	-71.8307	-103.3465	735
3/2/10	Deep Blue	-71.8102	-103.0809	743
3/2/10	Deep Blue	-71.7874	-102.8100	535
3/2/10	Deep Blue	-71.7537	-103.0781	730
3/2/10	Deep Blue	-71.7095	-103.4544	689

3/2/10	Deep Blue	-71.6772	-103.7351	638
3/2/10	Deep Blue	-71.6314	-104.1196	626
3/3/10	Deep Blue	-70.8295	-94.8437	510
3/3/10	Deep Blue	-70.6146	-94.6144	693
3/3/10	T-5	-70.5806	-94.5773	925
3/3/10	T-5	-70.5473	-94.5420	1114
3/3/10	T-5	-70.5048	-94.4971	1428

MEDDELANDEN från STOCKHOLMS UNIVERSITETS INSTITUTION för GEOLOGISKA VETENSKAPER No 341

Rapportserie
ISBN 978-633-7440-1

No. 331. IVARSSON, M. Fossilized microorganisms in volcanic rocks from sub-sea floor environments. Stockholm 2008.

No. 332. BJÖRKVALD, L. Landscape hydrogeochemistry of Fe, Mn, S and trace elements (As, Co, Pb) in a boreal stream network. Stockholm 2008.

No. 333. BÄCKSTRAND, K. Carbon gas biochemistry of a northern peatland – in a dynamic permafrost landscape. Stockholm 2008.

No. 334. BLAJ, T. Late Eocene through Oligocene calcareous nannofossil from the paleoequatorial Pacific Ocean – taxonomy, preservation history, biochronology and evolution. Stockholm 2009.

No. 335. COLLEONI, F. On the Late Saalian glaciations (160–140 ka): a climate modeling study. Stockholm 2009.

No. 336. KONN, C. Origin of organic compounds in fluids from ultramafic-hosted hydrothermal vents of the Mid-Atlantic Ridge. Stockholm 2009.

No.337. SELLÈN, E. Quaternary paleoceanography of the Arctic Ocean: A study of sediment stratigraphy and physical properties. Stockholm 2009.

No. 338. SUNDVALL, R. Water as a trace component in mantle pyroxene: Quantifying diffusion, storage capacity and variation with geological environment. Stockholm 2010.

No 339. PETTERSSON, C-H. The tectonic evolution of northwest Svalbard. Stockholm 2010.

No. 340. SVAHNBERG, H. Deformation behaviour and chemical signatures of anorthosites: Examples from southern West Greenland and south-central Sweden. Stockholm 2010.

Formerly/1990–2009: MEDDELANDEN från STOCKHOLMS UNIVERSITETS INSTITUTION för Geologi och Geokemi (ISSN 1101-1599)

Department of Geological Sciences
Stockholms universitet SE-106 91 Stockholm www.su.se

Stockholm University